Novel Fingermark Detection Techniques Using Upconverters with Anti-Stokes Luminescence

By

Rongliang MA

A thesis submitted for the degree of Doctor of Philosophy
University of Technology, Sydney

2012

Certificate of Authorship/Originality

I certify that the work in this thesis has not previously been submitted for a degree nor has it been submitted as part of requirements for a degree except as fully acknowledged within the text.

I also certify that the thesis has been written by me. Any help that I have received in my research work and the preparation of the thesis itself has been acknowledged. In addition, I certify that all information sources and literature used are indicated in the thesis.

Signature of Candidate

Acknowledgements

I would hereby sincerely like to acknowledge the assistance I received from various people during my studies at the University of Technology, Sydney (UTS).

First, I would like to convey my appreciation to my principal supervisor, Professor Claude Roux, for his support throughout my study. I thank him for assisting me with the scholarship, the visit to the Lausanne University in Switzerland and for taking the trouble to help me with many other aspects of my study.

I would also like to express my thanks to my external supervisor, Professor Chris Lennard at the University of Canberra, for all his help since my admittance to UTS, his assistance during the whole project and for teaching me how to write scientifically. I wish also to thank all my other supervisors: Dr Andrew McDonagh for his invaluable suggestions on the writing of my papers and thesis; Dr Ronald Shimmon for his help in the experiment, and especially his encouragement through the tough times at the beginning of my study; Dr Philip Maynard for his assistance during the experiment and the writing.

I wish to thank Professor Hilton Kobus from Flinders University who assisted with my visit to Australia in 2004, which resulted in my PhD study at UTS, and for many other helpful things throughout my study.

I would also express my appreciation to the following people:

Dr Congji Zha from the Commonwealth Science, Industry and Research Organization (CSIRO) for all his invaluable help and advice during the whole project.

Dr Linda Xiao for helping me with so many aspects.

Professor Fuyou Li for his precious advice in synthesising the functionalised UCs.

Dr Annette Dowd for her help in solving the imaging problem, which was critical to my project.

Dr Barry Liu for his assistance with the Par bomb device in the synthesis.

Dr Peter Osvath and Dr Andrew Scully from CSIRO for their assistance with my experiment.

Dr Mi Jung Choi for all the encouragement and kind support with my application since my arrival in Sydney in 2005.

Dr Mark Tatouh for his help and good ideas for the experiment.

Dr Xanthe Spindler for aiding me with my experiment and thesis writing.

Harry Simpson for all his kind and patient help with the experiment.

Jean-Pierre Guerbois for helping me with the heating devices in the experiment.

Dr Richard Wuher in the Microstructural Analysis Unit (MAU) at UTS for all his help with SEM.

Rochelle Seneviratne for all her kind assistance with my study.

Greg Dalsanto who helped me with the Teflon autoclave for the synthesis.

Professor Besim Ben-Nissan for the assistance with the synthesis and other invaluable advice.

Amir Moezzi for the assistance with some of the softwares in my thesis writing.

Dr Lucas Blanes, one of my best friends, not only for the best fingermark samples provided, but also for all the funny stories and laughs. You also taught me a different attitude to life: to keep a curiosity for all the new things and enjoy life.

A special thanks goes to my proofreader, Joanne Watson.

I would also like to thank some of my fellow students and the staff at UTS for their help. They are Mark Berkahn, Jim Franklin, Stuart Dines, Scott Chadwick, Amanda Van Gramberg, Adrian De Grazia, Ayling Rubin, Andrew Malecki, Gemma Armstrong and Adam Georgius.

Finally, I would like to thank my mother and father, and my sister and nephew. Thanks for the unconditional love you give to me. A big thank you to my wife, Kangling Ren, who gave up wonderful business opportunities to come to Sydney with me and live a ‘poor’ life. Thank you for your sacrifice. To my daughter, Yifan, who was born in the busiest time of my PhD study. You gave me so many sleepless nights, but I never regretted having your company. Your smile is the best reward for me and you are the driving force in my life.

Table of Contents

Table of Figures

List of Tables

Abbreviations

AA: Azelaic acid

AFIS: Automatic fingerprint identification system

AOT: Sodium bis(2-ethylhexyl) sulfosuccinate

CA: Cyanoacrylate

CAF: Cyanoacrylate Fuming

CTAB: cetyltrimethylammonium bromide

DNA: Deoxyribose Nucleic Acid

FTIR: Fourier transform infrared spectroscopy

IR: Infrared

NIR: Near infrared

PEI: Polyethylenimine

PVP: Polyvinylpyrrolidone

SEM: Scanning electron microscope

SLR camera: Single-Len Reflex camera

SPR: Small particle reagents

UC: Upconverter

UCNP: Upconverter nanoparticle

UC-AA: $NaYF_4$:Er,Yb/azelaic acid

UC (Ho)-AA: $NaYF_4$:Ho,Yb/azelaic acid

UC (Tm)-AA: $NaYF_4$:Tm,Yb/azelaic acid

UC-AOT: $NaYF_4$:Er,Yb /sodium bis(2-ethylhexyl) sulfosuccinate

UC-PEI: $NaYF_4$:Er,Yb/polyethylenimine

UC-PVP: $NaYF_4$:Er,Yb/polyvinyl pyrrolidone

UV: Ultraviolet

VSC: Video Spectral Comparator

XRD: X-ray diffraction

Publications and Manuscripts Arising From This Work

1. Rongliang Ma, Ronald Shimmon, Andrew McDonagh, Philip Maynard, Chris Lennard, and Claude Roux, Fingermark detection on non-porous and semi-porous surfaces using YVO_4:Er,Yb luminescent upconverting particles. Accepted， doi:10.1016/j.forsciint.2011.10.033.

2. Rongliang Ma, Elicia Bullock, Philip Maynard, Brian Reedy, Ronald Shimmon, Chris Lennard, Claude Roux, and Andrew McDonagh, Fingermark Detection on Non-Porous and Semi-Porous Surfaces Using NaYF4:Er,Yb Up-converter Particles, *Forensic Science International*, 207 (2011) 145-149 ， doi:10.1016/j.forsciint.2010.09.020.

3. Rongliang Ma, Andrew McDonagh, Chris Lennard, Ronald Shimmon, Philip Maynard, and Claude Roux, 'Latent Fingermark Detection Using Functionalised Upconvertors', presented for the BIT's 2nd Annual World Congress of Forensics, September, 2011, Chongqing.

4. Rongliang Ma, Ronald Shimmon, Andrew McDonagh, Philip Maynard, Chris Lennard, and Claude Roux, 'Further Research into Novel Fingermark Detection Techniques Using Upconversion Luminescence', presented for the 8th International Fingerprint Research Group (IFRG) Meeting, September, 2011, Helsinki.

5. Rongliang Ma, Ronald Shimmon, Andrew McDonagh, Philip Maynard, Chris Lennard, and Claude Roux, 'Fingermark Detection Using Anti-Stokes Luminescence Generated by Functionalized Up-onverters', paper presented on the 20th Symposium on the Forensic Sciences, Australian and New Zealand Forensic Science Society, 2010, Sydney.

6. Rongliang Ma, Ronald Shimmon, Philip Maynard, Chris Lennard, Andrew McDonagh, and Claude Roux, 'Further Research into Novel Fingermark Detection Techniques Using Anti-Stokes Luminescence', paper presented on the 5th European

Academy of Forensic Sciences, European Network of Forensic Science Institutes, 2009, Glasgow.

7. Rongliang Ma, Ronald Shimmon, Andrew McDonagh, Philip Maynard, Chris Lennard, and Claude Roux, 'Further Research into Novel Fingermark Detection Techniques Using Upconversion Luminescence', paper presented on the 7th International Fingerprint Research Group (IFRG) Meeting, June-July 2009, Lausanne.

Abstract

Fingerprinting is a mainstay of forensic science and has been used in crime investigation for more than one hundred years. However, most fingermarks found at a crime scene are latent; they may become visible through development and enhancement. Among all the fingermark development techniques, conventional luminescence methods are routinely employed, with the advantages of being both sensitive and selective on non-luminescent substrates (i.e., providing high contrast in developed marks).

Anti-Stokes luminescence or upconversion is an optical process of converting long-wavelength radiation into a shorter-wavelength emission, which is contrary to conventional Stokes luminescence. Upconversion mainly exits in rare-earth complexes and upconversion materials are referred to as upconverters. Commercially-available upconverters have been widely employed in security inks and biolabels.

Upconversion is unusual in both natural surfaces and in consumer products. If the upconverters are applied for fingermark detection and show selective affinity to fingermark materials, theoretically the strong luminescence of the upconverters can be visualised on fingermarks as bright regions on a totally dark background. This means that fingermark detection techniques using upconverters has the potential to eliminate interference from background printing and luminescence.

This thesis begins with the review of luminescence-based fingermark detection techniques and previous research on the application of upconverters for fingermark detection. The previous research showed that upconverters have an affinity for fingermark residues and are effective for fingermark detection.

Chapter 2 describes issues with respect to imaging the upconversion luminescence. Of the options tested, a 980 nm laser pointer with 700 mW output proved to be the most suitable light source for the excitation of the upconversion luminescence. Long exposure times were needed to record the upconversion

luminescence. A Rofin Poliview fitted with a 555 nm band-pass barrier filter was found to be a suitable recording system.

Chapter 3 investigates the application of the $NaYF_4$:Er,Yb upconverter powder for latent fingermark detection on non-porous and semi-porous surfaces. The $NaYF_4$:Er,Yb powder showed selective affinity to fingermark materials and the dry powdering method proved to be better than the suspension method. The upconverter powder showed strong luminescence when illuminated with 980 nm wavelength laser light and the developed fingermarks presented clear ridges with high contrast. A near-infrared laser diode and laser pointer are both effective light sources when used in conjunction with a 555 nm band-pass filter to block the IR light. In actual imaging, the fingermark substrate is still visible to some extent under long exposure times, but the interference is reduced compared to what is observed with conventional luminescence imaging and the fingermark detail is clear. In summary, the $NaYF_4$:Er,Yb powder can be used to detect fingermarks on various difficult surfaces that exhibit interfering background luminescence when using conventional luminescence techniques.

Chapter 4 investigates the application of another type of upconverter powder, YVO_4:Er,Yb, for fingermark detection on non-porous and semi-porous surfaces. The YVO_4:Er,Yb powder proved to be effective for latent fingermark development when used as a dry powder or as a suspension, with the former generally presenting the better result. The YVO_4:Er,Yb powder also showed selective affinity to fingermark residues on most surfaces and the developed fingermarks presented clear ridges against a clear background. The upconverter powder showed strong luminescence when illuminated with 980 nm wavelength laser light but was slightly less visually luminescent than the $NaYF_4$:Er,Yb powder. Both a laser diode and pointer are effective light sources when used in conjunction with a 555 nm band-pass filter to block the infrared light. As before, the fingermark substrate was visible to some extent in the upconversion luminescence mode with long exposure times, but the interference was reduced compared to that observed using conventional luminescence imaging. Clear fingermark detail was observed. In summary, the YVO_4:Er,Yb powder can be used to detect fingermarks on various difficult surfaces

that exhibit interfering background luminescence when using conventional luminescence techniques.

Cyanoacrylate fuming is probably the most important routine technique for fingermark detection on non-porous surfaces. In the fingermark detection process, the cyanoacrylate monomer forms a white fibrous layer of polycyanoacrylate on the fingermark ridges. There are numerous holes in the fibrous polycyanoacrylate layer, with an average diameter of 1–2 micrometres. Hence, it is worth investigating smaller $NaYF_4$:Er,Yb upconverter particles that can penetrate into the holes in the polymer structure and remain trapped inside. In Chapter 5, three methods (sieving, suspension and milling) were investigated to isolate the smaller particles from the commercial $NaYF_4$:Er,Yb powders. Owing to limitations with respect to instrumentation and time, no ideal results were acquired.

Conventional upconverter materials are insoluble in water and other solvents, and this limits their application when combined with cyanoacrylate fuming. The possibility of making upconverters soluble or dispersible in water was investigated by functionalizing them as nanoparticles with hydrophilic groups. Chapter 6 explores the synthesis and use of four functionalised upconverters including UC-PEI ($NaYF_4$:Er,Yb/polyethylenimine), UC-AA ($NaYF_4$:Er,Yb/azelaic acid), UC-PVP ($NaYF_4$:Er,Yb/polyvinyl pyrrolidone) and UC-AOT ($NaYF_4$:Er,Yb /sodium bis(2-ethylhexyl) sulfosuccinate) for staining CA-fumed fingermarks on various non-porous surfaces. Among them, the UC-PEI and UC-AA showed strong luminescence under 980 nm laser illumination, with the latter being more visually luminescent. The UC-PEI and UC-AA showed some advantages for fingermark detection on various difficult surfaces where background luminescence and printing interfered with conventional luminescence enhancement. Long exposure times under a Rofin Poliview system had to be employed in the imaging of fingermarks developed by the functionalised upconverters. These long exposure times resulted in the substrate itself being visible to some extent, which is different from the theoretical “ideal” scenario that would provide bright fingermarks against a totally dark background. However, functionalised upconverters still showed superior results to conventional

luminescence techniques for fingermark detection on some difficult substrates and they have great potential to be improved through further research.

General discussion and conclusions are presented in Chapter 7. Possible future directions for fingermark detection using upconverters are also presented.

Chapter 1:

Luminescence Techniques and Upconverters for Fingermark Detection

Chapter 1. Luminescence Techniques and Upconverters for Fingermark Detection

1.1. Introduction

1.1.1. Fingermarks

Fingerprinting is a mainstay of forensic science. The ridge patterns present on the fingers, palms and sole of the feet are immutable and highly polymorphic characteristics across individuals [1]. Because of these unique properties, fingerprinting has been used in crime investigation for more than one hundred years. With the rapid application of the automatic fingerprint identification system (AFIS), fingerprinting plays a more important role in both civil and criminal investigations all over the world.

Most fingermarks found at a crime scene or on an item related to a criminal matter are latent. Latent fingermarks are those that are present but invisible; they may become visible through development and enhancement.

Latent fingermarks deposited by the ridges of the finger or palm are complex mixtures of natural secretions and contaminants from the environment [1]. Three types of glands are responsible for the natural secretions of the skin: the sudoriferous eccrine and apocrine glands, and the sebaceous glands. The amount and constituents of individual secretions and individual glandular secretions are variable (Table 1.1). Environmental conditions such as temperature and humidity, exercise and stress affect the rate of production of eccrine sweat in an individual. The composition also varies in relation to age, sex, medical condition and diet. Eventually these factors influence the quality of developed fingermarks, along with environmental conditions post-deposition.

Table 1.1. Main chemical constituents of the glandular secretions relevant to fingermark [1].

Main Chemical Constituents of the Glandular Secretions

		Constituents	
Source	**location**	**inorganic**	**organic**
Eccrine glands	All over the body, but the only type of glands on the palms of the hands and the soles of the feet	Chloride Metal ions (Na^+, K^+, Ca^{2+}) Sulfate Phosphate Bicarbonate Ammonia Water (>98%)	Amino acids Proteins Urea Uric acid Lactic acid Sugars Creatinine Choline
Apocrine glands	In the groin and the armpits; associated with hair follicles around the genitals and mammary glands	Iron Water (>98%)	Proteins Carbohydrates Sterols
Sebaceous glands	All over the body, except on the palms of the hands and the soles of the feet; highest concentration is on the forehead and on the back; associated with hair roots	—	Glycerides (30–40%) Fatty acids (15–25%) Wax esters (20–25%) Squalene (10–12%) Sterol esters (2–3%) Sterols (1–3%)

1.1.2. Fingermark detection techniques

To make a latent fingermark become visible, various enhancement techniques can be used. The combination of optical methods (absorption, diffuse reflection, luminescence, UV absorption and reflection), physical methods (powdering, small particle reagents, vacuum metal deposition), physical/chemical methods [physical developer, multi-metal deposition, iodine, cyanoacrylate fuming (CAF)] and chemical methods [ninhydrin and its analogues, metal complexation after ninhydrin treatment, 1,8-diazafluoren-9-one (DFO), 1, 2-indanedione and genipin] allows for the development of fingermarks deposited on various surfaces. Despite all of the existing techniques, there remains a strong need for new and more efficient reagents to detect latent fingermarks [2].

The choice of the technique for fingermark development is dependent on the composition of latent fingermarks, on the type of substrate, on environmental conditions and on the suitability of the technique to be applied in sequence in the context of the case [2].

1.2. Luminescence Techniques for Fingermark Detection

1.2.1. Introduction

Luminescence techniques are the methods of choice to detect latent fingermarks, with the advantages being high sensitivity and in general high selectivity (high contrast), etc. Fluorescence is a type of luminescence where light emission results from the absorption of light (energy). When light interacts with matter, a photon of light may be absorbed by a molecule (or atom) of that matter. After absorption of the photon, the molecule has an excess of energy and is no longer in its normal (ground) state, but is promoted to a higher energy (excited) state. However, the molecule (or atom) tends to rapidly return to its ground state by releasing the excess energy in some form. If the molecule releases part of its excess energy to the immediate neighbours, in the form of an emission of another photon, this process is called photoluminescence. An emission can proceed either directly or indirectly. Direct emission is known as "fluorescence", which is most common in the photoluminescence process, while indirect emission through a metastable state is known as "phosphorescence". Generally, the energy of an emitted photon is smaller than the energy of an absorbed photon by the amount of shared energy. This means that the photoluminescence emission has a longer wavelength (lower energy) compared with the absorbed light that was used to excite the molecule (the "excitation" light). It is also said that the photoluminescence emission is "red-shifted" in comparison to the light. Stokes shift is the difference (in wavelength or frequency units) between positions of the band maxima of the absorption and emission spectra (**Figure 1.1**) [3].

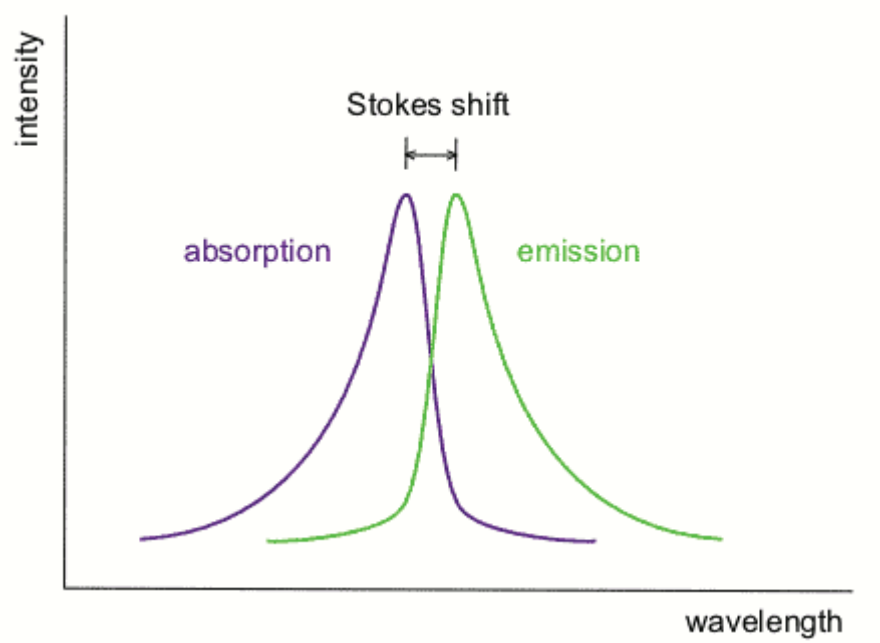

Figure 1.1. Schematic representation of the Stokes shift in a luminescence process [4].

Since the late 1970s, lasers have been proposed for the detection of the inherent luminescence of untreated fingermarks on non-luminescent surfaces. Positive results have been obtained in experiments on many surfaces, although the success rate of the technique in actual casework is relatively low [5]. However, the illumination of exhibits at different wavelengths using a suitable high-intensity light source (not necessarily a laser) while observing through appropriately filtered goggles is needed.

Many chemical techniques based on amino acid detection take advantage of the high level of sensitivity of luminescence methods. For example, ninhydrin and zinc or cadmium post-treatment has long been regarded as the best reagent to detect fingermarks on porous surfaces. A ninhydrin and metal salt-treated fingermark illuminates strong luminescence under liquid nitrogen temperature [1]. Moreover, the products of many ninhydrin analogues with amino acid also have good luminescence. In the 1990s, DFO was formally introduced to fingermark detection with even higher sensitivity than ninhydrin. DFO-developed latent marks produce excellent luminescence without any post-treatment or cooling. It has become a routine chemical in many fingerprint laboratories [1]. 1,2-Indanedione is another

excellent fluorescent fingermark reagent after DFO. It has a high sensitivity and a darker colour under white light, and is lower priced compared to DFO. It is gradually becoming an important fingermark reagent that may replace DFO in many forensic labs [6].

For fingermark detection on non-porous surfaces, luminescent powders and CAF (in conjunction with luminescent staining) are two of the most important techniques. Powders generally are preferred at crime scenes. The use of luminescent powders has advantages on reflective or multicoloured surfaces where contrast may be a problem with conventional powders. Background colours and substrate luminescence should be taken into consideration when selecting an appropriate luminescent powder [1, 7].

The most popular luminescent stains used after CAF include rhodamine 6G, Ardrox 970-P10, and basic yellow 40. The CA-fumed fingermarks strongly absorb the stain and emit good luminescence under approximate illumination, but no enhancement is obtained with luminescent stains if the surface itself is highly luminescent [1, 7].

1.2.2. Advanced luminescence techniques

This section is a description of the recent developments in fingermark detection using advanced luminescence techniques, i.e. beyond the scope of traditional amino acid reagents or CAF stains.

1.2.2.1. CdS/CdSe/CdTe luminescence techniques

Luminescent CdS nanoparticles

Menzel *et al.* focused their research on the use of photoluminescent semiconductor nanocrystals (also referred to as nanocrystallites, quantum dots, nanoparticles, nanoclusters or nanocomposites), formed from compounds such as ZnS, CdS, CdSe, CdTe, InP, InAs, which yield intense luminescence with a lifetime in the desired range [8, 9]. Moreover, the absorption and emission can be tailored by

adjusting the nanocrystal size. Basically, CdS nanoparticles were used as the luminescence resources after CAF. Cadmium nitrite and sodium sulfide were added in the dendrimer solution to form the CdS/dendrimer nanocomposites. After that, exhibits with fingermarks already fumed by cyanoacrylate (CA) were dipped into a CdS/dendrimer nanocomposites solution for a number of hours (often left over night) to endure the possible reaction between the amino functionality of the dendrimer and the carboxylic acid of the fingerprint residue. An interesting observation was that this method was only effective on CA ester-fumed fingermarks, but ineffective when applied to unfumed fingermarks. This could be explained by the use of ethanol in the solution causing the fingerprint residues to be washed away. Moreover, to improve the binding of the fingermark to the dendrimer, Bouldin *et al.* used diimide to pretreat the fingermark to convert the carboxylic acid moieties of the fingerprint residue to esters that then reacted with the dendrimer amino groups to form amide linkages [10]. The effect of the reaction temperature of CdS/dendrimer nanocomposites with fingerprint residues was also considered and some positive results were acquired. In summary, the CdS/dendrimer nanocomposites improved the binding of nanoparticles with fingerprint residues and seemed an interesting direction in the wet powdering techniques, but the complexity of the operation, for example, long development time, also limited its further application. In addition, Jin *et al.* used CdS/PAMAM nanocomposites to develop sebaceous fingermarks on tinfoil and observed similar results [11].

A CdS/chitosan nanocomposite was explored for fingermark detection by Dilag *et al* [12]. The CdS quantum dots (QDs) were encapsulated in an inexpensive biopolymeric chitosan matrix with the help of sodium sulphide (Na_2S). The transmission electron microscopy (TEM) showed that the average size of the QDs varied from ~7 to ~12 nm depending on the concentration of Na_2S. When excited at 450 nm, the QDs showed two emissions: one narrow peak at 531nm and a broad emission between 600 and 850 nm with a maximum at 716 nm. Latent fingermarks on aluminium foil were successfully developed by this QDs powders with identifiable ridge characteristics. However, further research may be needed to improve the particle size of this CdS/chitosan nanocomposite and the application method should be investigated too.

Algarra *et al* assembled two CdS nanocomposite in a porous phosphate heterostructures (PPH) functionalized respectively with mercaptopropyl (PPH-SH) or propionitrile (PPH-CN) [13]. Both the PPH-SH-CdS and the PPH-CN-CdS showed luminescence in the 450–700 nm wavelength range with a large Stokes shift higher than 300 nm. The PPH-SH-CdS is far more luminescent than the PPH-CN-CdS and fingermarks on various surfaces were developed successfully by the PPH-SH-CdS.

Luminescent CdSe nanoparticles

Sametband and coworkers developed two types of nanoparticles: gold stabilized by n-alkanethiols and CdSe/ZnS stabilized by n-alkaneamine [14]. Both nanoparticles were dissolved in organic solution and adhere to the fingermark ridges preferentially. The gold nanoparticles can improve the effectiveness of physical developer (PD) by catalysing the deposit of silver on the fingermark ridges on porous surfaces. The CdSe/ZnS nanoparticles successfully detected fingermarks on non-porous surfaces and the luminescence of the developed fingermark can be viewed directly under the illumination of UV light.

Wang et al used mercaptoacetic acid (TGA) as the stabiliser to synthesise the CdSe nanoparticles in an aqueous solution and applied this nanoparticles to fingermark detection on adhesives [15]. They investigated the effects of stabilizer, precursor, pH value, etc. on the luminescence of the CdSe nanoparticles. The result showed that the nanoparticles exhibited strong luminescence under 380 nm illumination and the intensity of the luminescence can be remarkably increased when adding excess cadmium ion, under controlled ion ratio and at pH 8. Fingermarks on adhesives were successfully detected with better resolving rate compared with traditional gentian violet.

Luminescent CdTe nanoparticles

Becue et al synthesised a novel luminescent reagent based on the use of the CdTe quantam dots in aqueous solution [16]. The maximum emission of this CdTe

quantam dots was centred in the green range of the visible when excited under UV light. This luminescent CdTe reagent was applied to detect fingermarks in blood on a variety of non-porous surfaces and compared with another very efficient blood reagent, Acid Yellow7 (AY7). The result showed that the CdTe quantam dots were equally effective to AY7 for fingermark detection on glass, polyethylene and polypropylene surfaces and were better than AY7 for fingermark detection on aluminium.

Gao and co-workers synthesised an efficient, positively charged CdTe–$COONH_3NH^+3$ QDs for fingermark detection on a variety of smooth surfaces [17]. In the preparation process, they used hydrazine hydrate as both the surface stabilizer and pH adjuster that led to enhanced luminescence. Another $CdTe^-COO^-$ QDs were also synthesized for fingermark detection and compared with the $COONH_3NH^+3$ QDs. The result illustrated that the $COONH_3NH^+3$ QDs are effective for fingermark detection on many surfaces such as smooth objects such as glass, polymer materials, plastic film, rubber, transparent polypropylene, marble and aluminum. The $COONH_3NH^+3$ QDs also showed superior detection capability than the $CdTe^-COO^-$ QDs.

1.2.2.2. Luminescent oxide nanoparticles

Luminescent TiO_2 nanoparticles

Choi *et al*. used functionalised titanium dioxide (TiO_2) powder doped with a new perylene diimide dye to detect sebaceous fingermarks on non-porous surfaces [18]. A new, highly fluorescent dye—perylene dianhydride—was synthesised using oleylamine and was adsorbed into TiO_2 nanoparticles to form the new fingermark detection powder. The powder exhibiting strong luminescence at 650-700 nm under excitation at 505 nm led to similar results to those obtained with commercial fluorescent powders (**Figure 1.1**). On glass surfaces, the new powder gave images showing tertiary-level detail of the fingermark ridges. The luminescence intensity of the new powder was slightly weaker, but background development was much less, which led to good contrast between the fingermark and the substrate.

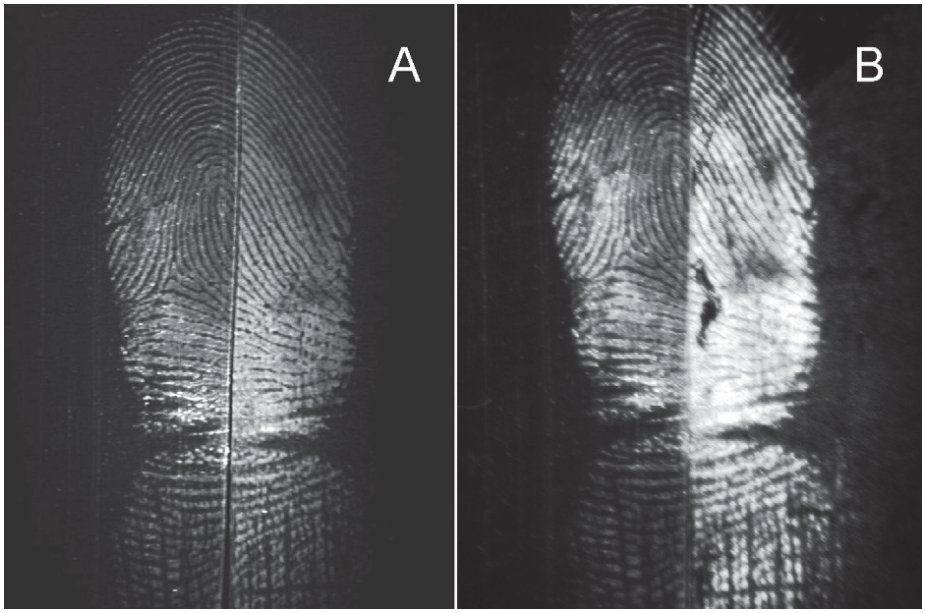

Figure 1.2. Comparison of perylene dye on TiO_2 and commercial fluorescent powders, viewed using a 575 nm long-pass filter and 505 nm illumination. (A) (Left) Perylene dye/TiO_2 particles (Degussa), and (right) Black Emerald fluorescent magnetic powder on polyethylene. (B) (Left) Fluorescent dye/TiO_2 particles (Degussa), and (right) Blitz Green fluorescent magnetic powder on polyethylene [18].

Luminescent ZnO nanoparticles

Moreover, Choi *et al*. used zinc oxide (ZnO) as fluorescent powder for fingermark detection [19]. Pure and lithium-doped nanostructured ZnO powders were applied to fresh and aged fingermarks on non-porous surfaces such as glass, polyethylene and aluminium foil. ZnO was found to produce clear fluorescent impressions when illuminated with long-wave UV light.

Becue *et al*. used the in situ deposition of zinc oxide (ZnO) on gold nanoparticles to detect fingermarks on various non-porous surfaces [20]. It resulted in a great improvement on the multimetal deposition (MMD) technique, showing better selectivity and sensitivity, especially on black surfaces.

Luminescent SiO_2 nanoparticles

Liu *et al*. used silicon dioxide (SiO_2) nanocomposites doped with fluorescent Eu^{3+}/sensitizer complex for fingermark detection [21]. Because of the large loading capacity and high surface area to volume ratio of SiO_2, it has great potential to form nanocomposites with other molecules. They trapped the highly fluorescent and photo-stable Eu^{3+} metal ions/sensitizer complex in SiO_2-based xerogels. They also tried other sensitizers but the results indicated that 1,10-phenanthroline (OP) in tetrathoxysilane (TEOS) was the best for fingermark detection. Both fresh and aged eccrine fingermarks were left on various surfaces such as metal foil, glass, plastic, coloured paper and a green leaf. A magnetic brushing technique was used for fingermark development with a magnetic applicator. The strong and narrow ligand-sensitized luminescence emission of Eu^{3+} was observed from the above fingermarks.

Theaker *et al*. used the hydrophobic silica doped with either fluorescent or coloured dyes to form both nano- and micro-particles for developing latent fingermarks [22]. Nanoparticles were applied as an aqueous suspension, and the microparticles as dusting agents using brushes or a magnetic wand. Good samples were achieved from both the coloured and luminescence images for both fresh and aged fingermarks left on glass microscope slides.

1.2.2.3. Time-resolved and phase-resolved techniques

The time-resolved (TR) technique has been proposed to detect the luminescence of fingermarks recently [23-25]. However, it is not a new technique but one developed by Murdock and Menzel in the 1990s [26]. TR spectroscopy is a method which utilizes the difference in luminescence lifetime between a substrate and a sample [27]. Luminescence lifetime is the average decay time of the luminescence emitted by a molecule after excitation with a short laser (or other light resource) pulse [25]. It has been extensively applied in biology, but not widely used in fingermark detection. So far the TR technique has been successfully applied to fingermark development with milli-, micro- and even nanosecond resolution.

Generally the TR technique needs complex and expensive devices such as laser, CCD camera, image intensifier, programmable timing generator, and so on. This greatly limits the application of the TR technique, but it does have a significant advantage. It can address the issue caused by background luminescence interference.

A more complicated technique named the phase-resolved (PR) technique was also applied with the similar theoretical principle [28, 29]. The PR technique is based on the phase shift that occurs in luminescence emissions. In this method, the sample (fingerprint) is excited with an intensity-modulated laser. The luminescence emissions from the sample and the background will be phase shifted with respect to the excitation. Then the heterodyne technique is applied to acquire the frequencies of different emissions from the fingerprints and the background. The heterodyne signal obtained will be further processed to resolve the phase information by mixing it electronically with a square wave pulse. Finally, the fingerprint is "separated" from the background. The PR technique can image the luminescence emission even when the fingermark's luminescence lifetime is shorter than that of the background, which is not at all possible with the TR technique. Moreover, the PR technique offers better contrast for fingermark detection than the TR technique [28]. However, the PR technique also faces many of the same disadvantages as the TR technique, which limits its further application.

1.2.2.4. Europium (Eu) related techniques

Allred and Menzel used an Eu-bioconjugate method to detect sebaceous fingerprints [30]. First, ethylenediaminetetraacetic acid (EDTA) was applied as a conjugating ligand that formed a non-luminescent complex with the Eu ion. The complex then covalently reacted with the lipids of the latent fingerprint. In the reaction process, additional sensitizing reagents, such as 1, 10-phenanthroline and thenoyltrifluoroacetone (TFA), were added to replace EDTA which finally led to the production of luminescence. A spray method was applied to fingerprints on a variety of porous and non-porous surfaces including brown paper, cardboard, smooth wood, rough wood, cloth, metal and clear plastic. The treated fingerprints were observed

under the excitation of near-ultraviolet (UV). Only poor fingerprints were seen on the rough wood and cloth, but good fingerprints with detailed ridges could be found on the other surfaces.

Wilkinson explored a one-step fluorescent Eu chelate, whose generic formula can be represented as Eu(organic ligand)$_3$ 2(synegic reagent), to develop lipid fingermarks on porous and non-porous surfaces [31]. Several chelates and synegic reagents were evaluated, but europium tri(thenoyltrifluoroacetone) (thenoyl europium chelate; TEC) with trioctylphosphine oxide (TOPO) was found to achieve the best results. The exhibits were dipped in the TECTOPO solution to develop the fingermarks and the compatibility of the technique with sequential methods such as ninhydrin and DFO was also studied. The results showed that TECTOPO was very good for recovering fresh fingermarks, but inferior to a physical developer (PD) for the detection of aged fingerprints. Moreover, Wilkinson and Watkin also attempted to use a europium complex to detect fingermarks on human skin, but few positive results were acquired [32].

Lock *et al*. used Eu chelate as a fluorescent dye for CA fumed fingermarks [33]. Five Eu reagents were tried for the post-CA treatment of fingermarks, but Eu ThenoylTrifluoroAcetone ortho-Phenanthroline (EuTTAPhen) was determined to be the most efficient complex. The EuTTAPhen was then applied to fingermark detection on a variety of non-porous surfaces and mixed with Basic Yellow 40. The result showed that EuTTAPhen was an excellent reagent with strong luminescence and a big Stokes shift (262 nm), and could be used with other common CA dyes, such as Rhodamine 6G and Basic Yellow 40.

1.2.2.5. Other luminescence techniques

In 1990, Meylan *et al*. introduced a gaseous electrical discharge method to induce luminescence in latent fingermarks [34]. A gaseous electrical discharge (20,000 V), followed with the vapours formed by heating ammonium hydrogen carbonate, induced UV excited luminescence in latent prints. Good visibility with a bluish-

white luminescence was achieved on a number of surfaces. The technique was effective on both fresh prints and prints aged for several weeks, and developed prints even remained luminescent for over a year after initial treatment. The method did not prohibit the subsequent application of conventional fingerprint development techniques. In addition, it can be used to induce luminescence in prints developed with CA.

Davies *et al.* conducted experiments to investigate the principle of the electrical discharge approach [35]. Similarly, they exposed the fingermark residue to a gaseous electrical discharge in nitrogen followed by treatment with ammonium hydrogen carbonate vapours to produce luminescence. They used a laser illumination at 514 nm instead of UV. After that, the fingermark residues were separated by thin-layer chromatograph (TLC) and analyzed. The result indicated that the luminescence observed was from the previously non-fluorescent fractions of the fingermark residue, and lipid derivatives were possible sources of the luminescence.

Interestingly, Worley *et al.* selected micro-X-ray luminescence (MXRF) imaging/mapping to detect fingermarks [36]. They used the spatial imaging of inorganic elements existing in fingerprint residues, mainly potassium and chlorine. The result showed that fingermarks containing sweat, lotion, saliva, and sunscreen could be detected by MXRF.

1.3. Upconversion (Anti-Stokes Luminescence)

Anti-Stokes luminescence or upconversion was discovered independently by Auzel and Ovsyankin and Feofilov in the mid-1960s [37]. Anti-Stokes luminescence is a luminescence process contrary to conventional Stokes luminescence. In most cases, during the process, some special materials absorb two photons from an intense radiation source with energy-transfer from a host metal ion to a dopant, followed by the emission of a single photon. The process can be complicated and several mechanisms are well established, but the net result is the absorption of long-wavelength illuminating radiation and the emission of a shorter-wavelength photon (**Figure 1.3**; **Figure 1.4**). This process is also called photon upconversion or upconversion. Upconversion mainly exits in rare-earth complexes. Some

commercially available upconversion materials exist and are often known as upconverters (UCs). For example, Artemis Chemicals Company (UK) supplies five kinds of UCs with various emission colours. They emit in the blue (UC-B), green (UC-G), yellow (UC-Y), orange (UC-O) and red (UC-R) regions of the visible spectrum with infrared (IR) 980 nm excitation [38].

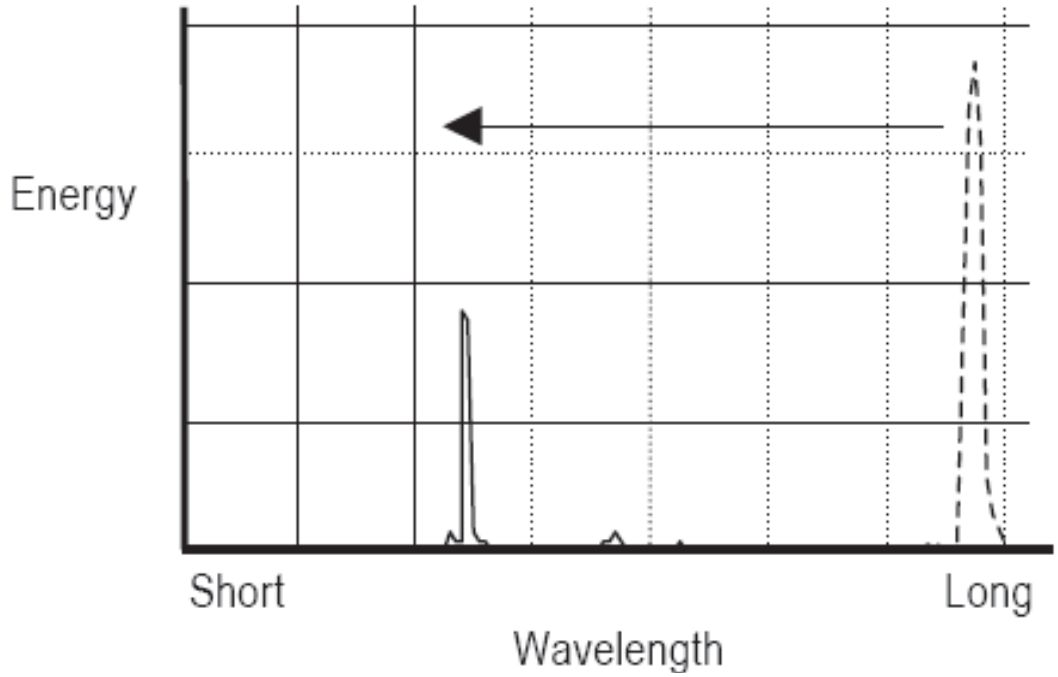

Figure 1.3. Schematic representation of anti-Stokes photoluminescence; Stokes shift is considered negative [39].

Heer *et al.* described a method for synthesizing $NaYF_4$ codoped with Er^{3+} and Yb^{3+} ions, which has the highest upconversion efficiencies known today [40]. They also succeeded in dispersing it into a transparent colloid solution, which is important for the application of biolabelling, but difficult to do considering the submicrometer to micrometer-size of the crystal. Moreover, they found that upconversion intensity of the complex in the colloid state is 10^2-10^3 times higher than in the solid state because of the abundant existence of a cubic α-phase in the crystal which is about an order of magnitude less efficient than the corresponding hexagonal β-phase.

Since $NaYF_4$ is one of the most efficient hosting materials, many scientists pay much attention to it. Wang *et al*. reported a method for one-pot synthesis of

polyethylenimine(PEI)/$NaYF_4$ (UC-PEI) nanoparticles [41]. The UC-PEI showed great potential for use in biological labelling and imaging. The amino groups of PEI attached to the UC core made the whole complex soluble in water and biocompatible. The average size of the nanoparticles was about 50 nm and they had a spherical shape. Different lanthanide ions (Yb^{3+}, Er^{3+} and Tm^{3+}) were also doped into the nanoparticles to check the luminescence property. Under excitation at 980 nmby a powerful laser all the three showed strong upconversion luminescence of different colours in aqueous solutions.

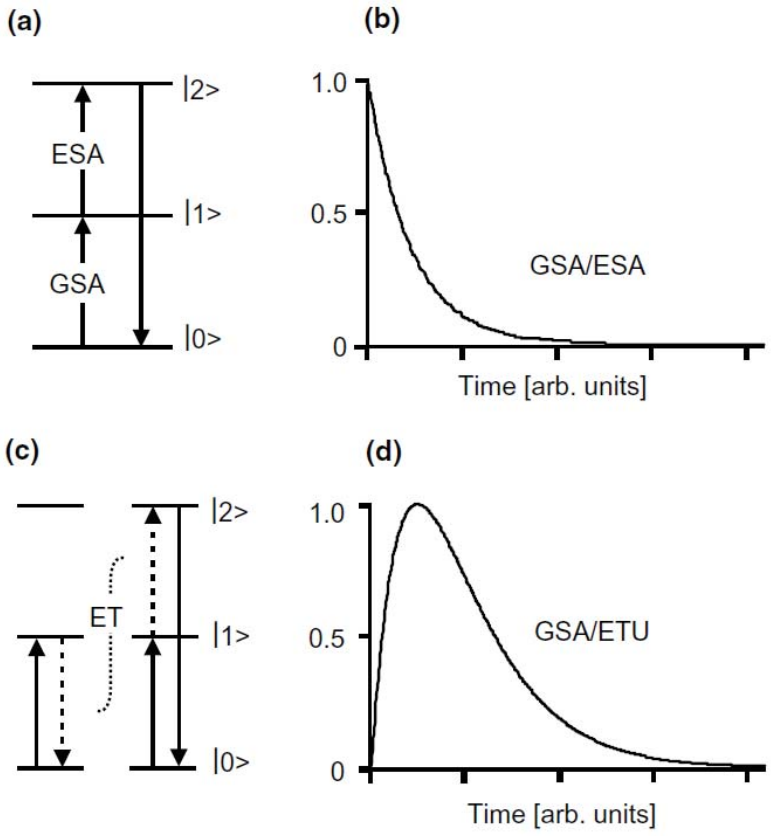

Figure 1.4. Schematic representation of the two most prominent UC mechanisms: (1) ground-state absorption (GSA), excited-state absorption (ESA) and (2) ground-state absorption (GSA), energy transfer upconversion (ETU). The dotted arrows represent non-radiative energy transfer (ET) processes. The straight arrows indicate radiative transitions. The transients indicated in (b) and (d) describe the time-evolution of the emission of the upconversion luminescence after a short excitation pulse [37].

In 2005 Suyer *et al*. gave an overview of the upconversion spectroscopy of $NaYF_4$ nanoparticles doped with lanthanide ions [37]. First, the near-infrared (NIR) to visible efficiencies for $NaYF_4$, one of the most efficient lattice known to date, were discussed when codoped with Er^{3+}, Yb^{3+}/Er^{3+} or Yb^{3+}/Tm^{3+}, respectively. The result shows that the $NaYF_4$:2% Er^{3+},18% Yb^{3+} is an efficient UC because about 50% of all NIR excitation energy are converted to the upconversion emission with two most significant bands in the visible. However, the $NaYF_4$:0.3% Tm^{3+}, 25% Yb^{3+} is much worse in the NIR to visible (mainly blue/violet) UC efficiency which is only about 2%). Similarly, the UC efficiency of the samples only doped with Er^{3+} is also much lower than the Er^3/ Yb^{3+} codoped samples. In $NaYF_4$ crystal, the hexagonal β-phase has much higher emission efficiency than the cubic α-phase. Moreover, the two above complexes showed strong visible upconversion spectroscopy in their nanocrystalline solutions. It could be extremely important in the future application of nanolabels or biolabels. Finally, the mechanism of mixed transition metal/rare-earth systems was also described. The rare-earth ion is the sensitizer and upconversion occurs on the transition metal ion.

Pires *et al*. studied Y_2O_3 and Y_2O_2S—two different Y^{3+} hosting materials or matrixes [42]. Different precursors including polymeric resin, oxalate and basic carbonate were used to acquire UCs with different percentages of Er^{3+} and Yb^{3+} as doping ions. The upconversion luminescence spectra were recorded at 298 K for all the doped samples in the visible region. The upconversion efficiency was also measured and the green/red emission relative intensity was compared as well. The result showed that the upconversion luminescence was affected enormously by the doping ion concentration, particle size and host lattice.

Recently, Bai *et al*. investigated the infrared-to-visible upconversion luminescence in Li^+ and Er^{3+} codoped Y_2O_3 nanocrystals [43]. They found that Li^+ ions can greatly enhance the intensity of upconversion luminescence in the Y_2O_3 matrix. The possible reason for this increase is believed to be the modification of the local crystal field and the homogeneous distribution of the Er^{3+}caused by the Li^+ ions. Similarly, doping Li^+can also increase the upconversion intensity of Er^{3+} ions in some other Er^{3+} doped oxides, such as ZnO, ZrO_2, etc.,.

Although most of the UCs are inorganic compounds consisting of rare-earth metal, some organic UCs have been reported. Zhuo *et al*. synthesised a new organic dye trans-4-[p-(N-ethyl-N-hydroxyethylamino)styryl]-N-methylpyridinium iodide (abbreviated as HEASPI). This HEASPI has a large two-photon absorption (TPA) cross section leading to excellent upconverted properties [44]. The upconversion luminescence was excited by a mode-locked Nd :YAG picosecond laser with a pump energy[1] [45] of 2.07 mJ. The net upconversion efficiency can be as high as 19.6%. Moreover, Zhao *et al*. also found metal-to-ligand upconverted luminescence from pyrene and di-tert-butylpyrene using Ir(ppy)3 as triplet sensitizer [46].

1.4. Possible Approaches to Use UCs in Fingermark Detection

Upconversion luminescence has been widely employed in security ink [47]. It is increasingly used in biolabels or nanolabels [37]. Upconversion is unusual in both natural surfaces and in consumer products [38]. If the UCs are applied for fingermark detection and show selective affinity to fingermark materials rather than the background, theoretically the strong luminescence of the UCs can be visualised on fingermarks as bright regions on a total dark background. This means that fingermark detection techniques using UCs can eliminate the interference of the background printing, pattern and luminescence. As the result, fingermark detection techniques based on UCs are potentially extremely sensitive and selective.

[1] The pump energy in laser refers to the incontinuous energy transferred from the external source into the gain medium of a laser to produce the laser beam.

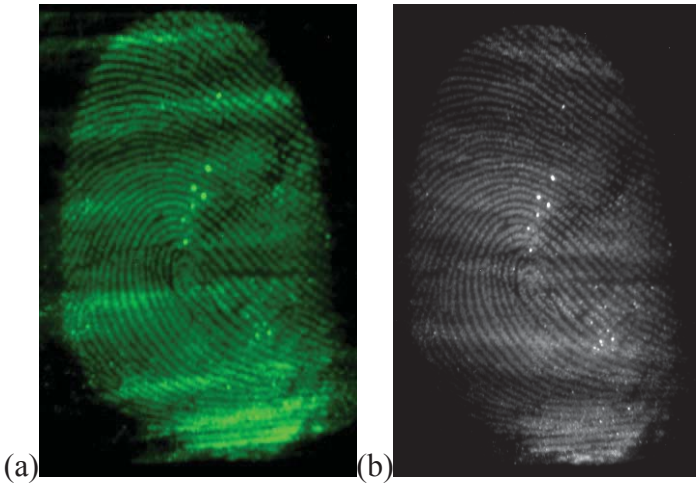

Figure 1.5. UC-G powder developed latent marks (a) viewed using a low pass filter (b) viewed using a 513 nm centred band pass filter. 980 nm excitation and 10.19 x magnification by a Visual Spectral Recorder [(VSC) it was not mentioned on what substrate the fingermark was developed] [38].

Bullock investigated the use of UCs emitting in the blue, green, yellow, orange and red regions for the detection of latent fingermarks [38]. The best performing phosphor was the UC-G powder, as it gave the most intense luminescence and adhered well to the fingermarks (**Figure 1.5**). It was also found that most surfaces revealed little to no background development. Imaged fingermarks showed good ridge detail without providing tertiary-level detail when used as dry powder. However, the main drawback was their inability to be used as a stain or a wet powder. To overcome some of the disadvantages described above, three possible directions will be proposed in this thesis.

1.4.1. UCs as a dry powder and as a suspension

Previous work showed that UC phosphors were effective for fingermark detection. The background showed no anti-Stokes luminescence and the strong luminescence of the phosphors could be seen on these backgrounds as bright images on a black background. However, this potential should be fully explored and compared with

traditional fingerprint powders. Besides this, the possibility of using an UC as a suspension is also investigated.

The idea of employing an UC as a suspension may come from the successful application of small particle reagents (SPR) and sticky-side powder [1, 48]. The principle of suspension is to disperse UCs into solvents with the help of surfactants or other coating reagents such as silica. Compared to dry powdering, the suspension or wet powdering method is probably a more flexible method achieving better results on some difficult surfaces, for example, the sticky side of adhesive tapes or water-dipped surfaces [1]. In order to obtain an ideal suspension, the accurate physical properties of UCs, including size, grain structure, electric charge etc. should be known. Research should also be conducted into identify the most appropriate surfactants. There are thousands of surfactants in existence that show a large variability in their physical and chemical characteristics. For example, emulsifiers and suspending agents are entirely different in application. In addition, finding an appropriate solvent to disperse UCs is also a challenge. A water solution may be the preferred method to dissolve UCs, but polar and non-polar organic solvents should be tried as well.

1.4.2. UCs of smaller particle size for inserting in CA fumed (CAF) fingermarks matrices

CAF is universally used in fingerprint laboratories and probably the most important technique for fingermark detection on non-porous surfaces [1]. CA ester (generally the ethyl ester) liquid forms a vapour that reacts with certain eccrine and sebaceous components in a latent fingerprint. The vapour selectively polymerizes on the fingermark ridges to form a hard, white polymer known as polycyanoacrylate [1]. The size of the holes in CA polymer is approximately 1 to 2 micrometres [49]. As a result, if the size of the UC is smaller than the size of those holes in the CA polymer, it can go into and may stay inside the polymer and become an ideal staining reagent.

However, the size of many commercial UCs is much bigger than that of the holes in the Polymer, according to the previous research. Hence these big UC particles can only stay outside the CA polymer. There may be several methods to get smaller UCs. One possible option is to synthesise UCs under controlled conditions, while another option is to ground UCs by mechanical mills or separate them by sieves. However, the luminescence properties of a material are related to its size. Once we achieve UCs with smaller sizes, we may see a change in the emission spectra. This will need to be carefully investigated.

There is much literature that describes synthesising UCs under controlled conditions. Li *et al*. developed an efficient method for the synthesis of uniform hexagonal-phase $NaYF_4$: Er,Yb/Tm nanocrystals by forming small solid-state crystal nuclei and further growth and ripening of the nuclei. $NaYF_4$: Er,Yb/Tm nanoplates, nanospheres and nanoellipses were selectively produced by varying the concentration of the surfactant [50]. All the nanocrystals showed strong upconversion luminescence under laser illumination. These nanocrystals have great potential for use in biology image probes, and in our opinion, they could be applied to CA-fumed fingermark staining.

1.4.3. Functionalised UC nanoparticles

Coated, modified, or functionalised powders have attracted great attention from fingerprint scientists [2, 8, 9, 18-21]. To use functional molecules to coat or modify UCs is undoubtedly an interesting approach. Because UCs are notoriously insoluble in water and other solvents, this disadvantage seriously limits their application for staining CA-fumed fingermarks. Since CAF is probably the most used technique in laboratories for fingermark detection on non-porous surfaces, it is worth investigating the possibility of making UCs soluble or dispersable in water by functionalizing them with hydrophilic groups.

Recently there have been numerous papers published on functionalised UCs. As we described above, Wang *et al*. used a one-pot synthesis to attach an organic

surfactant molecule, polyethylenimine (PEI), to $NaYF_4$:Er,Yb(Tm) UC particles [41]. The TEM image showed that the PEI/$NaYF_4$:Er(Tm),Yb complex had an average size of 50 nm and the amino groups of PEI endowed the complex molecule solubility in water. The luminescence spectra also showed that the doping PEI molecule did not change the upconversion luminescence. However, the new water-soluble complex showed great potential for use in biological labelling and imaging, and certainly it could be applied to fingermark detection, especially for CA-fumed fingermark staining.

Li *et al*. used an amphiphilic surfactant, pyrrolidone (PVP) attached to $NaYF_4$:Er,Yb UC nanocrystals [51]. The PVP/$NaYF_4$:Er,Yb (UC-PVP) nanocrystals are polyhedral in shape and very uniform in size, with an average size of about 30 nm, and can be well dispersed in some of the most commonly used solvents, from weakly polar chloroform to strongly polar water. Strong green and red luminescence was observed from these nanocrystals under the excitation of a 980 nm NIR laser. Furthermore, the authors also coated these UC-PVP nanocrystals with silica to improve the photostability and biocompatibility Both the silica-coated and uncoated PVP/$NaYF_4$:Er,Yb nanocrystals showed great potential for fingermark detection since they were well dispersed in common solvents and strong upconversion luminescence.

Chen *et al*. developed a simple and versatile strategy to attach oleic acid to upconverting rare-earth nanophosphors (UCNPs) [52]. This oleic acid ligand was then oxidized to carboxylic acid directly by Lemieux Rufloff reagent. The carboxylic acid-functionalised UCNPs were water-soluble and showed strong luminescence under the illumination of 980 nm laser. These biocompatible UCNPs could be ideal reagents for CA-fumed fingermark staining.

Hu *et al*. converted hydrophobic upconverting rare-earth nanophosphors (UCNPs) into amphiphilic ones based on epoxidation of the surface oleic acid (OA) ligand and further coupling with polyethylene glycol monomethyl ether (m-PEG-OH) [53]. The amphiphilic m-PEG-UCNPs showed strong upconversion luminescence and could be a potentially promising reagent for fingermark detection.

Although these functionalised UCs could be ideal reagents for biolabelling and fingermark detection, it should be noted that they are not exhaustive and other attempts may be tried such as doping other possible elements to the known UCs and looking for, or synthesizing, new efficient UCs.

1.5. Conclusions

Because of their high sensitivity, luminescence techniques are always among the most important fingermark detection methods. However, it often occurs that background surfaces produce an emission at the same wavelength as, or very close to, the wavelength emitted by a treated or untreated fingermark. This cannot be solved with the conventional fluorescent techniques, but upconversion may be the solution. UCs exhibit anti-Stokes luminescence, which is unusual in both natural surfaces and consumer products. This means that fingermark detection techniques using UCs are potentially extremely sensitive and selective. And this has been tested in the preliminary study we described above.

This thesis presents the results of work towards the goals. Imaging upconverted fingermarks is described in Chapter 2. Chapters 3 and 4, respectively, illustrate the application of fingermark detection using two types of UC particles: $NaYF_4$: Er,Yb and YVO_4:Er,Yb. The investigation into achieving smaller particles is presented in Chapter 5. The synthesis and application of functionalised UCs are discussed in Chapter 6.

Chapter 2:

Imaging for Upconversion Luminescence

Chapter 2. Imaging for Upconversion Luminescence

2.1. Introduction

The process of photon upconversion is a way of converting long-wavelength excitation radiation into shorter wavelength output radiation. Upconversion is one of the most studied nonlinear optical processes [37, 54], and there is a variety of well-established UC mechanisms. The majority of these involve absorption and non-radioactive energy transfer steps. Early studies mainly used UC phosphors as coatings for IR sensor cards or IR quantum counters [37, 47, 54]. The recent discovery of UC in a transparent colloidal solution is an important first step towards the development of functional materials, with considerable application potential as luminescent markers for immunoassays and bio-imaging in fluid media [37]. Recent studies using UCs as fingermark detection reagent also reveal their great potential in this area [55]. However, the upconversion process is not as efficient as conventional luminescence using the Stokes shift, as it needs to be excited by high intensity light [54, 56]. As a result, a laser system is preferable for the illumination for fingermarks developed by UCs and a suitable imaging system is required for capturing results. These topics are discussed below.

2.2. Materials and Methods

2.2.1. General

Fingermarks were detected using $NaYF_4$: Er,Yb UC powder by dry powdering method only to test the effectiveness of different light sources and image recording devices. $NaYF_4$:Er,Yb powder (Artemis Limited, UK) were used as received. Two

donors supplied latent fingermarks for this work. Fingermarks were deposited after the donors wiped their fingers over their forehead or facial area just prior to fingermark deposition and used for detection in two hours after they were deposited. $NaYF_4$: Er,Yb powders were applied to fingermarks using squirrel brushes (Optimum Technology, Australia). Two surfaces, glass (microscope slides) and plastics (polyethylene bags) were investigated.

Safety goggles（a Dioptika LG 001S OD 7+ and LG 001 OD 7+ laser glasses) were worn to prevent IR light from entering the eyes. An IR display card, made to show the laser beam (since IR light is invisible to the naked eye), was also employed. Laser warning signs were placed on the door of the dark room warning other people from entering.

2.2.2. Comparison of Different Light Sources

The $NaYF_4$: Er,Yb powder-developed fingermarks were illuminated with white light (for conventional reflection mode imaging), by a modified Polilight PL-10 (Rofin, Australia), a laser diode (a Roithner RLDH-980-200-3), a laser pointer (Techlasers Enforcer) and a Crime-Lite ASV (Foster and Freeman, UK) respectively (for upconverting mode imaging). The laser diode and the laser pointer operated at a wavelength of 980 nm and the Crime Lite at 976 nm. Both wavelengths are within the range that stimulate the upconverters considered.

The Roithner RLDH-980-200-3 laser diode had a maximum 200 mW output. It was connected to a DC power supply (TTi, England). Two C cell batteries purchased from local supermarkets were used to provide electricity for the Techlasers laser pointer. The laser output power was measured using a laser power meter (Laser Check, Edmund Optics Inc).

Images were recorded using a Rofin Poliview (Rofin Australia Pty. Ltd.). When imaging in upconverting mode, a 555nm band pass filter with bandwidth of 28nm

(type 702.0212, manufactured by Rofin, Australia) was put in front of the lens to block the IR light from the laser.

2.2.3. Comparison of Different Image Recording Devices

The $NaYF_4$: Er,Yb powder-developed fingermarks were illuminated with a laser pointer (Techlasers Enforcer), then recorded using a Rofin Poliview (Rofin Australia Pty. Ltd.), a video spectral comparator (VSC 2000/HR; Foster and Freeman, UK) and a Canon EOS 450 D single-lens reflex (SLR) camera.

2.3. Results and Discussion

2.3.1. The Wavelength and Intensity of Laser Applied for UC Illumination

The UC powders used in this project required a low energy wavelength of 980 ± 5 nm [37, 38]. Such wavelengths were needed owing to the small distances between energy levels and f-f transitions [38, 57]. The correct excitation energy was required for the absorption and transfer of energy in order for luminescence emission to occur.

The intensity of the light source is fundamental for the excitation of the phosphors. This is owing to the multi-photon absorption during excitation, requiring at least double the photon input as that of the expected output. Most lanthanide (or rare earth metal) ions are not great light absorbers, too [38]. Upconversion often has high efficiencies at very low temperature (for example, 15K) and the efficiency drops dramatically when temperature increases [37]. However, in our research, only upconversion at room temperature is meaningful which more powerful light resources are needed. Therefore, the light source requires a high intensity of greater than 80 mW. This is the cut-off point below which no significant luminescence emission can be visualized [38].

2.3.2. Comparison of Different Light Sources

2.3.2.1. Modified Polilight forensic light source

The first attempt at finding a suitable excitation source was to modify a Polilight PL-10, a high-intensity filtered light source specially developed for use in forensic science. An interference long-pass filter was used to isolate the IR output, with approximately 3 to 4 optical watts of light output achieved for wavelengths longer than 900 nm as measured. The IR output was via a 2-metre fibre light guide from the side while the original port and guide (in the front) for UV and visible light were untouched. An adjust cap was assembled in the front of the light guide with a 38mm diameter aperture in order to get a large light spot to illuminate the developed fingermarks.

However, the result from this modified Polilight was not promising. Although green upconversion luminescence for $NaYF_4$: Er,Yb UCs could be observed with the naked eye using the illumination of the Polilight, it was weak. Clear luminescence images could not be seen and photographed under the Polilight for fingermarks developed with UCs (**Figure 2.1**). It was assumed that the needed IR light (around 980 nm) only occupied a small portion of the total IR light that the modified Poligiht produced and the power output of IR light around 980 nm was much less than 80 mW, the threshold power output.

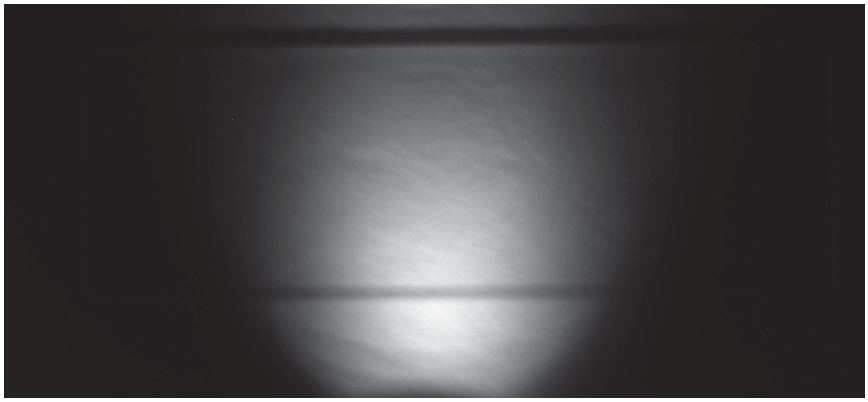

Figure 2.1. Fingermark developed by $NaYF_4$: Er,Yb UCs and then illuminated by the modified Polilight. No fingermark detail can be seen under this illumination.

The heat side-effect was also enormous in that the plastic samples would bend and burn under long exposure times (approximately ≥30 seconds) with illumination from the modified Polilight. The heat side-effect may be due to the large power output (3 to 4 optical watts of light output achieved for wavelengths longer than 900 nm). Second, the IR has an intrinsic "heat effect". The heat may also consist of a large proportion of the total energy at around 980 nm. In summary, the modified Polilight is unsuitable as a light source to excite the luminescence of the UCs under consideration.

2.3.2.2. Laser diode

The Roithner RLDH-980-200-3 laser diode with a maximum 200 mW output was used at the beginning of this project. It was connected to a DC power supply (TTi, England, **Figure 2.2**). The operating voltage should be set at 3 V all the time and the current should not exceed 0.25 mA avoiding damage the laser diode.

However, it was found that the power output of the laser diode was not 200 mW as described in the datasheet, but around 100 mW when the current was set at 0.25 mA which was the maximum current suggested by the manufacturer. The power output decreased to 30 mW when the electric current was set at 0.15 ampere which was often used in the previous research [38]. Thus, the use of 0.25 mA was applied with most of the experiments.

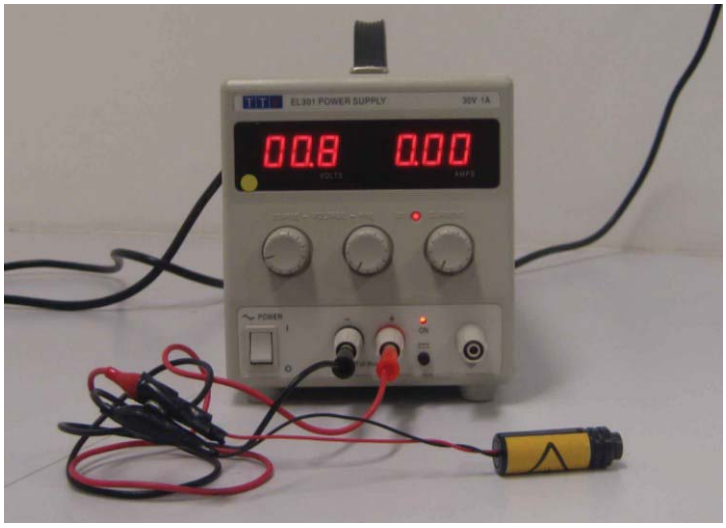

Figure 2.2. Laser diode with power supply (Roithner Australia).

The laser diode can excite the luminescence of the $NaYF_4$: Er,Yb developed fingermarks. However, the luminescence of the developed fingermarks illuminated by the diode was not strong. The fingermark images were often incomplete owing to the small aperture of the diode unless very long exposure time (> 5 seconds) was employed.

2. 3.2.3. Laser pointer

In this project, a Techlasers Enforcer laser pointer (**Figure 2.3**) was used most of the time, with two C-cell batteries as the power source. In theory, the maximum power output was 700mW. However, with the gradual depletion of the batteries, the power output would drop dramatically (from 700 to 100 mW). Therefore, full batteries were used all the time. The light aperture of the laser pointer was around 7 mm x 7 mm, which was also much bigger than the laser diode.

Figure 2.3. Laser pointer (Techlasers, Hong Kong).

The power output of the pointer was much higher than that of the diode. Accordingly, the luminescence intensity of developed fingermarks excited by the pointer was much greater than that achieved with the diode. **Figure 2.4** shows the same fingermarks developed by $NaYF_4$: Er,Yb dry powdering and then illuminated respectively by the diode (A) and the pointer (B) using the Rofin Poliview system with the same exposure time. The luminescence emission when illuminated by the pointer was clearly much brighter than that was observed with the diode. Due to this advantage, the laser pointer was used as the light source for most of the experiments described in this project.

Laser scanning and long exposure time

Because the light aperture of both the diode (approximately 1 mm x 5 mm) and the pointer (around 7 mm x 7 mm) was very small and the fingermark area was much bigger, during the imaging process the laser diode or pointer had to be scanned across the fingermark area. Because there was no mechanical system available, this had to be done manually. Long exposure times (generally from several seconds to less than one minute) were also employed because the laser spot was much smaller than the fingermark area. Another solution to replace the manual scanning is to employ a very powerful laser with a power output to several or tens of watts, and enlarge its aperture to ideal size, for example, the size of a palm print. However, in this case a separate room has to be allocated due to the safety protocols of UTS. The cost would increase dramatically and the application and setup process is also time-consuming. All the above made this approach with powerful lasers impossible in the limited time of this PhD project.

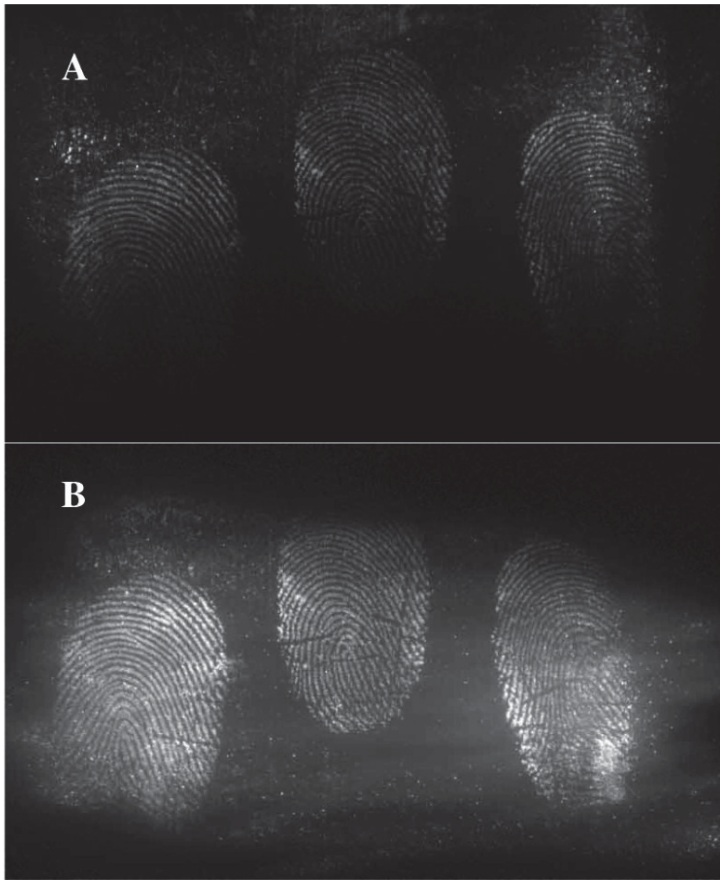

Figure 2.4. The same fresh fingermarks on plastic developed by $NaYF_4$: Er,Yb dry powdering, under the illumination of a 980 nm laser diode (**A**) and pointer (**B**) and observed using a Rofin Poliview system with the 555nm band pass filter and 5 s exposure time.

2.3.2.4. The Crime-Lite ASV from Foster & Freeman

The Crime-Lite ASV is a bench-mounted laser viewing enclosure for the stimulation of UC fingerprint powders (**Figure 2.5**). It has two 6-Watt 976 nm lasers inside and a large laser illumination area (45 mm x 60 mm). It also has a 45mm x 60 mm laser blocking fingerprint viewing/imaging window. It is specially designed for the illumination of specimens treated with UCs. **Figure 2.6** shows fingermarks on glass developed by $NaYF_4$: Er,Yb dry powdering, under the illumination of the Crime-Lite ASV and imaged using a Canon SLR camera.

Figure 2.5. The Crime-Lite ASV (Foster and Freeman, UK).

Figure 2.6. Fresh fingermarks on glass developed by $NaYF_4$: Er,Yb dry powdering, under the illumination of The Crime-Lite ASV and imaged using a Canon EOS 450 D SLR camera with F 5.6 and 2.0 second exposure time.

However, the ASV has no computer connection with an image processing software, making it impossible to see real-time images. Being able to view real-time images is important as, without them, it is difficult to decide on the appropriate exposure time for fingermarks developed by UCs. Quite often, the fingermark images acquired were overexposed as shown in **Figure 2.6** because of the powerful built-in lasers. Also, due to the enormous heat effect of the powerful lasers, it is not suitable for the illumination of fingermarks on plastic, paper and other substrates that have a low ignition point. A plastic sample was damaged even with an exposure time

of about one second (**Figure 2.7**). Currently the switch-on and –off button was only controlled manually which made the long-time exposure (seconds) of fingermark samples to the laser inevitable.

Figure 2.7. A plastic specimen that was deformed by the heat produced by the Crime-Lite ASV.

Table 2.1 shows the comparison of light sources used in this project. The results proved that all light sources can excite the luminescence of UC-developed fingermarks except the modified Polilight. The laser pointer was the best light source under current conditions.

Table 2.1. Comparison of different light sources

	Laser diode	Laser pointer	Modified Polilight	Crime-Lite ASV
Intensity of laser	weak	good	very weak	Very strong
Effectiveness for fingermark detection	Below satisfactory because of weak luminescence intensity and small aperture.	Good, but long exposure times and manual scanning were generally employed.	Unable to develop any satisfactory fingermarks developed with UCs.	Laser was too powerful; fingermarks were often overexposed and samples with low ignition points were destroyed.

2.3.3. Recording Device

2.3.3.1. The Rofin Poliview system

A Rofin Poliview system was the most used imaging set-up in this project to record the luminescence of the fingermarks developed by UCs (**Figure 2.8**). The Poliview is a forensic imaging system that offers the fine tuning of light bands both for illumination and observation over the range 350–1100 nm (UV-Vis and near-IR).

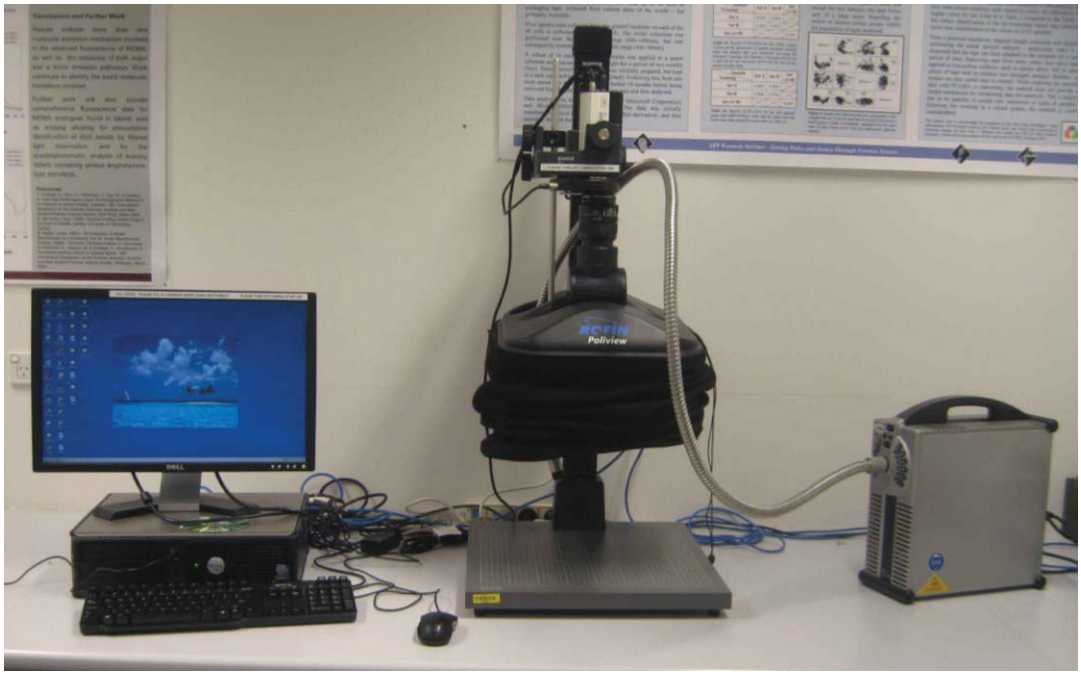

Figure 2.8. The Rofin Poliview system

Properties of the Poliview system

The Poliview system includes a colour (RGB) liquid crystal filter slider that is designed to slide in and out of the optical path. This allows the user to select monochrome (black and white) or full colour images. Luminescence images should always be captured in monochrome according to the manufacturer.

The Poliview system camera, with a resolution of 1024 x 1280 pixels, has selectable 12 bit and 8 bit pixel depth resolution. When 12 bit is selected, each pixel has a grey scale of 4096, while 8 bit is 256. This means that each pixel can have

4096 or 256 possible levels of grey (or colour with the colour module). Software features enable these levels to be seen by the eye.

The Poliview achieves the best sensitivity by eliminating all stray light and cooling the CCD by a Peltier cooling technique. Peltier cooling is electronic cooling (not water or gas) and, importantly, allows for long exposure times for up to several minutes without the interference that would otherwise result from thermal electronic camera noise.

The Poliview provides variable electronic CCD camera exposure allowing samples to have long integration exposure times into the minutes which is crucial for upconversion luminescence imaging.

The Poliview uses special software to provide a full computer screen live display. When electronic integration is selected, an integrated live image is displayed and updated. Several real-time overlay comparison features are provided. The biggest advantages of the Poliview are that real-time images can be seen on the computer screen and the exposure time can be adjusted by the software until ideal images are achieved.

There are over 100 digital imaging functions within the Poli-V®++ forensic software that is provided with the Poliview system. Common routines include brightness and contrast adjustment, and sharpening and smoothing filters that are essential for upconversion luminescence imaging.

All of the above features made the Poliview the most ideal system, of those available for this research, for the imaging of upconverted fingermarks. However, because the CCD that the Poliview employs is sensitive to IR light, a 555 nm band-pass filter with a bandwidth of 28 nm (type 702.0212, manufactured by Rofin, Australia) was put in front of the lens to block the reflected IR light from the laser. The passing wavelength (541-569 nm) of this filter also corresponds to the emission maximum of the UCs used in this project. **Figure 2.9** shows fingermarks developed by $NaYF_4$: Er,Yb powder that were imaged with and without the 555 nm band-pass filter, respectively. It can be seen that, without the filter, the reflected IR light

resulted in significant background interference and good ridge detail and contrast could not be achieved (**Figure 2.9**).

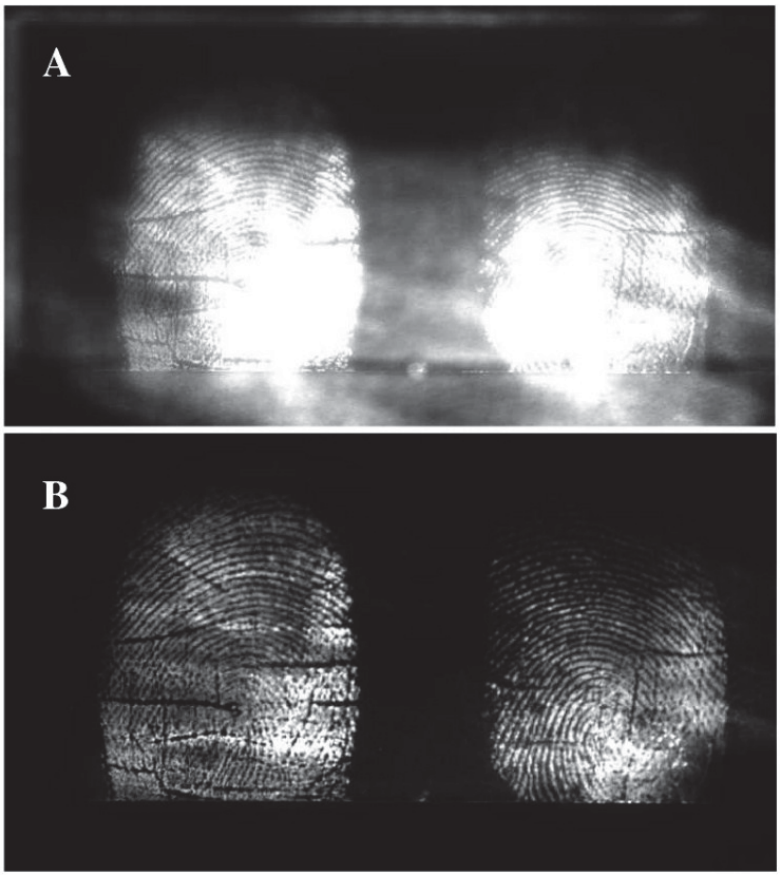

Figure 2.9. Fingermark developed by $NaYF_4$: Er,Yb powder and illuminated by laser pointer, imaged under the Poliview without the 555nm band pass filter showing the interference from the IR light (**A**) and with the 555 nm band pass filter (**B**).

2.3.3.2. Video Spectral Comparator (VSC)

In previous research at UTS, a Video Spectral Comparator (VSC2000/HR) was employed to record fingermarks in the upconversion mode [38] (**Figure 2.10.A**). After the fingermarks were developed, the samples were placed into the VSC chamber and illuminated with white light to allow the fingermarks to be focused. The white light was then turned off and the VSC set to a low-pass filter and 4 second integration time. The fingermark was then illuminated using the laser diode system (980 nm). The luminescence was photographed and recorded by the VSC2000/HR.

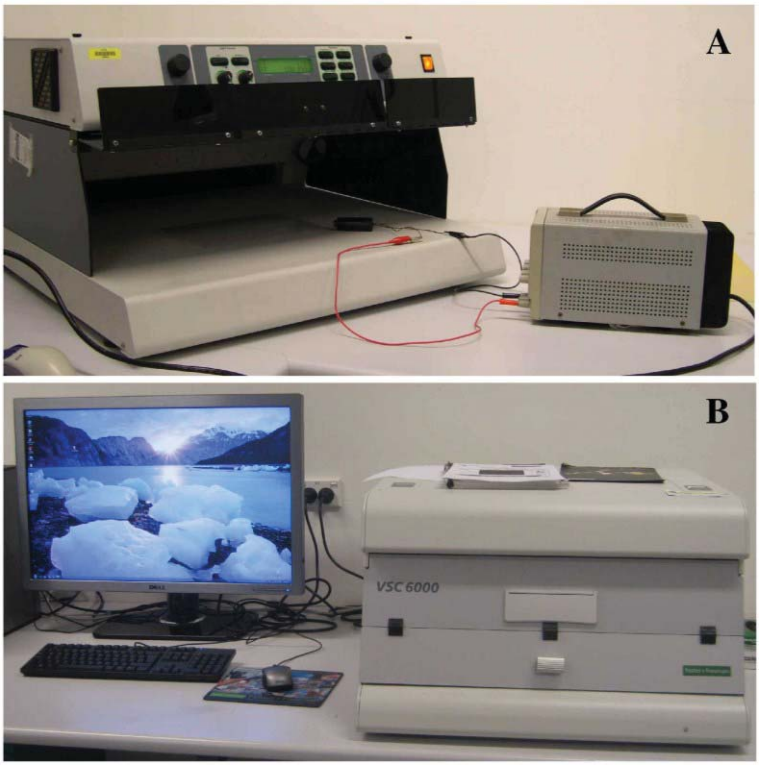

Figure 2.10. Video Spectral Comparator (Foster and Freeman, UK): A. 2000/HR; B. VSC6000.

The new VSC6000 (**Figure 2.10.B**) has an upconversion mode for imaging. However, the fingermark images taken by this method only showed blurred luminescence without clear fingermark detail. Hence, the VSC was not used for fingermark detection in this project.

2.3.3.3. Digital Single-Len Reflex (SLR) camera

A Canon SLR camera was used to photograph the upconverted fingermarks (**Figure 2.11**). Because most cameras have a filter mounted in front of the sensor to block IR light, it is not necessary to use an additional IR block filter or the 555 nm band-pass filter used with the Poliview [7]. The photos acquired by this method depicted a green coloured luminescence as shown in Figure 2.6. However, since most upconversion luminescence is relatively weak compared to normal 'down conversion' luminescence, long exposure times are usually required. Nevertheless, it was not possible to see a real-time image using the Canon digital camera. This

limited the use of the digital SLR camera in the photographing of upconversion luminescence.

Figure 2.11. The Cannon EOS 450 D SLR camera.

Table 2.2 shows the comparison of different recording devices for the recording the upconversion luminescence of fingermarks developed by UCs. The overall result showed that the Poliview was the most satisfactory device followed by the SLR camera, whereas the VSC proved not suitable for the recording of upconversion luminescence.

Table 2.2. Comparison of recording devices

	Poliview	SLR camera	VSC
Advantage	Real-time images; Exposure time easily controlled.	Filter not needed because generally SLR cameras are not sensitive to IR light.	Nil
Disadvantage	Filter needed to block IR light from the laser.	Real time image cannot be seen; Difficult to control exposure time.	No satisfactory image with clear ridges can be seen.
Overall effectiveness for recording UC-developed fingermarks	Good	medium	poor

2.3.4. Safety Measures

Today, it is accepted that even low-power lasers with only a few milliwatts of output power can be hazardous to human eyesight, when the beam from such a laser hits the eye directly or after reflection from a shiny surface. At wavelengths at which the cornea and the lens can focus well, the coherence and low divergence of laser light means that it can be focused by the eye into an extremely small spot on the retina, resulting in localized burning and permanent damage within seconds or even less [58].

The power output of the laser used in this project was from 200 mW to 700 mW. It could burn skin and cause serious eye damage [58]. Strict safety measures were adopted when the lasers were applied to fingermark detection. These measures were in the form of the following:

- Safety goggles (**Figure 2.12**) worn to prevent the IR light entering the eyes;
- An IR display card made to show the laser beam, since IR light (invisible to the naked eye) was being used; and
- Laser warning signs placed on the door of the dark room warning other people from entering.

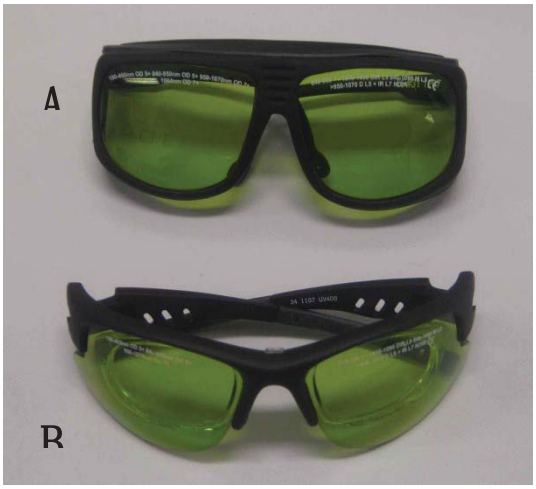

Figure 2.12. Safety goggles (A: Dioptika LG 001S OD 7+ glasses; B: LG 001 OD 7+ laser glasses)

2.4. Conclusions

The successful imaging of fingermarks developed by UCs is crucial in this project. A 980 nm laser pointer with 700 mW output proved to be the most suitable light source for the excitation of the upconversion luminescence. Long exposure times were generally required for the recording of the upconversion luminescence. A Rofin Poliview fitted with a 555 nm band-pass barrier filter was determined to be the most suitable recording system of those available for this research. Safety measures had to be adopted at all times during the experiments to avoid potential eye damage.

Chapter 3

Fingermark Detection on Non-Porous and Semi-Porous Surfaces Using $NaYF_4$:Er,Yb Upconverter Particles

Chapter 3. Fingermark Detection on Non-Porous and Semi-Porous Surfaces Using $NaYF_4$:Er,Yb Upconverter Particles

3.1. Introduction

As mentioned in Chapter 1, fingermark detection techniques based on luminescence are well-established and can be very sensitive on a variety of surfaces [1, 7, 59]. These techniques can provide greater contrast between the developed fingermark and the background compared to non-luminescent methods [1, 7]. However, there are a number of surfaces where conventional luminescence techniques provide poor contrast because of background luminescence. This is due to the fact that many consumer products exhibit luminescence under the conditions used for traditional luminescent fingermark detection techniques [1, 5]. These products commonly have brightly-coloured surfaces containing dyes that are designed to emit broadband luminescence. Printed surfaces with complex, non-luminescent patterns may also be difficult to image because the printed pattern may interfere with the fingermark ridges in the image; banknotes are one example where this problem may arise.

To date, fingermark development studies have focused on luminescent materials that emit light of a longer wavelength than that of the excitation source, i.e., 'traditional' Stokes luminescence. In the current work, we explore the application of anti-Stokes luminescent materials [or so-called "upconverters (UCs)"] for fingermark detection. In these materials, two photons are absorbed followed by emission of a single photon of higher energy (i.e., shorter wavelength). Importantly,

anti-Stokes luminescence is quite rare in most materials and so this provides an excellent opportunity to develop and image fingermarks that are virtually free of background interference. A number of rare-earth complexes have been discovered that can absorb two photons and then transfer the energy to a dopant atom, which subsequently emits a single photon [38, 47]. Currently, some commercial anti-Stokes materials are available. One of them is Sodium yttrium tetrafluoride doped with erbium and ytterbium ($NaYF_4$: Er,Yb), a material known as the most efficient UC to date [40]. This compound absorbs light in the near infrared (NIR) region of the spectrum and emits green visible luminescence. Previously this material has been investigated for fingermark detection by Bullock at the University of Technology Sydney [38]. In this chapter, the application of $NaYF_4$: Er,Yb powders for fingermark detection is further explored in depth including its affinity for fingermark materials, its methods for fingermark detection and its effect for fingermark detection on a range of difficult surfaces. The overall aim of this in-depth research is to fully explore the possibility of $NaYF_4$: Er,Yb UC for fingermark detection and its advantage over traditional fluorescence techniques.

3.2. Materials and methods

3.2.1. General

Fingermarks were detected using both $NaYF_4$: Er,Yb and aluminium powders to explore UCs' effectiveness for fingermark detection compared to traditional fingerprint powders. Images of developed fingermarks were studied under microscope to check UCs' affinity to fingermark materials. Fingermarks on luminescent and patterned surfaces were also treated with UCs to check its advantage over traditional fluorescent techniques.

$NaYF_4$:Er,Yb powder (Artemis Limited, UK) and cetyltrimethylammonium bromide (CTAB, BDH Laboratory Supplies, UK) were used as received. These powders were characterised by fluorescence spectra, scanning electron microscopy, and also by x-ray diffraction experiments. Fluorescence spectrum was measured by

an Ocean Optics USB2000+ spectrometer with the excitation of a 700 mW laser pointer (Techlasers Enforcer) at 980nm. Scanning electron microscope images were obtained using a LEO Supra 55 VP microscope (Zeiss) equipped with an in-lens secondary-electron detector. X-ray diffraction experiments were performed using a Siemens D5000 X-ray diffractometer with a graphite post monochromator with the following parameters: wavelength 1.5406 Å (Cu Ka), tube power 1.6 kW (40 kV at 40 mA), step size = 0.02°, time per step = 3 s, divergent slit = 1°, receiving slit = 0.02 mm, scan angle range = 3–80°.

Six donors supplied latent fingermarks for this work. Fingermarks were deposited after the donors slightly wiped their fingers over their forehead or facial area just prior to fingermark deposition. A collection of fingermarks on glass from two donors was stored for up to 19 months for experiments on aged fingermarks. Surfaces investigated in this work include: glass (microscope slides), plastics (polyethylene bags and soft drink labels), aluminium foil, beer cans, glossy paper and electrical tape (PVC). Australian polymer banknotes were also tested as they are known to be a difficult semi-porous surface for fingermark development [60].

Developed fingermarks were illuminated either with white light (for conventional reflection mode imaging) or by a laser (either a Roithner RLDH-980-200-3 or a Techlasers Enforcer) operating at a wavelength of 980 nm (for upconverting mode imaging). Images were recorded using either a Rofin Poliview (Rofin Australia Pty. Ltd.). When imaging in upconversion mode, a 555nm band pass filter with bandwidth of 28nm (type 702.0212, manufactured by Rofin, Australia) was used to exclude the IR light of from the laser.

3.2.2. Fingermark Development with Dry Powder

$NaYF_4$: Er,Yb powders were applied to fingermarks on the various surfaces using squirrel brushes (Optitech Company, Australia). For comparison purposes, fingermarks were also developed using aluminium powder and black powder (Lightning Powder Company, USA) using the same technique.

3.2.3. Fingermark Development Using a Wet Powder Method

To further investigate the utility of $NaYF_4$: Er,Yb, the material was assessed for use in a wet powdering procedure. The powder was dispersed in aqueous media and applied to fingermarks on a range of nonporous surfaces. Fingermarks were developed using one of the following three methods.

1. Powder suspension using surfactants: $NaYF_4$: Er,Yb powder (0.5% w/v) was added to a solution of CTAB (0.1% w/v) in Milli Q water and stirred for 10 minutes using a magnetic stirrer. The suspension was poured into Petri dishes and fingermark specimens were immersed in the suspension for around 3 minutes and then rinsed with deionised water.

2. Homogenised suspension: $NaYF_4$: Er,Yb powder (0.5% w/v) was added to MilliQ water in a glass beaker and agitated using an IKA Ultra-Turrax T25 digital homogenisation instrument at 6,000 rpm for about 3 minutes. Fingermark specimens were then developed as described above.

3. Sticky-side wet powder: A slurry of $NaYF_4$: Er,Yb powder in Photoflo 200 (Eastman Kodak Company)/deionised water (50/50 mix) was prepared and then painted over the latent fingermark area, allowed to develop for 30 seconds and then rinsed off using deionised water. Traditional silver sticky-side powder (Lightning Powder Company Inc, USA) was also used for comparison.

3.2.4. Comparison with CAF / rhodamine 6G Staining

Sets of three fingermarks (index, middle and ring fingers) were deposited on plastic soft drink labels, and then these samples were cut in halves (down the centre of the middle finger impression). The left side of each set was treated by CAF/rhodamine 6G staining and the right side treated by $NaYF_4$: Er,Yb dry powdering. CAF was performed in a CAF cabinet (FCC171; Carter-Scott Design, Melbourne) using the preset mode for fresh fingermarks (5 minutes initial fume time). After being fumed, the specimens were dipped into the rhodamine 6G working solution for about 10 seconds, air dried and then illuminated at 530 nm with a 610 nm band pass barrier filter using the Rofin Poliview. The formulation of the

rhodamine 6G working solution was prepared according to the National Centre for Forensic Studies Workshop Manual [48]. The right side of each set was treated by $NaYF_4$: Er,Yb dry powder using a squirrel brush (Optitech Company, Australia). Then, the dry powder-treated fingermarks were illuminated using the Enforcer laser and recorded in upconversion mode as described in Section 3.2.1. In summary, both sides were treated and visualized under the optimal conditions for each half and then the recorded images compared.

3.2.5. Comparison and Assessment of Developed Fingermarks

There were several different fingermark comparison and assessment systems described in literature [61-63]. Because most fingermark comparison happened in sets of three fingermarks (index, middle and ring fingers) with the middle fingermarks cut in halves, generally it was easy to compare and evaluate the images of the developed fingermark on each side by bare eyes. Furthermore, the main aim of this project was to evaluate the effectiveness of (functionalised) UCs for fingermark development on luminescent and patterned backgrounds. It was difficult to grade the interference of background luminescence and pattern which also resulted that it was also difficult to grade the developed fingermarks on such backgrounds. As a result, in this project developed prints were not necessarily graded in general to evaluate the sensitivity and selectivity of UCs for fingermark detection.

For the comparison between UCs and aluminium powders (to decide if UC is suitable for fingermark detection), the amount of clear ridge detail present on the fingermark images was the main criterion. Other things such as the contrast and observable 3rd level characteristics (pores and ridge contours) were also considered as a minor criterion. To compare the fingermark developed by UCs (in Chapters 3 and 4) or functionalised UCs (in Chapters 6 and 7) vs. rhodamine 6G staining, the fingermarks with more luminescent ridge details and less interference of background luminescence and pattern were better. The amount of clear ridge detail present on the fingermark images was also a less important criteria. In conclusion, fingermark comparisons in this project was a subjective assessment rather than a quantitative one.

3.3. Results and Discussion

3.3.1. Characterisation of $NaYF_4$: Er,Yb Powder

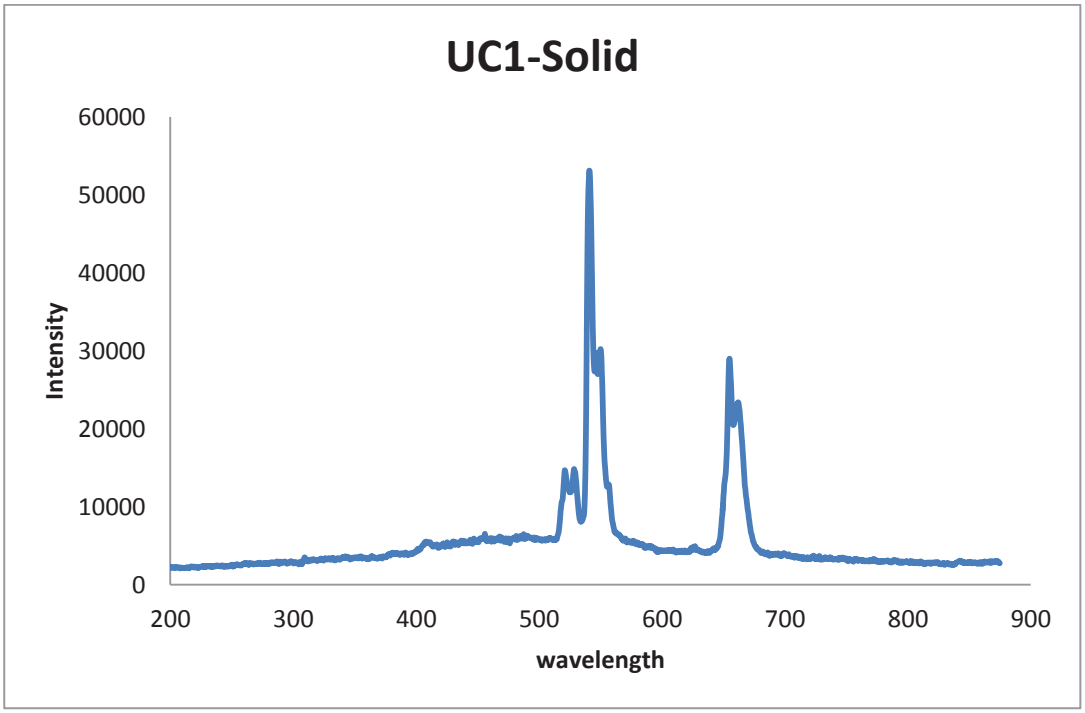

Figure 3.1. Fluorescence emission spectrum of $NaYF_4$: Er,Yb, excitated by a 980 nm laser.

The fluorescence spectra revealed that two emission maxima were produced under the 980 nm laser illumination as shown in **Figure 3.1.** One peak is at ~560 nm in the green visible region, while another peaked at ~670 nm, which is in the red visible region. The intensity of the green emission is much higher than that of the red emission making the overall emission appear green to the eye.

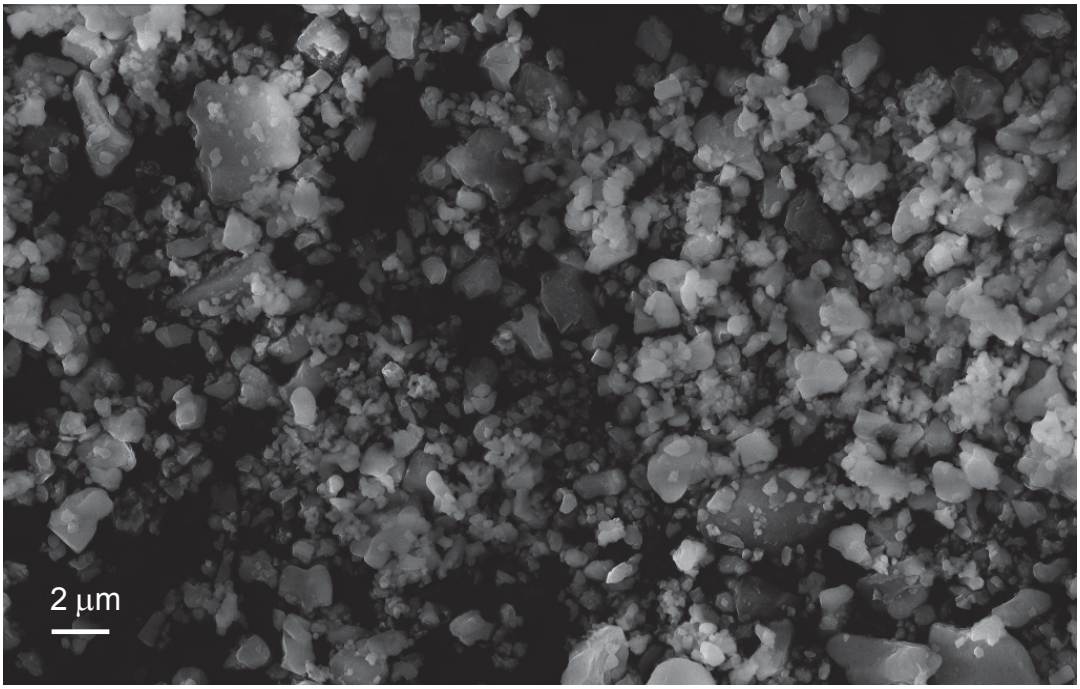

Figure 3.2. Scanning electron micrograph of $NaYF_4$: Er,Yb powder.

Figure 3.2 shows a representative image of the $NaYF_4$: Er,Yb powder and reveals that most of the particles have sizes ranging from ~0.5 to ~5 μm. [38].

Two crystal phases of $NaYF_4$:Er,Yb have been reported, the α-cubic and β-hexagonal phases [37]. Analysis by X-ray diffraction (**Figure 3.3**) showed that the particles consisted mostly of the β-hexagonal phase (diffraction peaks marked with blue lines, JCPDS standard card 28-1192), although some α-cubic phase was also evident (peaks marked with grey lines, JCPDS standard card 77-2042). Importantly, the luminescence intensity of the β-hexagonal phase is approximately ten times greater than that of the α-cubic phase [40].

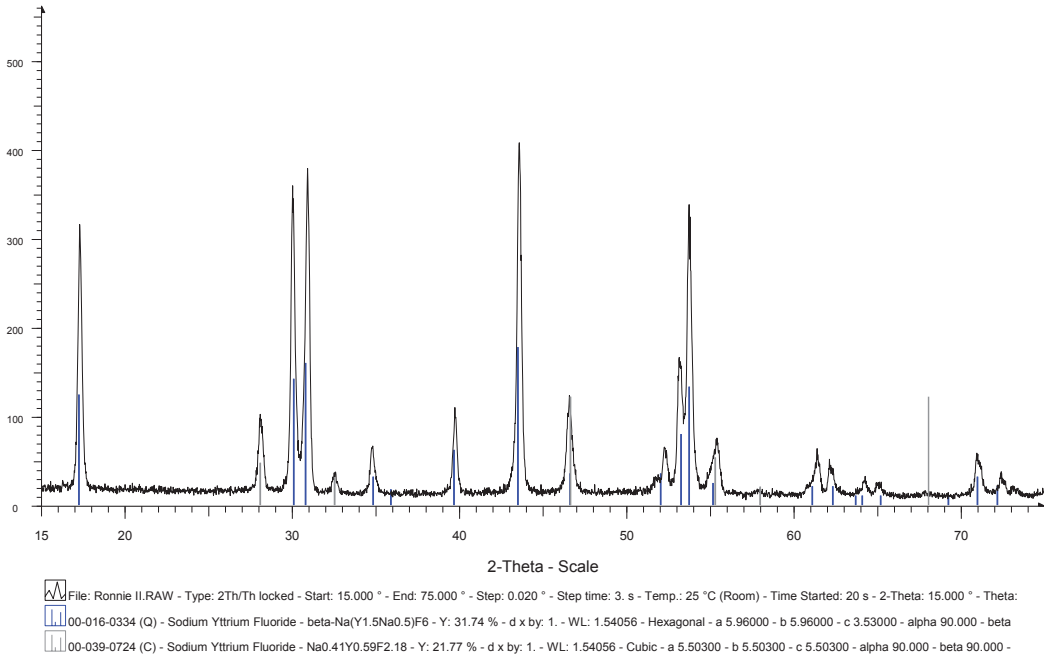

Figure 3.3. XRD spectrum of $NaYF_4$: Er,Yb.

3.3.2. Fingermarks Developed with $NaYF_4$: Er,Yb Powder

The $NaYF_4$:Er,Yb powder showed a good affinity for fingermark ridges on glass, plastic and aluminium surfaces. Most surfaces showed little to no background development upon application of $NaYF_4$:Er,Yb powder and the developed fingermarks were of a similar quality to those developed by aluminium powder. **Figure 3.4** shows representative images of fresh fingermarks on glass (A), plastic (B), and aluminium foil (C) developed with aluminium powder and with $NaYF_4$:Er,Yb powder under white light illumination. The $NaYF_4$:Er,Yb powders revealed minutiae detail and also exhibited significantly less background staining compared to the aluminium powder. Less background staining and slightly better affinity for fingermark materials for $NaYF_4$:Er,Yb powder was also confirmed by image taken under microscope showed in **Figure 3.5**. This may be a result of the smaller $NaYF_4$:Er,Yb particle size compared to the 1 to 10 μm average size of the aluminium fingerprint powder (as measured by SEM). Generally, smaller particles exhibit a stronger affinity to fingermark ridges than larger, coarser particles [64].

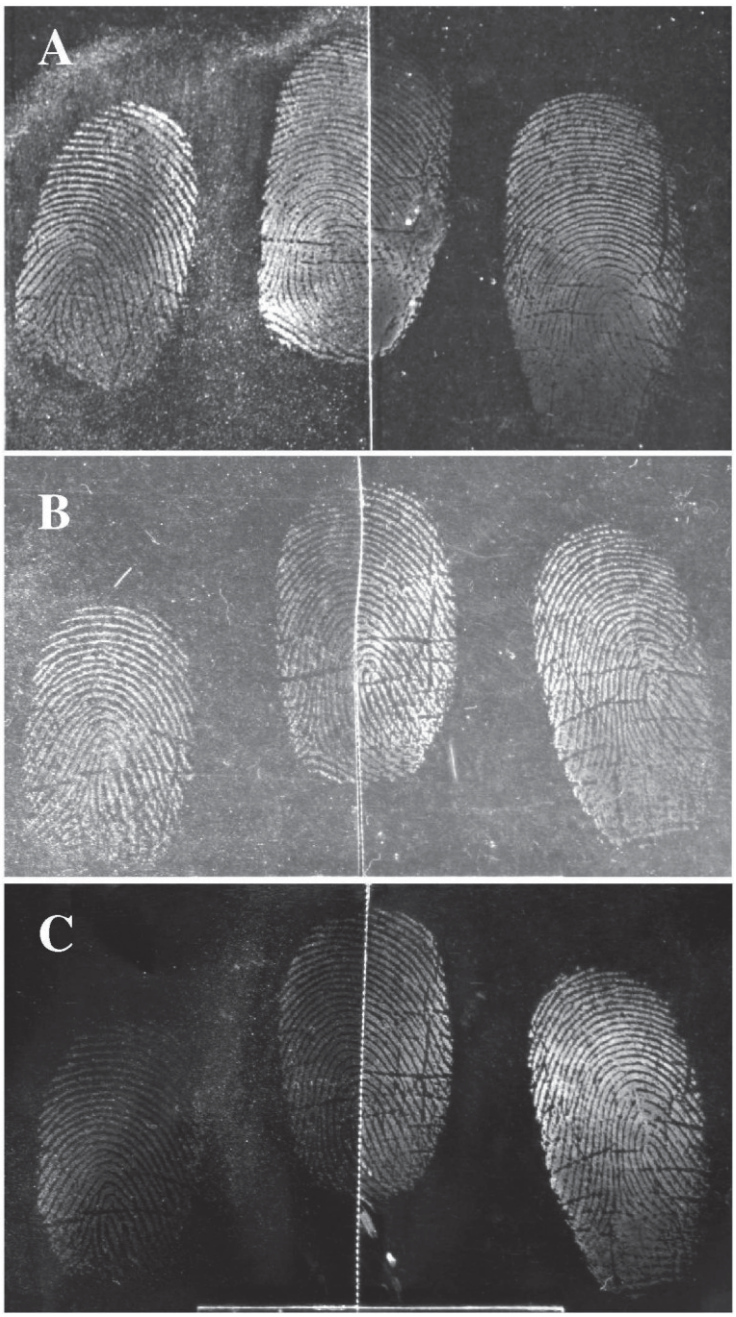

Figure 3.4. Fresh fingermarks (<12 hrs old) on glass (**A**), polyethylene plastic (**B**) and Aluminium foil (**C**) developed with: (left) aluminium powder and (right) $NaYF_4$:Er,Yb powder, visualised in the reflection mode under white light.

Fingermarks on glass that had been aged for up to 19 months were also successfully developed with $NaYF_4$:Er,Yb powder (**Figure 3.6**). It was concluded from these experiments that the $NaYF_4$:Er,Yb powder is a practical fingermark powder with good affinity for fingermarks on non-porous surfaces.

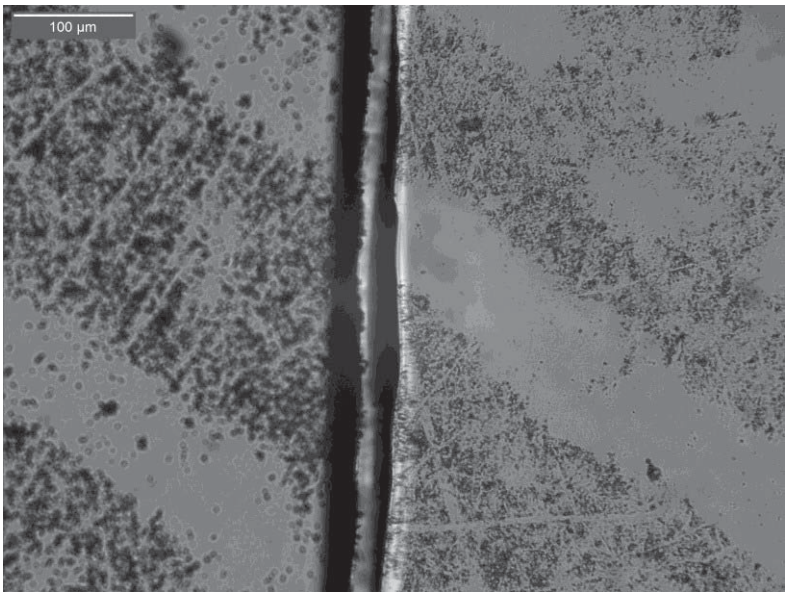

Figure 3.5. Fresh fingermarks on glass developed with: (left) Al powder and (right) $NaYF_4$:Er,Yb powder. This image was taken in transmission mode with white light illumination. Fingermarks are shown as the darker features. The right-handed side image shows less powder deposited in the fingermark valley regions compared to the image on the left.

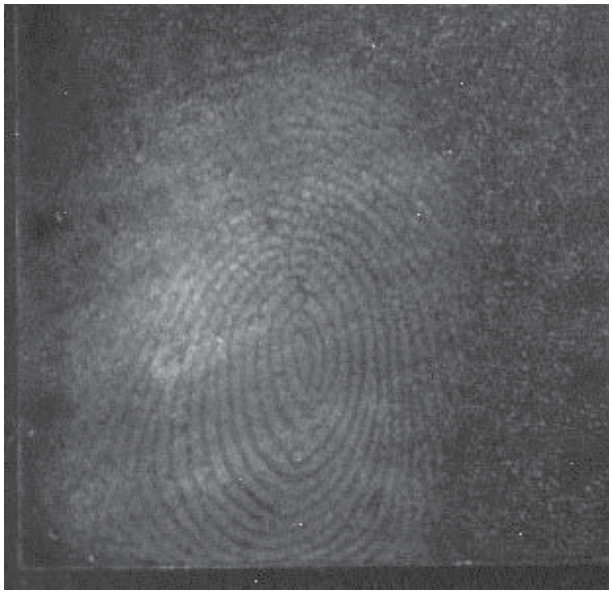

Figure 3.6. 19-month-old fingermark glass developed by dry powdering with $NaYF_4$: Er,Yb under the illumination of 980 nm laser pointer with a 555nm band pass filter and 15.2 s exposure time.

To utilise the upconversion properties of $NaYF_4$:Er,Yb powder for fingermark detection, specimens were illuminated using laser light with a wavelength of 980 nm and imaged using a 555nm band pass filter to receive the green light from the upconversion luminescence. Fingermarks were successfully developed using $NaYF_4$:Er,Yb powder and imaged in upconversion mode on various difficult surfaces including glossy magazine paper (**Figure 3.7**), beer cans (**Figure 3.8**), and plastic labels (**Figure 3.9**).

Theoretically the luminescence of the background should not interfere with the image at all as it was not excited by the 980 nm laser light. However, in the actual imaging process some very faint light was still essential for the operator to evaluate the location of the fingermarks when scanning with the laser. This led to some background being visible when long exposure time was applied (reflection). Owing to inexperience, at the beginning of this project some lights from computer screen and electricity power board were not excluded using black foam board that resulted in very apparent background (**Figure 3.8-3.9**). Another reason to cause the background interference in the image was the upconversion luminescence from the treated fingermark that can also cause the background visible to some extent, especially under long exposure time. In the further experiment some black foam board was used to block most light from the computer screen and the electricity power board and much less background was shown in the images, for example, **Figure 3.10** and **Figure 3.12**. Experiments were also done by illuminating the backgrounds with the 980 nm laser pointer and the result showed they were not upconverted or had no upconversion luminescence. These results illustrate the potential of UCs for the detection of latent fingermarks on difficult surfaces.

Figure 3.7. Fresh fingermark on magazine paper developed by dry powdering method of UC particles, under the illumination of 980 nm laser pointer with a 555nm band pass filter and 10.3 s exposure time.

Figure 3.8. Fresh fingermark on beer can developed by dry powdering method of UC particles, under the illumination of 980 nm laser pointer with a 555nm band pass filter and 15.2 s exposure time.

Figure 3.9. Fresh fingermark on Coca cola plastic tag developed by dry powdering method of UC particles, under the illumination of 980 nm laser pointer with a 555nm band pass filter and 10.3 s exposure time.

Figure 3.10 showed fresh fingermarks (<5 hrs old) on an Australian five dollar polymer banknote developed by dry powdering with $NaYF_4$:Er,Yb and illuminated using 980 nm laser light. Australian polymer banknote is a notoriously difficult surface for fingermark detection. The coating of these banknotes is a modified polyurethane lacquer over patterned offset and intaglio printing and each of the denominations exhibited broadband luminescence [60]. The ridge detail was remarkably clear on this surface, a surface that has proved to be challenging unless examined using a time consuming detection sequence and/or a highly specialised technique [60, 65]. However, the effectiveness of $NaYF_4$:Er,Yb particles for aged fingermarks was not investigated.

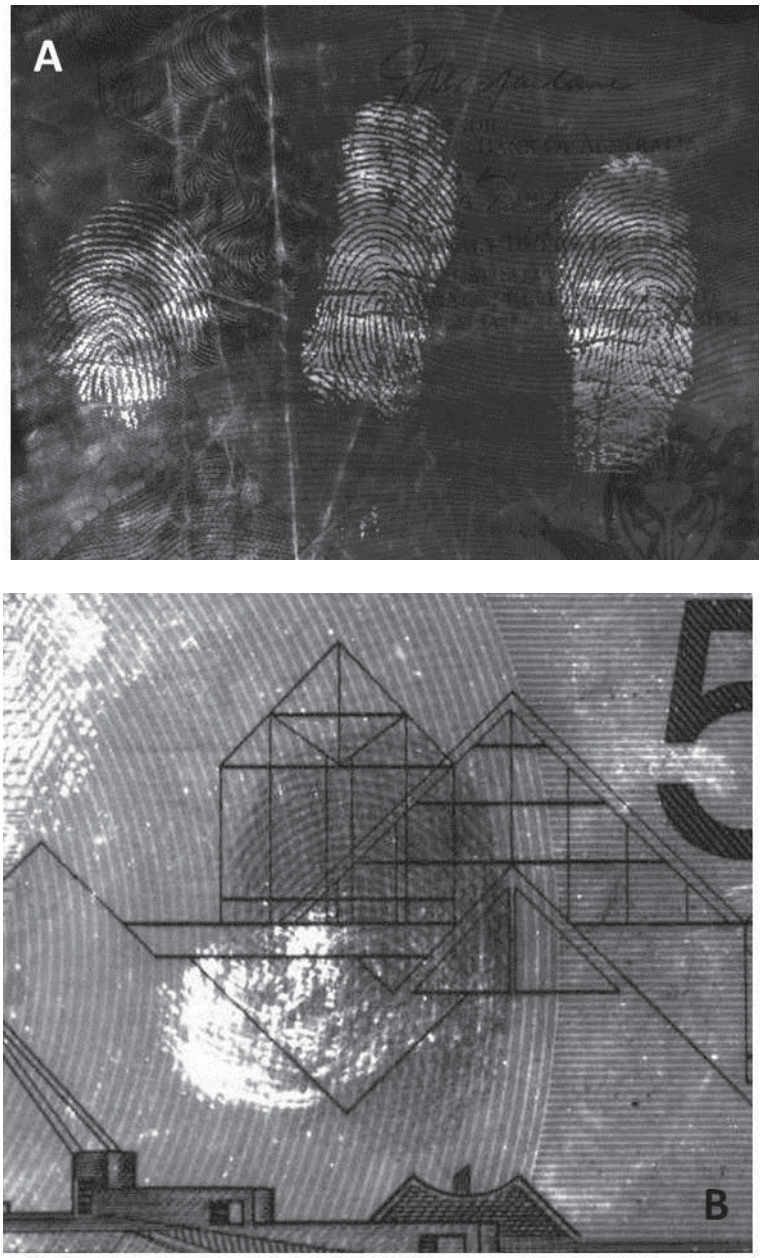

Figure 3.10. A: Fresh fingermarks (<5 hrs old) on an Australian five dollar polymer banknote developed with $NaYF_4$: Er,Yb. Illuminated using 980 nm laser light and imaged using a Rofin Poliview fitted with a 555nm band pass filter and using an exposure time of approximately 15 seconds. B: A fresh fingermark (<1 hr old) on an Australian five dollar polymer banknote developed with Aluminium powder. Illuminated using 530 nm Rofin Polilight and imaged using a Rofin Poliview fitted with a 610nm long pass filter and using an exposure time of 1.33 seconds.

3.3.3. $NaYF_4$: Er,Yb as a wet Powder

To further investigate the utility of $NaYF_4$: Er,Yb, the material was assessed for use in a wet powdering procedure.

On glass (**Figure 3.11** A), the homogenised suspension revealed much clearer fingermark details than the CTAB-containing suspension, which stained not only the fingermark ridges but also the background. The homogenised suspension of $NaYF_4$: Er,Yb yielded similar results to the dry powdering method although the dry powdered specimens had less background staining but also weaker luminescence. Both methods were able to show tertiary level details in the fingermark deposits. On aluminium foil (**Figure 3.11** B), the homogenised suspension adhered to the fingermarks as well as the background. The CTAB-containing suspension demonstrated only weak fingermark and background adhesion. On plastics (**Figure 3.11** C), overall results were generally poorer than on glass or aluminium foil using either method. Overall, the dry powdering method revealed fingermark detail with higher clarity than either of the wet powdering techniques.

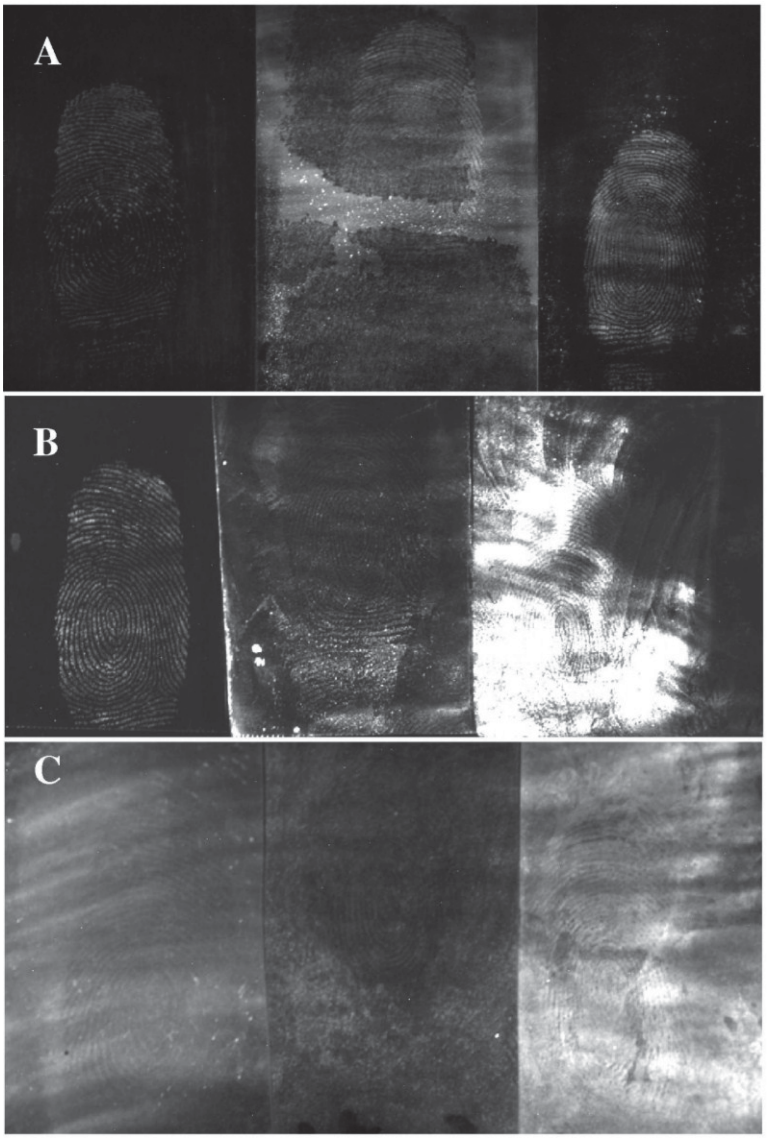

Figure 3.11. Comparison of fresh fingermarks glass (**A**), aluminium foil (**B**) and plastic **(C)** developed using $NaYF_4$: Er,Yb by different methods under the illumination of 980 nm laser pointer with a 555nm band pass filter and 20.3 s exposure time. (Left) dry powdering, (Middle) CTAB suspension and (Right) homogenization suspension.

An aqueous sticky-side powder incorporating $NaYF_4$: Er,Yb was used to develop latent fingermarks on the adhesive side of the black electrical tape but, as the tape was itself non-luminescent, no advantage over traditional sticky-side (luminescent or non-luminescent) powder was apparent. On adhesive-backed foam, neither the new

sticky-side powder nor traditional sticky-side powder was able to develop any latent fingermarks.

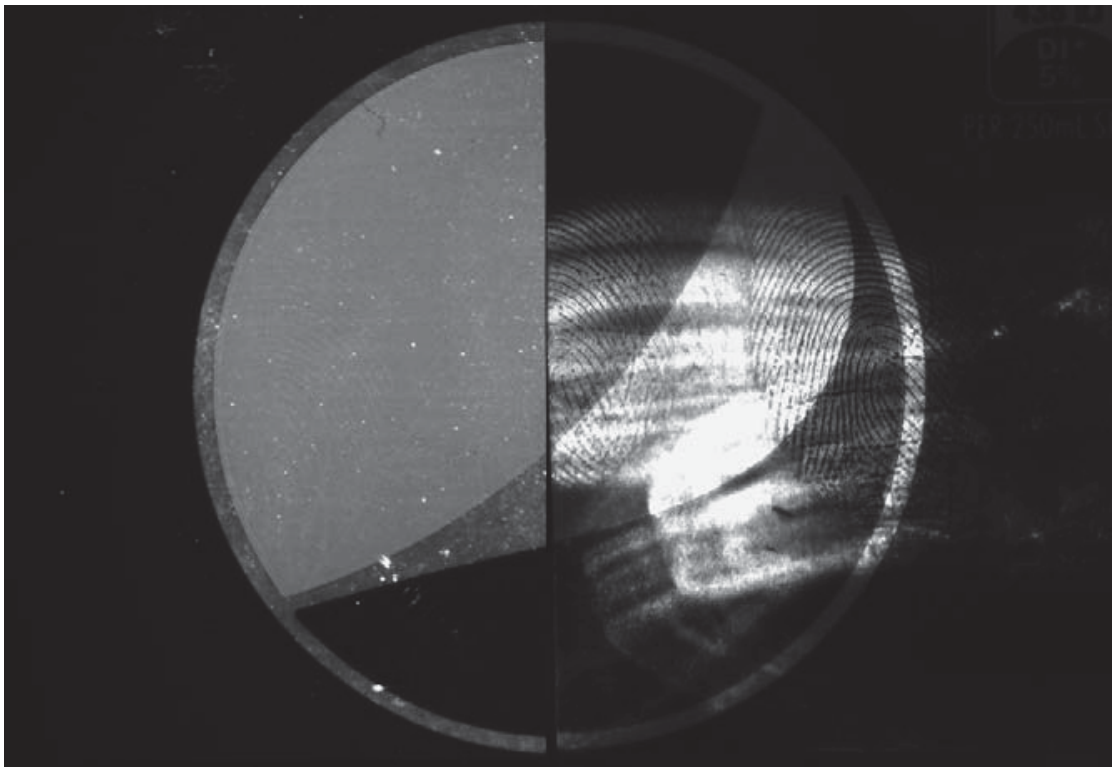

Figure 3.12. Comparison of a fresh fingermark left on soft drink plastic trademark developed by CAF and rhodamine 6G staining, illuminated at 505 nm for 1.23 s and observed at 610 nm (left half) and $NaYF_4$:Er,Yb dry powdering, illuminated using a 980 nm laser pointer with 1.68 s exposure time and a 555nm band pass filter (right half).

3.3.4. Comparison with CAF / rhodamine 6G Staining

For the comparison between $NaYF_4$: Er,Yb powdering vs. CAF/rhodamine 6G staining on plastic soft drink labels, it proved that under most conditions, both $NaYF_4$: Er,Yb powdering vs. CAF/rhodamine 6G staining can developed satisfactory fingermarks. However, on certain areas of some soft drink labels, owing to the strong absorption of background colour or the interference of luminescence, CAF/rhodamine 6G staining failed to develop ideal fingermarks while $NaYF_4$: Er,Yb

powdering showed promising results (**Figure 3.12**). This fully illustrated the advantage and potential of upconversion luminescence over conventional luminescence for fingermark detection.

3.4. Conclusions

The $NaYF_4$:Er,Yb powder is effective for latent fingermark development when used as dry powder or as a suspension with the former method is better than the latter. The $NaYF_4$:Er,Yb powder showed selective affinity to fingermark materials rather than the background on most surfaces and the developed fingermarks presented clear ridges with high contrast. The UC powder showed strong luminescence when illuminated with 980 nm wavelength laser light. A laser diode or pointer was found to be an effective light source when used in conjunction with a 555nm band pass filter to block the IR light from the laser. Theoretically the strong luminescence of the UCs can be visualised on fingermarks as bright regions on a total dark background, but in actual imaging the background is still visible to some extent especially under long exposure time owing to both the instrumental inefficiency and the illumination of upconversion luminescence itself. However, the interference from background was reduced compared to the conventional luminescence reagent and the fingermark detail was clear. In summary The $NaYF_4$:Er,Yb powder can be used to detect fingermarks on various difficult surfaces that exhibit interfering background luminescence when using conventional luminescence techniques.

Chapter 4

Fingermark Detection Using YVO_4:Er,Yb Upconverter particles

Chapter 4. Fingermark Detection Using YVO_4:Er,Yb Upconverter particles

4.1. Introduction

Chapter 3 presented an investigation into the application of anti-Stokes luminescence to detect fingermarks using sodium yttrium tetrafluoride doped with erbium and ytterbium ($NaYF_4$:Er,Yb) UC particles [55]. In this Chapter, the application of another type of UC particles, yttrium vanadate doped with ytterbium and erbium (YVO_4:Er,Yb) is investigated. This compound is an efficient anti-Stokes luminescent material that absorbs light in the NIR region of the spectrum and emits green luminescence [2]. In this study, we investigated the application of YVO_4:Er,Yb for the development of latent fingermarks on a range of non-porous and semi-porous surfaces.

4.2. Materials and Methods

Fingermarks were detected using YVO_4:Er,Yb particles on a range of surfaces to explore its effectiveness for fingermark detection. YVO_4:Er,Yb particles was compared with aluminium powders to explore its effectiveness for fingermark detection and affinity for fingermark materials compared to traditional fingerprint powders. YVO_4:Er,Yb particles was also compared with $NaYF_4$: Er,Yb to evaluate its effectiveness since the latter was already proved an excellent UC for fingermark detection. Images of developed fingermarks were studied under microscope to further confirm UCs' affinity to fingermark materials. Fingermarks on luminescent and patterned surfaces were also treated with YVO_4:Er,Yb particles to check its effect on difficult background and advantage over traditional luminescent techniques.

4.2.1. Synthesis and Characterisation of YVO_4:Er,Yb Particles

YVO_4:Er,Yb particles were synthesised at the Molecular and Health Technologies facility, Commonwealth Scientific and Industrial Research Organisation (CSIRO), Clayton, Australia. The particles were analysed with XRD, SEM, fluorescence spectrometry and size distribution analysis. However, the conditions are commercial in confidence and cannot be disclosed now.

4.2.2. Fingermark Deposition and Imaging

Fingermarks were obtained from two donors known to be good secretors. The fingermarks were deposited after the donors slightly wiped their fingers over their forehead or facial area just prior to fingermark deposition (to increase the sebaceous content in the deposited fingermarks). These highly sebaceous fingermarks are not realistic in actual cases, but they gave a baseline for the best case scenario of fingermark detection and they were often used in the research work [11, 18, 19, 22, 66]. Surfaces investigated in this work included: glass (microscope slides), plastic (polyethylene bags and plastic soft drink labels), soft drink cans, glossy magazine paper, adhesive tapes (Clingtape series including: clear tape with plastic backing, black cloth tape, yellow cloth tape and PVC duct tape; manufactured by Henkel International) and Australian polymer banknotes. This latter substrate is considered to be a difficult semi-porous surface for fingermark development [60].

Developed fingermarks were illuminated either with white light (for conventional reflection mode imaging), or using a laser pointer (Techlasers Enforcer) at a wavelength of 980 nm (for upconversion mode imaging). Images were recorded using a Rofin Poliview (Rofin Australia Pty Ltd). When imaging in the upconversion mode, a 555 nm band pass filter with bandwidth of 28nm (type 702.0212, manufactured by Rofin, Australia) was used to exclude the IR light of from the laser. Rhodamine 6G stained fingermarks were illuminated at 530 nm (Rofin Polilight PL500) and imaged through a 610 nm band pass filter using the Rofin Poliview.

4.2.3. Fingermark Development with Dry Powder

The dry YVO_4:Er,Yb powder was applied to fingermarks on the various test surfaces using squirrel hair brushes (Optimum Technology Australia). Fingermarks were also developed using aluminium powder (Lightning Powder Company, USA) and $NaYF_4$:Er,Yb particles (purchased from Artemis Limited, UK, and used as received.) using the same powdering technique for comparison purposes.

Moreover, fresh fingermarks on a five-dollar Australian banknote were also developed by YVO_4:Er,Yb dry powdering to test the effectiveness of this method on a surface that is notoriously difficult due to high background fluorescence and printing pattern interference.

4.2.4. Fingermark Development Using a Wet Powder Method

YVO_4:Er,Yb particles were assessed for use in a wet powdering procedure. The powder was dispersed in aqueous media and applied to fingermarks on a range of non-porous surfaces. Fingermarks were developed using one of the following three methods.

Powder suspension using surfactants: YVO_4:Er,Yb powder (0.5% w/v) was added to a solution of Tergitol NP9 (purchased from Sigma-Aldrich, used at 0.1% w/v) in Milli-Q water and stirred for 10 minutes using a magnetic stirrer. The suspension was poured into Petri dishes and fingermark specimens were immersed in the suspension for ~ 3 minutes and then rinsed with deionised water.

Homogenised suspension: 0.5% (w/v) YVO_4:Er,Yb powder (0.5% w/v) was added to Milli-Q water in a glass beaker and agitated using an IKA Ultra-Turrax T25 digital homogenisation instrument at 6,000 rpm for about 3 minutes. Fingermark specimens were then developed as described above.

Sticky-side wet powder: A paint-like slurry of YVO_4:Er,Yb powder in Photoflo 200 (Eastman Kodak Company)/deionised water (50/50 mix) was prepared and then painted over the latent fingermark area using a squirrel-hair brush. The suspension

was left in contact with the fingermarks for 30 seconds and then rinsed off using deionised water.

4.2.5. Comparison with CAF and Staining on Luminescent Substrates

Sets of three fingermarks (index, middle and ring fingers) were deposited on a soft drink can, plastic soft drink labels and glossy magazine paper, and then these samples were cut in halves (down the centre of the middle finger impression). The left side of each set was treated by CAF/rhodamine 6G staining and the right side treated by YVO_4:Er,Yb dry powdering. CAF was performed in a CAF cabinet (FCC171; Carter-Scott Design, Melbourne) using the preset mode for fresh fingermarks (5 minutes initial fume time). After being fumed, the specimens were dipped into the rhodamine 6G working solution for about 20 seconds, air dried and then illuminated at 530 nm with a 610 nm band pass barrier filter using the Rofin Poliview. The formulation of the rhodamine 6G working solution was prepared according to the National Centre for Forensic Studies Workshop Manual [48]. The right side of each set was treated by YVO_4:Er,Yb dry powder using a squirrel brush (Optimum Technology, Australia). Then, the dry powder-treated fingermarks were illuminated using the Enforcer laser and recorded using the Rofin Poliview in upconversion mode as described in Section 4.2.2. In summary, both sides were treated and visualized under the optimal conditions for each half and then the recorded images compared.

4.2.6. Comparison and Assessment of Developed Fingermarks

This was done as described in Section 3.2.5.

4.3. Results and Discussion

4.3.1. Properties of YVO_4:Er,Yb Powder

The YVO_4:Er,Yb phosphor emitted green visible light under the 980 nm laser illumination. The quantum efficiency of the green emission for the YVO_4:Er,Yb

phosphor is lower than that of $NaYF_4$:Er,Yb, which is known as the most efficient upconversion crystal studied to-date, but the luminescence of the former is still bright enough for fingermark detection [37, 55].

The size of the YVO_4:Er,Yb phosphor particles is similar to that of aluminium flake powder, one of the most commonly used fingerprint powders [1]. This was confirmed under SEM and by optical microscopy (**Figure 4.1**).

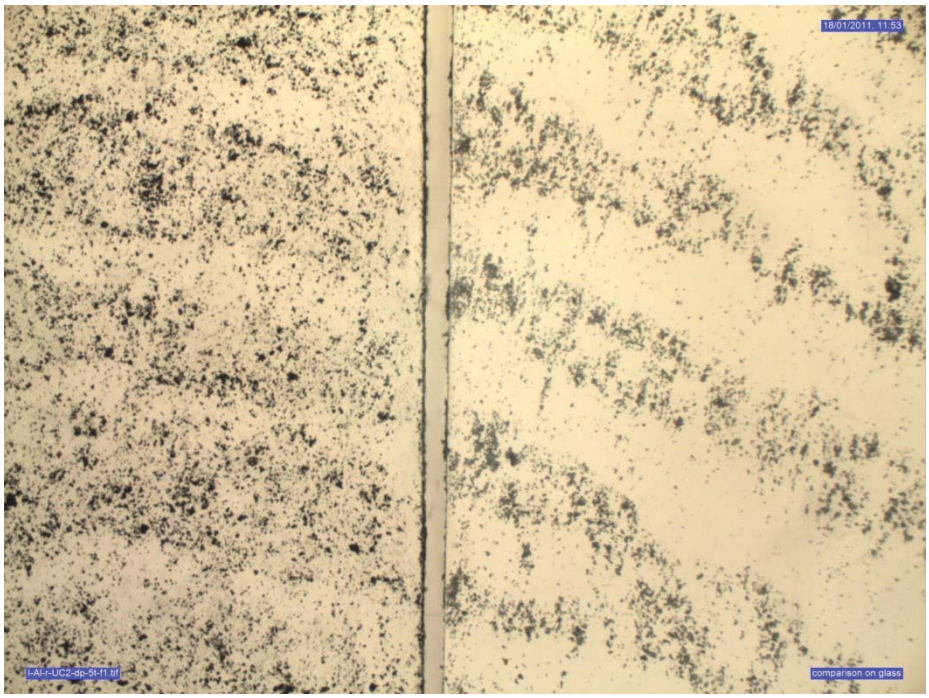

Figure 4.1. Comparison of fingermark developed on glass slides by Al (left) and YVO_4: Er,Yb (right) under a Leica DMC comparison microscope. This image was taken in the transmission mode with white light illumination.

4.3.2. Fingermarks Developed with YVO_4:Er,Yb Dry Powder

The YVO_4:Er,Yb powder showed a good affinity for fingermark ridges on glass, plastic (polyethylene bag) surfaces and glossy magazine paper. Most surfaces showed little to no background development upon application of the YVO_4:Er,Yb powder and the developed fingermarks were of a higher quality than those developed using aluminium powder. **Figure 4.2** shows images of fresh fingermarks on glass (A)

and plastic (B), developed using aluminium powder (left) and YVO_4:Er,Yb powder (right), with visualisation under white light illumination. The YVO_4:Er,Yb powders revealed fine minutiae and also exhibited significantly less background development compared to the aluminium powder as shown in microscope image (**Figure 4.1**).

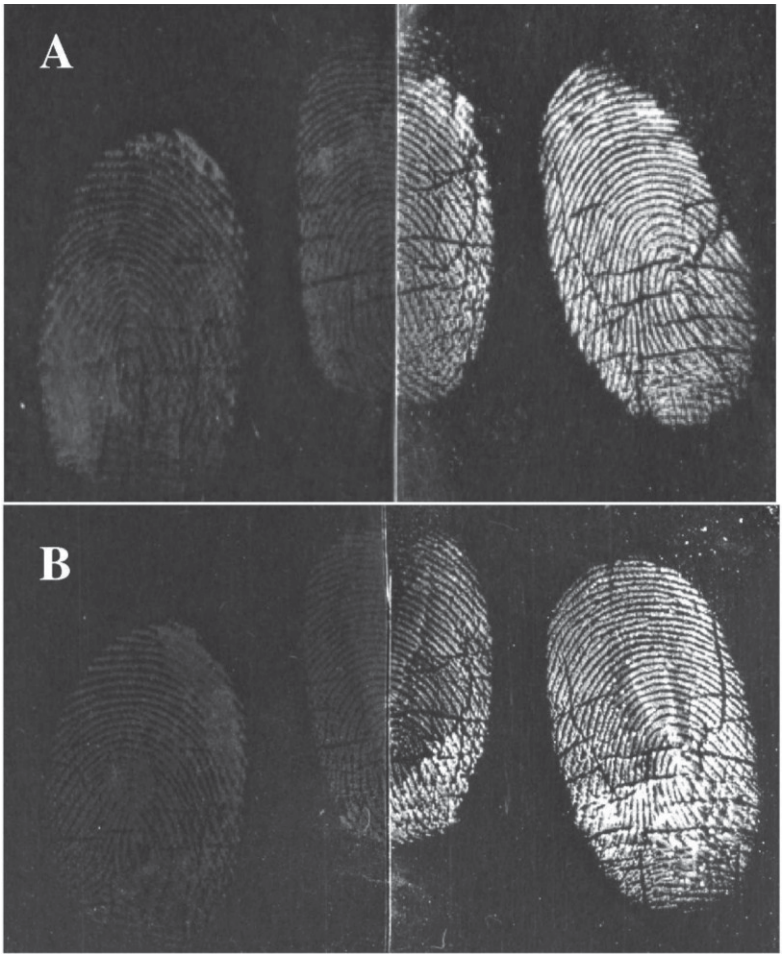

Figure 4.2. Fresh fingermarks (<1 hr old) on glass (**A**) and plastic (**B**) developed by dry powdering with (left) aluminium powder and (right) YVO_4:Er,Yb powder, recorded in the reflection mode under white light.

From **Figure 4.3**, we can see that the YVO_4:Er,Yb powder has similar affinity for fingermark ridges as for the $NaYF_4$: Er,Yb powders. However, it can be seen that the luminescence intensity of the YVO_4:Er,Yb particles is less than that observed for the $NaYF_4$:Er,Yb as shown in **Figure 4.4**, which is consistent with the latter being

considered as the most efficient upconversion material currently available [37, 55]. However, the luminescence intensity of the YVO_4:Er,Yb particles is sufficient to yield satisfactory fingermark images under the laser illumination system employed.

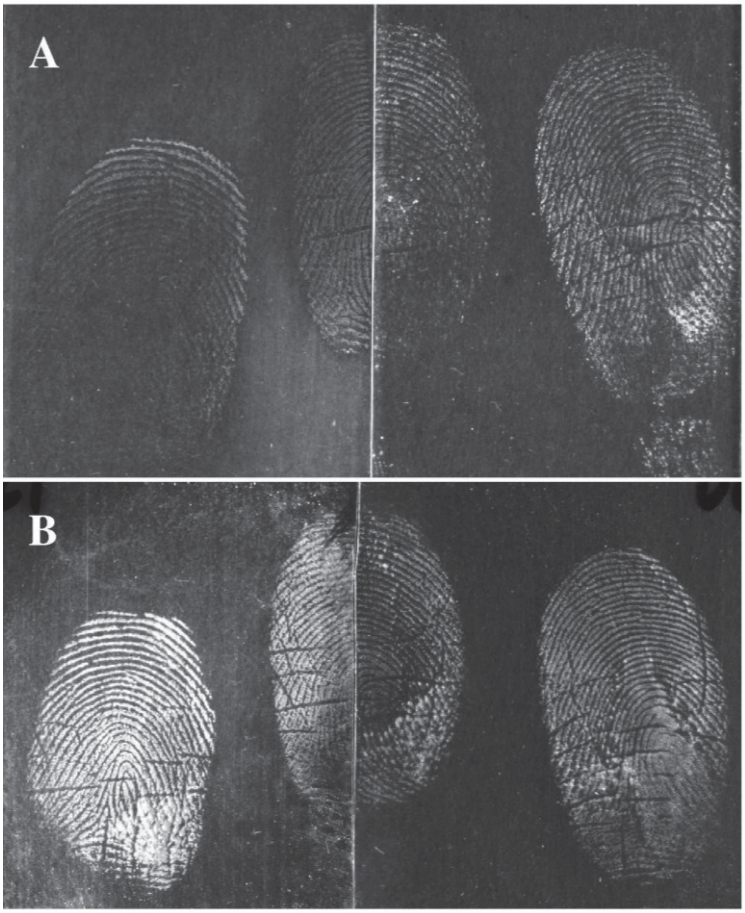

Figure 4.3. Fresh fingermarks on glass (**A**) and plastic (**B**) developed with: (left) $NaYF_4$: Er, Yb powders and (right) by YVO_4: Er,Yb powder in reflection mode under white light.

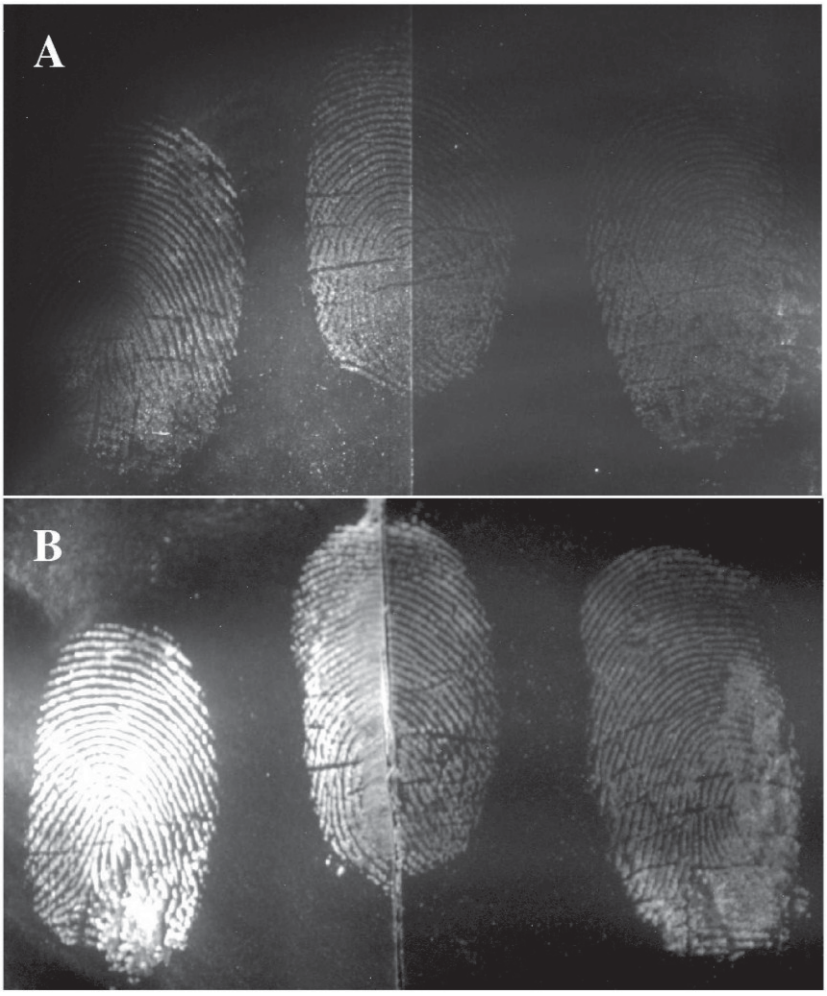

Figure 4.4. Fresh fingermarks (< 2 hours old) on glass (A) and plastic (B) developed with: (left) $NaYF_4$: Er, Yb powders and (right) by YVO_4: Er,Yb powder, under the illumination of a 980 nm laser pointer with a 555nm band pass filter.

Latent fingermarks aged for up to one year were also developed with clear ridge detail (**Figure 4.5**). It is concluded from these experiments that the YVO_4:Er,Yb particles can be used as a practical fingermark powder with good affinity for latent marks on a range of non-porous and semi-porous surfaces.

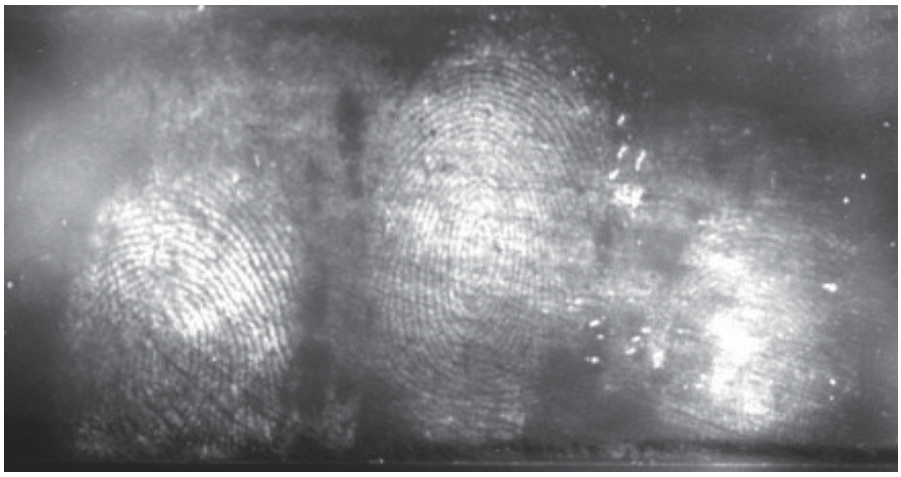

Figure 4.5. Aged fingermarks (1 year old) on glass developed by dry powdering with YVO_4:Er,Yb. Illumination at 980 nm and imaged with a 555nm band pass filter.

Figure 4.6. Fresh fingermark (< 2 hrs old) on an Australian five dollar polymer banknote developed with YVO_4:Er,Yb dry powdering. Illuminated at 980 nm and imaged with a 555nm band pass filter. The absence of visible background should be noted.

Figure 4.6 shows an Australian five dollar polymer banknote with a fresh fingermark (< 2 hours old) which has been developed by dry powdering with YVO_4:Er,Yb and illuminated using 980 nm laser light. The coating on these

banknotes is a modified polyurethane lacquer over patterned offset and intaglio printing, and each of the denominations exhibits broadband fluorescence emission under various excitation wavelengths [60]. In the reflection mode, no fingermark was readily visible. In the upconversion mode, the ridge detail was remarkably clear on this surface – a surface that has proved to be otherwise very challenging, unless a time consuming detection sequence and/or highly specialised techniques are applied [24-26, 60, 65].

4.3.3. YVO_4:Er,Yb as a Wet Powder

On glass, the homogenised suspension revealed clearer fingermark details than the Tergitol-containing suspension, but both methods led to significant undesirable background staining (**Figure 4.7**.A). The homogenised suspension of YVO_4:Er,Yb yielded similar results to the dry powdering method, and while the dry powdered specimens had less background staining, they also exhibited weaker luminescence. Both methods showed tertiary detail in the resulting fingermark images. On plastic (**Figure 4.7.B**), the homogenised suspension adhered to the fingermarks as well as to the background, resulting in poor contrast. The Tergitol-containing suspension gave relatively weak fingermark visualisation with significant background adhesion. The dry powdering method showed much better results on these substrates, with clear fingermark ridges and no significant background development.

An aqueous sticky-side powder incorporating YVO_4:Er,Yb was used to successfully develop latent fingermarks on the adhesive side of cloth-backed tape (**Figure 4.8**); but, as the tape itself was non-luminescent, there is no obvious advantage over traditional sticky-side powder methods.

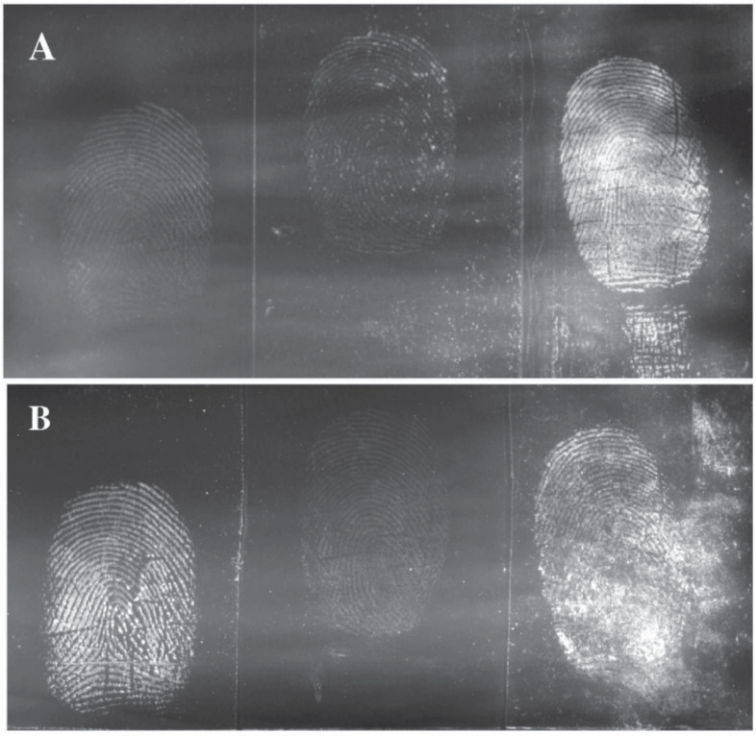

Figure 4.7. Fresh fingermarks (<2 hrs old) on glass (**A**) and plastic (**B**) developed by different methods: (left) dry powdering; (middle) Tergitol suspension; and (right) homogenised suspension. Illumination at 980 nm using a laser pointer and imaged using a Rofin Poliview with a 555 nm band pass filter.

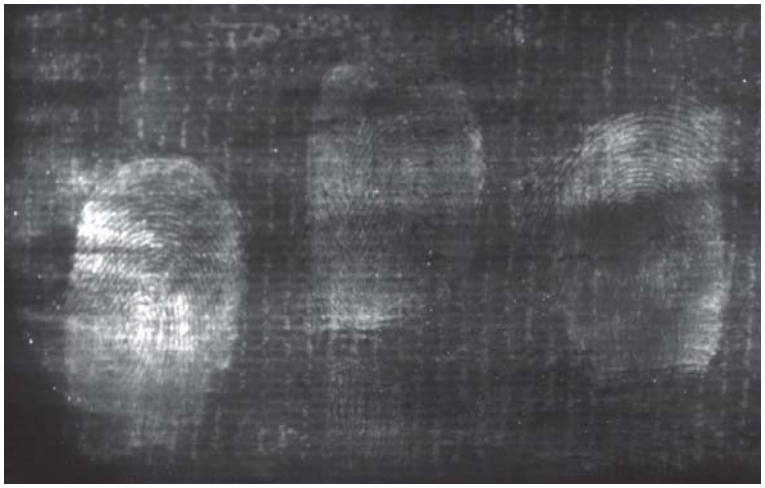

Figure 4.8. Fresh fingermarks developed on the sticky side of the black cloth tape using a YVO_4: Er,Yb suspension in a Kodak Photoflo 200/water (50:50) solution. Illumination using a 980 nm laser pointer, imaged using a Rofin Poliview with a 555nm band pass filter.

Table 4.1. Comparison of $NaYF_4$: Er,Yb and YVO_4:Er,Yb UC powders.

	Effective excitation light sources	Emission wavelenth	Luminescence intensity	Affinity to fingermark residues	Fingermark detection
$NaYF_4$: Er,Yb UC powder	980 nm laser	Major peak: ~560 nm Minor peak: ~670 nm	Very strong (Strongest known to date)	Good	Good
YVO_4:Er,Yb UC powder	980 nm laser	Major peak was green visible[†].	Very strong	Good	Good

Table 4.1 shows the comparison of $NaYF_4$: Er,Yb and YVO_4:Er,Yb UC powders. The result proved both the powders were similar in the properties of luminescence and the application for fingermark detection.

4.3.4. Comparison with CAF/staining on Luminescent Substrates

Fingermarks on a "difficult" surface, namely a popular soft drink label, were successfully developed using YVO_4:Er,Yb dry powder and imaged in the upconversion mode. A representative image is shown in **Figure 4.9**. The background luminescence of the label did not interfere with the UC image, which was in stark contrast to the interference observed with the traditional rhodamine 6G staining process. Fingermarks developed using YVO_4:Er,Yb powder were also successfully

[†] The actual values for these emissions are protected under a confidentiality agreement, therefore only the wavelength region in which they are found can be disclosed.

imaged in the upconversion mode on a range of other surfaces, including aluminium soft drink cans (**Figure 4.10**), and glossy magazine paper (**Figure 4.11**). Similar to the imaging of the $NaYF_4$: Er,Yb powders, the backgrounds of the fingermarks developed by the YVO_4:Er,Yb powder were still visible to some extent. The reasons for this visible background are also similar: the faint light essential for the operator to see the location of the fingermarks when scanning with the laser, and the illumination of the upconversion luminescence from the treated fingermarks. Under the long exposure time both the faint light and the upconversion luminescence become light sources that made the background visible. Differently, the lights from computer screen and electricity power board were excluded using black foam board that resulted less background interference compared those in Chapter 3. These results illustrate the potential of anti-Stokes luminescent materials for the detection of latent fingermarks on difficult surfaces.

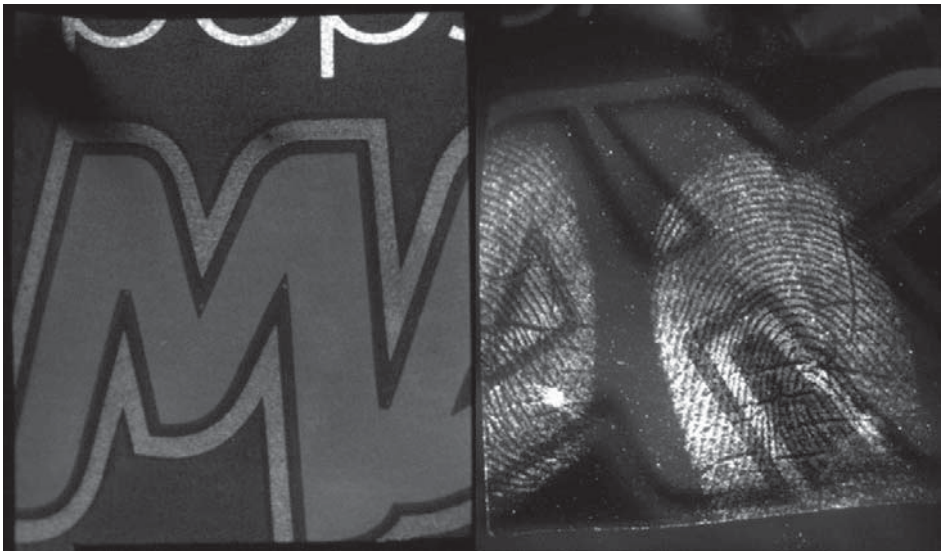

Figure 4.9. Fresh fingermarks (< 2 hrs old) developed on a plastic soft drink label: (left) CAF and rhodamine 6G staining, illuminated at 530 nm and with a 610 nm band pass filter; (right) YVO_4:Er,Yb dry-powdered, illuminated using a 980 nm laser pointer and with a 555nm band pass filter.

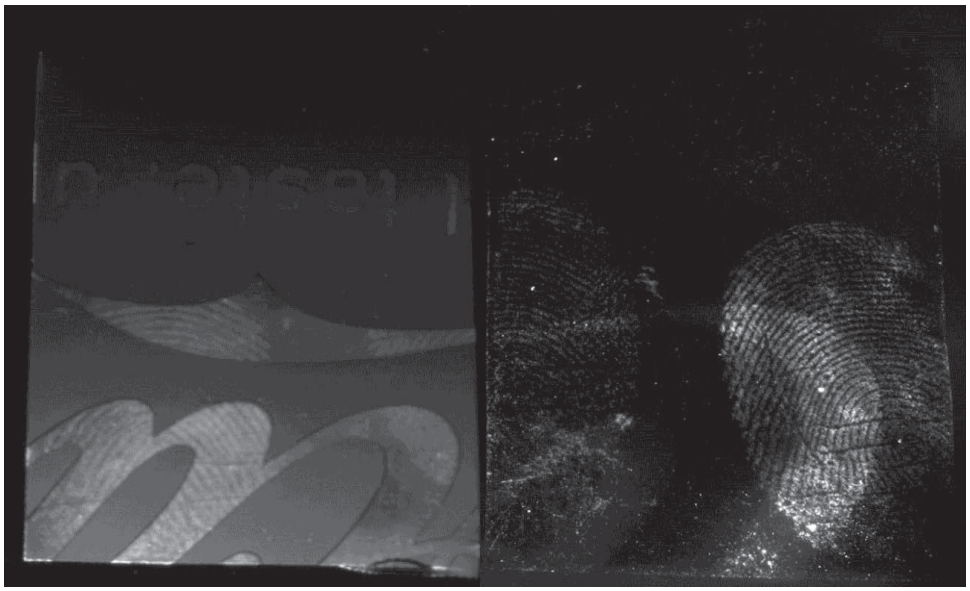

Figure 4.10. Fresh fingermarks (<2 hrs old) developed on a soft drink can. (left) CAF and rhodamine 6G staining, illuminated at 530 nm with a 610 nm band pass filter; (right) YVO_4: Er,Yb dry-powdered, illuminated using a 980 nm laser pointer with a 555nm band pass filter.

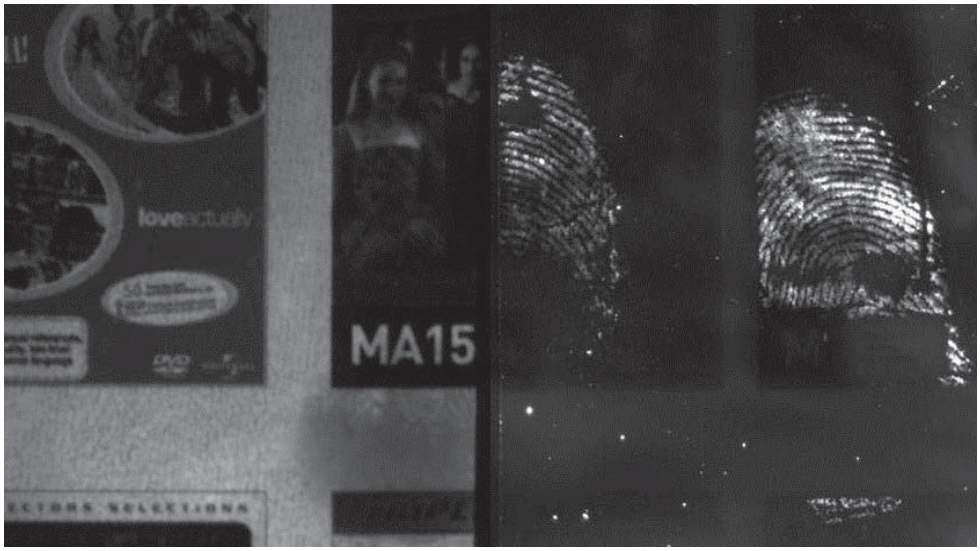

Figure 4.11. left: Fresh fingermarks (<2 hrs old) developed on glossy magazine paper. (left) CAF and rhodamine 6G staining, illuminated at 530 nm and with a 610 nm band pass filter; (right) YVO_4: Er,Yb dry-powdered, illuminated using a 980 nm laser pointer with a 555nm band pass filter.

4.4. Conclusions

The YVO_4:Er,Yb powder is effective for latent fingermark development when used as a dry powder or as a suspension, with the dry powdering generally presenting better results. The YVO_4:Er,Yb powder showed selective affinity to fingermark materials on most surfaces and the developed fingermarks presented clear ridges against a clear background. The UC powder showed strong luminescence when illuminated with a 980 nm wavelength laser light. A laser pointer was found to be an effective light source when used in conjunction with a 555 nm band-pass filter. Theoretically, the strong luminescence of the UCs should be visualised on fingermarks as bright regions against a completely dark background. However, in actual practice, the background was more or less visible mainly due to being illuminated by the UC emission under the long exposure times. However, the background interference was reduced compared to the results from the conventional luminescence reagent and the fingermark ridges were remarkably clear. In summary, the YVO_4:Er,Yb powder can be used to detect fingermarks on various difficult surfaces that exhibit interfering background luminescence when using conventional luminescence techniques.

Chapter 5

Smaller Upconverter Particles as a Staining Reagent for Cyanoacrylate-Fumed Fingermarks

Chapter 5. Smaller Upconverter Particles as a Staining Reagent for Cyanoacrylate-Fumed Fingermarks

5.1. Introduction

CAF is probably the most important fingermark detection method on non-porous and semi-porous surfaces [1, 7]. CA esters (generally the ethyl ester) are colourless, monomeric liquids that are sold commercially as rapid, high-strength glues (e.g. "superglue"). When heated (or under low atmospheric pressure), CA liquid forms a vapour that reacts with certain eccrine and sebaceous components in a latent fingerprint [67]. The moisture or water in the fingermark ridges prior to fuming has been also found to be important to trigger the polymerization of CA ester [61, 68]. Finally the vapour selectively polymerises on the fingerprint ridges to form a hard, white polymer known as polycyanoacrylate (**Figure 5.1**) [1, 7]. In this way, CA vapour develops latent fingermarks on semi-porous and non-porous surfaces [1, 7].

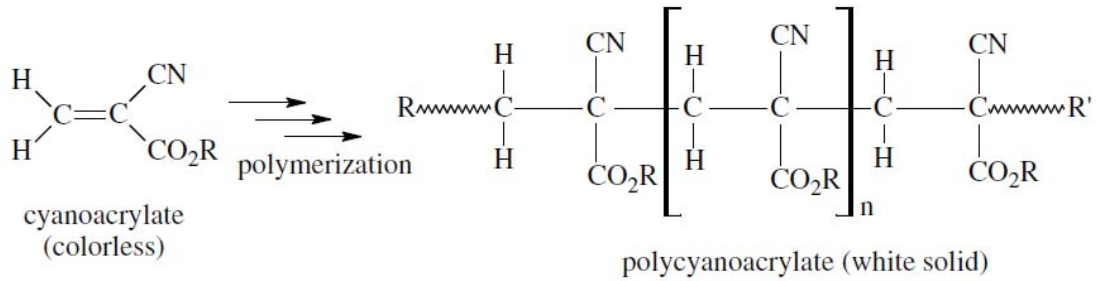

Figure 5.1. CA polymerisation reaction that results in the formation of a hard, white polymer known as polycyanoacrylate [1].

The polycyanoacrylate forms a fibrous layer on fingermark ridges [61]. There are many holes with diameters of around 1 to 2 micrometres within the fibrous layer (**Figure 5.2**) [69].

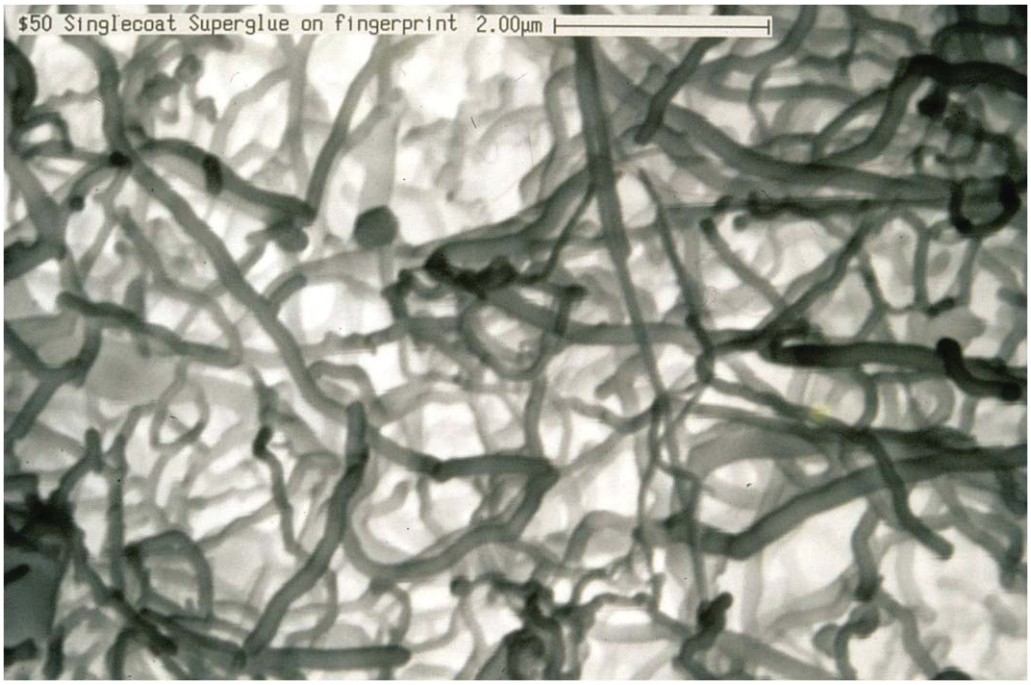

Figure 5.2. Polycyanoacrylate structure on a developed fingermark as imaged by SEM [69].

CAF is generally considered a more sensitive method than powdering [61] and is therefore used more often, especially in a laboratory setting.

In the case of weak CA development, or for light coloured or multi-coloured surfaces, some enhancement is necessary to extract fingermark detail from the background. Two enhancement procedures are commonly used: staining and powdering.

Enhancement with stains

Enhancement can be achieved with coloured or luminescent stains (e.g. Rhodamine 6G). In general, luminescent stains are recommended because of the higher sensitivity of the luminescent mode [1, 7].

Enhancement with powders

The enhancement of CA developed marks can sometimes be achieved on semi-porous, light coloured or luminescent surfaces using common fingerprint powders. However, this only happens when stain solutions cannot be applied [1]. Similarly, luminescent powders generally offer greater sensitivity than non-luminescent powders [7].

Since CAF is probably the most common technique in laboratories for fingermark detection on non-porous surfaces, it is worth investigating the possibility of using an UC as an enhancement technique to eliminate the background disturbance on highly luminescent or patterned substrate. The basic idea is to get smaller $NaYF_4$:Er,Yb UC particles that can penetrate into the holes of the polycyanoacrylate and remain trapped inside. Since the holes in the polycyanoacrylate structure are around 1–2 micrometres, the ideal particles should be smaller than 2 micrometres. Because the commercial $NaYF_4$:Er,Yb UC powder (purchased from Artemis Limited, UK) is a mixture of particles with sizes of ~0.1 to ~15 micrometres when observed under SEM (the majority of the particles ranges from ~0.5 to ~5 μm as seen from **Figure 3.2**), appropriate methods, including sieving, suspension and milling, were investigated to produce a smaller average particle size.

5.2. Sieving

The first attempt to separate smaller particles from larger ones was to use sieves. The experiments were limited to the sieves that were available at the University of Technology, Sydney.

5.2.1. Materials and Methods

To accelerate the sieving process, a Julabo SW 22 shaking bath (John Morris Scientific Ltd., Australia) was used.

A Millipore filter with 1.6 micrometer glass microfiber filter (Whatman, cat No 1820150) was attached to a flask. Two test-sieves (Endecotts Ltd, England), with 15 and 10 micrometre pore sizes respectively, were put above the Millipore filter in order to retain particles bigger than 10 micrometres. Then 5 grams of $NaYF_4$:Er,Yb particles were suspended in 100 mL Milli-Q water and stirred for around 5 minutes. After that, the $NaYF_4$:Er,Yb water suspension was poured into the 15 micrometer sieve. Finally, the whole device was put on the Julabo SW 22 shaking bath at 70 rpm, 25 ℃ for 48 hours to avoid the possible blockage in the holes of the sieves.

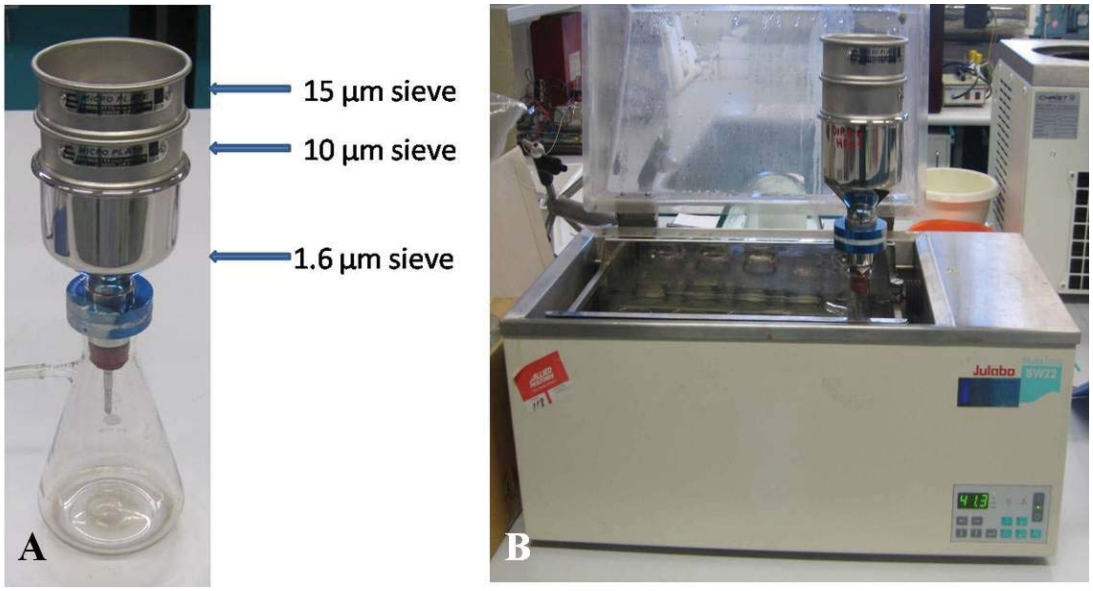

Figure 5.3. Sieving device for the commercial $NaYF_4$:Er,Yb powder showing the order of sieves (**A)**; Sieving device placed in the shaking bath (**B**).

5.2.2. Results and Discussion

Only a small amount (less than 0.5 gram) of UC particles were able to penetrate the first sieve (15 µm). No particles were observed on the glass fibre sieve on the third layer, and there were no visible UC particles on the second sieve (10µm). The smaller particles were unable to get through the three layers to reach the bottom of the flask.

The results demonstrated that sieving is not an ideal method to separate the UC particles, and this was for several reasons. First, the holes in the 15- and 10- μm sieves were so few that it made the speed of separation very low. The Julabo SW 22 shaking bath was supposed to be used to reduce the possible blockage, but it proved not useful for 15- and 10- μm sieves. Second, the cellulose structure of the 1.6 μm glass fibre filter may have retained the smaller particles. Third, from the SEM image (**Figure 3.2**) we can see that the particles smaller than 1.6μm only occupied a very low proportion of the mixture, which resulted in fewer particles available to penetrate all three sieves. Due to the reasons above, sieving was not an ideal method to separate the small particles from the commercial $NaYF_4$:Er,Yb powder.

5.3. Suspension Method

5.3.1. Introduction

According to Stokes' law, the sedimentation rate of a certain type of uncharged particle in a certain liquid is decided by the dimensions of the particle. The bigger the size of the particle is, the quicker it will precipitate in the liquid [70]. Since the $NaYF_4$:Er,Yb powder is a mixture of particles with sizes from 0.1 to 20 micrometres (**Figure 3.2**), in its water suspension particles of different size will precipitate successively, i.e. the larger particles separate and fall first. Accordingly, the particles in the upper suspension should be smaller than those in the precipitate, and the smaller the particles are, the longer they will stay in the upper solution. Hence it may be possible to get the smaller particles by suspending the $NaYF_4$:Er,Yb powder in water and get the upper suspension of a different timing

5.3.2 Materials and Methods

Preparation of Suspension

One gram of $NaYF_4$:Er,Yb powder was suspended in 10 mL Milli-Q water and the suspension sonicated for 30 minutes. After that, it was allowed to rest to wait for the larger particles to settle. In 0.5 hour after 100 μL upper solutions was taken using

a pipette for SEM imaging later, the upper suspension was carefully poured into a clean beaker avoiding carrying the precipitate on the bottom. Then this 0.5 hour's upper suspension rest and larger particles will precipitate on the bottom again. Similarly, in 0.5 hour after 100 μL upper solutions was taken using a pipette, the upper suspension was carefully poured into a clean beaker again and this upper suspension was 1 hour's suspension (from when the sonication finished). Similarly, the 1.5 hour's suspension and 2 hour's suspension were made. Then 100 μL upper solutions of 0.5, 1, 1.5, 2 hours, respectively, was dropped on a silicon wafer, which had previously been sequentially cleaned with ethanol and acetone. The wafer was put in a clean drawer for 48 hours until the water had evaporated, and the particles were then analysed by a LEO Supra 55 VP SEM (Zeiss) equipped with an in-lens secondary-electron detector.

Fingermark detection

Fingermarks were left on glass slides and fumed immediately in a CAF cabinet (FCC171; Carter-Scott Design, Melbourne) using the pre-set mode for fresh fingermarks (5 minutes initial fume time).

The suspension was poured into Petri dishes directly after it was made. CA-fumed glass slide fingermark specimens were immersed in the suspension for around 3 minutes and then rinsed with deionised water and air dried.

Developed fingermarks were illuminated using a laser pointer (Techlasers Enforcer) at a wavelength of 980 nm, and photographed using a Canon single-lens reflex (SLR) camera (EOS 500D).

5.3.3. Results and Discussion

According to Stokes' law, in the $NaYF_4$:Er,Yb powder suspension, the 20 micrometres particles should precipitate first and the particles 0.1 micrometres or smaller in diameter should precipitate last. All the other particles should precipitate in the middle and theoretically a suitable time can be worked out for particles bigger than 2 micrometres to precipitate from the suspension. In this experiment, 4 timings,

0.5, 1, 1.5 and 2 hours were investigated in order to get the upper solution with particles smaller than 2 micrometres.

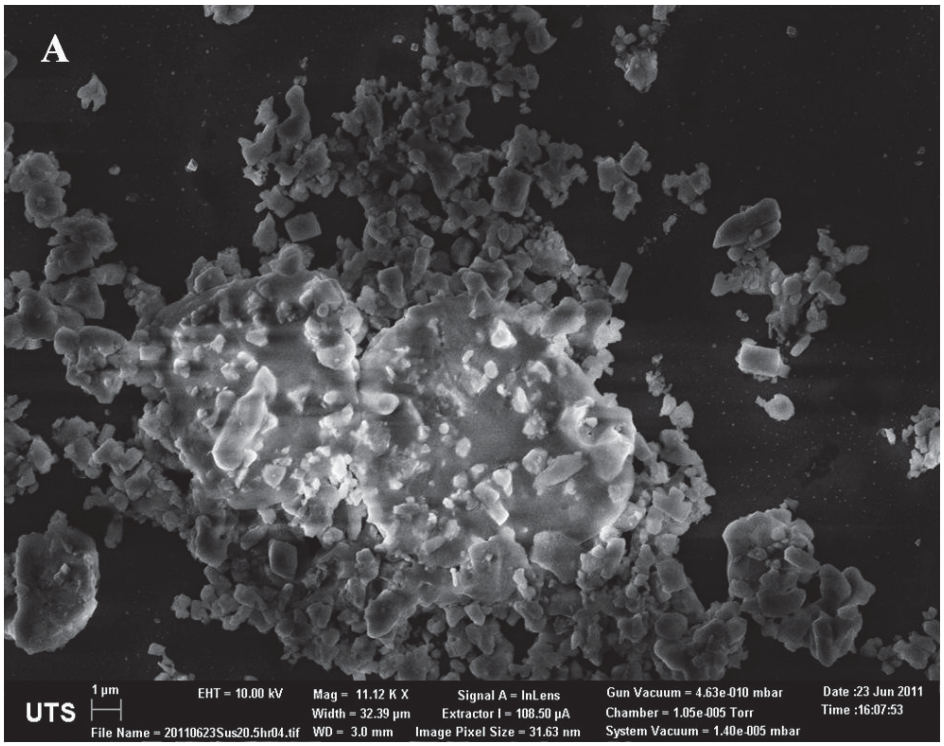

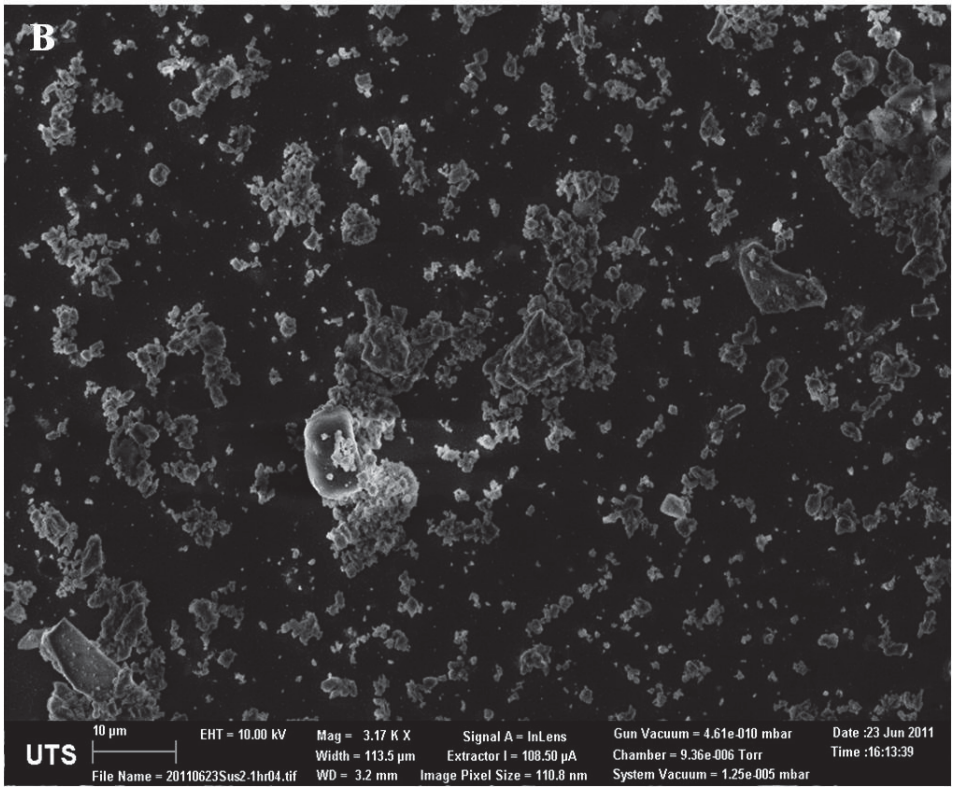

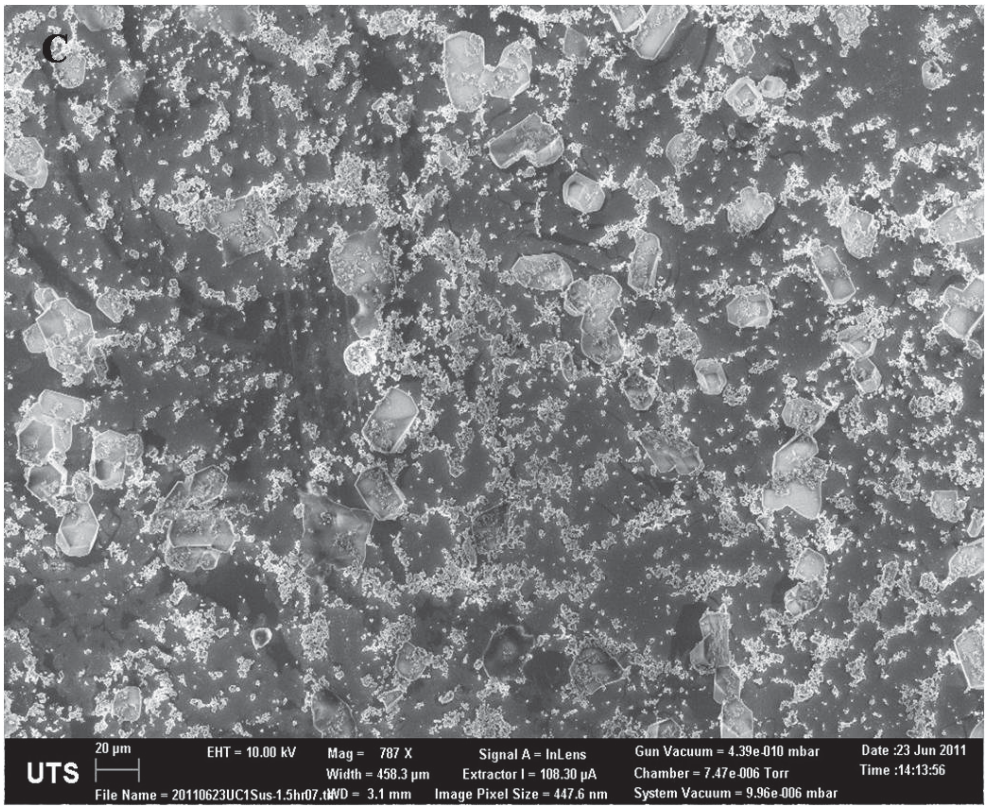

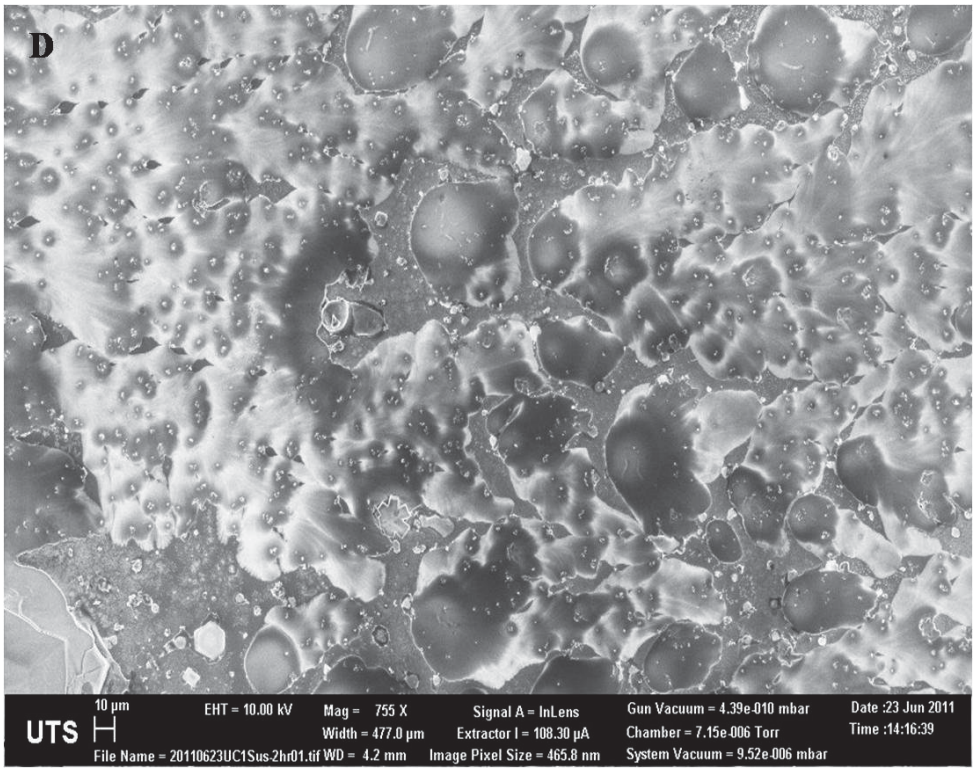

Figure 5.4. The SEM image of 0.5 hour (**A**), 1 hour (**B**), 1.5 hour (**C**), and 2 hour (**D**) suspension of $NaYF_4$:Er,Yb particles.

Figure 5.4 A to D showed the SEM images of the particles in 0.5, 1, 1.5 and 2 hour(s) suspension respectively. In the 0.5 hour suspension (Figure 5.5 A), most particles were smaller than 2 micrometres, but there were a few particles bigger than 2 micrometres or some small particles aggregated into bigger ones with the size of about 6 to 9 micrometres. It was not clear whether the aggregated particles existed in the suspension or the process of evaporation lead to the particles' aggregation. In the 1 hour suspension (Figure 5.5 B), most particles were smaller than 2 micrometres, but there were some particles even bigger than 10 micrometres. There were less particles than the 0.5 hour suspension. In the 1.5 hour suspension (Figure 5.5 C), there were two types of particles: the majority was the particles smaller than 2 micrometres and the minority was the particles with the size around 20 micrometres which was assumed by possible contamination. In the 2 hour suspension (Figure 5.5 D), it seemed the majority was the particles smaller than 2 micrometre with very few bigger particles existing. From the SEM images it can be seen that large particles existed in the 0.5 to 1.5 hour(s) suspension, but settled down in the 2 hour suspension. It seems less particles (rather than less big particles) were found in the later-acquired upper suspension, which agrees with Stokes' law.

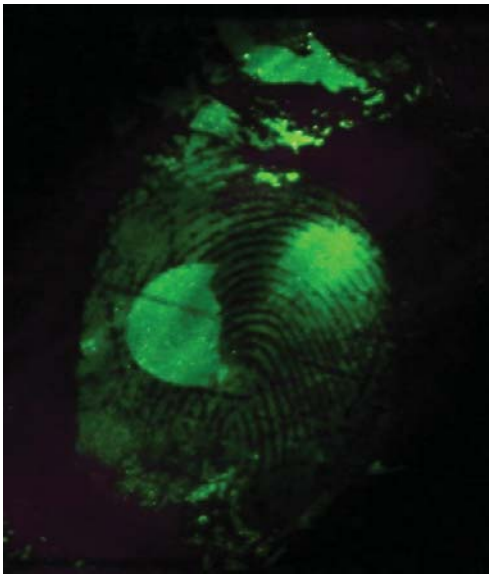

Figure 5.5. Fingermark developed by the 0.5 hour suspension of $NaYF_4$:Er,Yb particles. Photographed using a Canon SLR Digital Camera (EOS 500D) at ISO 400, F6.3, 2S exposure time with illumination from a 980 nm laser pointer.

In terms of fingermark detection, only the 0.5 hour upper solution successfully detected fingermarks (**Figure 5.5**). It accorded with less powder existing in the later suspension. Consequently, the reason for other suspensions not being able to develop ideal fingermarks was probably owing to too few particles existing in the upper suspension after 0.5 hour when most particles already settle on the bottom.

5.4. Ball Milling

5.4.1. Introduction

A ball mill is a type of cylindrical grinder used to grind materials into extremely fine powder, and is used in grinding (or mixing) materials like ores, chemicals, ceramic raw materials and paints. Ball mills rotate around a horizontal axis partially filled with the material to be ground plus the grinding medium. Different materials are used as media, including ceramic balls, flint pebbles and stainless steel balls. High-quality ball mills can be expensive but are able to grind mixture particles to as small as 5 nm, thereby enormously increasing surface area and reaction rates [71].

5.4.2. Materials and Methods

Five grams of $NaYF_4$:Er,Yb powder was weighed and put in the bowl of a Fritsch Pulverisette (type 07.302) milling machine (**Figure 5.6**). Then the balling mill was started at the lowest speed, adjusted to the highest speed, and then running at the highest speed for 10 minutes. The milling process was repeated and the powders were taken out and viewed under a LEO Supra 55 VP SEM (Zeiss) equipped with an in-lens secondary-electron detector.

Figure 5.6. The Fritsch Pulverisette (type 07.302) milling machine used in this study.

5.4.3. Results and Discussion

Although the manual described the average fineness of powders milled by this instrument as being smaller than 1 μm, from the SEM it was observed that the size of the UC particles was not apparently changed. There were still a large number of particles bigger than 10μm as shown in **Figure 5.7**. This resulted showed that the Fritsch Pulverisette (type 07.302) milling machine was not able to grind the commercial $NaYF_4$:Er,Yb powder into the particles smaller than 2 micrometres.

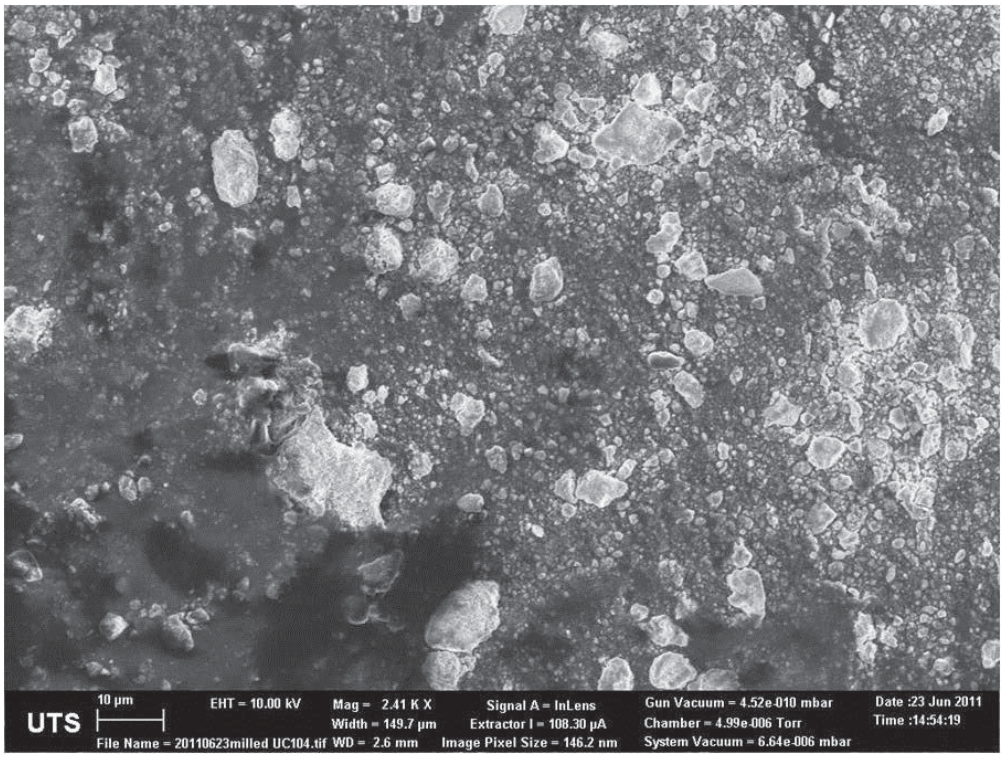

Figure 5.7. The SEM image of $NaYF_4$:Er,Yb particles after being milled.

5.5. Conclusions

In this Chapter, three methods, sieving, suspension and milling, were investigated to separate the smaller particles from the commercial $NaYF_4$:Er,Yb powders. Owing to the limitation of instrumentation and time, no ideal results were acquired. However, this does not mean that the pursuit of smaller particle sizes for these UC powders is flawed, and further research is justified in the future.

Chapter 6

Fingermark Detection by Functionalised UCs

Chapter 6. Fingermark Detection by Functionalised Upconverters

6.1. Introduction

Fingermark detection techniques based on UCs with anti-Stokes luminescence have been investigated in Chapters 3 and 4 and also reported in previous papers [55, 72]. These materials show promising results on a variety of luminescent and/or patterned backgrounds where traditional luminescent fingermark reagents give poor results. However, these UC materials are often insoluble in water and other solvents and this limits their application in staining CA-fumed fingermarks. Since CAF is probably the most common laboratory technique for fingermark detection on non-porous surfaces, it is worth investigating the possibility of making UCs soluble or dispersible in water by functionalizing them with hydrophilic groups [1, 7, 61]. These functionalised UC nanoparticles (UCNPs) are being increasingly used in medical imaging or as biological labels [37, 51, 52, 73-79]. In medical applications, UCNPs are generally illuminated by IR light with better penetration and less damage to human tissues compared to ultraviolet or short-wavelength visible radiation, which conventional luminescent labels need. Among these functionalised UCNPs the functionalised $NaYF_4$:Er,Yb is particularly interesting because $NaYF_4$:Er,Yb is one of the most efficient upconversion lattices known to date [37, 40]. In this Chapter, the synthesis and assessment of several functionalised $NaYF_4$:Er,Yb complexes is described for fingermark detection on a range of non-porous and semi-porous surfaces. These water-soluble UCNPs are polyethylenimine/$NaYF_4$:Er,Yb (UC-PEI), $NaYF_4$:Er,Yb-azelaic acid (UC-AA), polyvinyl pyrrolidone/$NaYF_4$:Er,Yb (UC-PVP) and sodium bis (2-ethylhexyl) sulfosuccinate/ $NaYF_4$:Er,Yb (UC-AOT).

Branched PEI is an organic polymer surfactant with a number of primary, secondary and tertiary amino groups (**Figure 6.1**) which can form complexes with

metal ions via coordination [41, 80]. The hydrophilic and positively charged amino groups of PEI can stabilize the nanoparticles in solution and also make the functionalised complexes (UC-PEI) soluble or well dispersed in water [41, 80]. The high decomposition temperature of PEI (approximate 310 °C for the 25 kD PEI) also makes it the polymer of choice for some hydrothermal synthesis reactions.

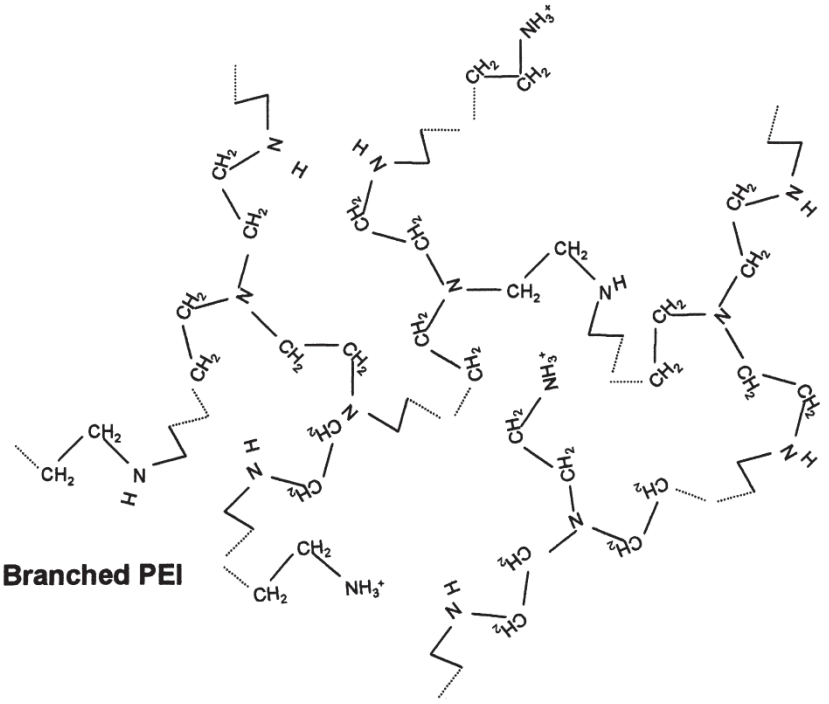

Figure 6.1. The structure of branched PEI [80]

Today oleic acid has been widely used as the capping ligand in many synthesis reactions for functionalised UCs and other nanoparticles [52, 81]. Herein, a two-step reaction was introduced for synthesising water-soluble UCNPs by functionalising UCs with oleic acid first and then oxidising the oleic acid ligands into carboxylic acid with the Lemieux-von Rudloff reagent [52]. **Figure 6.2** shows the simplified synthesis mechanism of this new approach. In the first reaction the UCNP core was synthesised and the oleic acid was attached to the UCNP via the carboxylic end; in the second reaction the –CH=CH– group in the oleic acid was cleaved and oxidised by the Lemieux-von Rudloff reagent into azelaic acid (AA). The Lemieux-von Rudloff agent (a mixture of permanganate and periodate solutions) is well-known to oxidise selectively a carbon-carbon double bond (R-CH=CH-R') to give two

carboxylic acids ($HOOC(CH_2)_7COOH$) which is hydrophilic [82]. The product in the first reaction, the oleic acid-functionalised nanoparticles are not soluble in water due to the hydrophobic property of the oleic acid end but the final product, the azelaic acid-functionalised nanoparticles, are soluble in water with many hydrophilic carboxylic acid groups as the end.

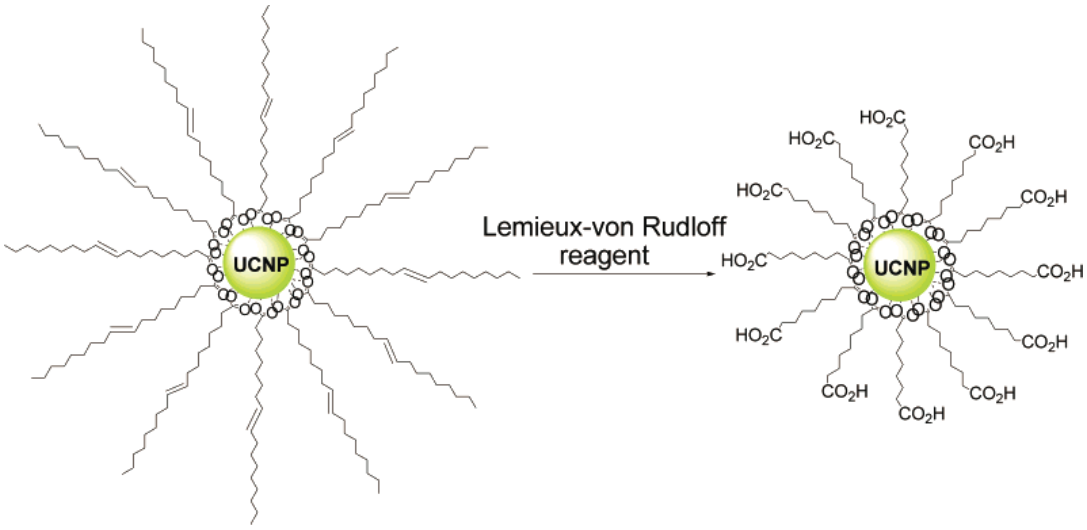

Figure 6.2. Synthesis mechanism of carboxylic acid-functionalised UCs from oleic acid-capped precursors [52].

Polyvinylpyrrolidone (PVP) is an amphiphilic surfactant which can make the nanoparticles dispersible in water and its pyrrolidone groups can coordinate with lanthanide ions [51]. PVP was used in this work as the chelating agent to synthesise $NaYF_4$ nanocrystals with controlled size and shape (**Figure 6.3**). Furthermore, the UC/PVP nanocrystals could be directly coated with a uniform layer of silica to produce a surface for the conjugation of biomolecules. The silica coating can also improve the photostability of the nanoparticles [51].

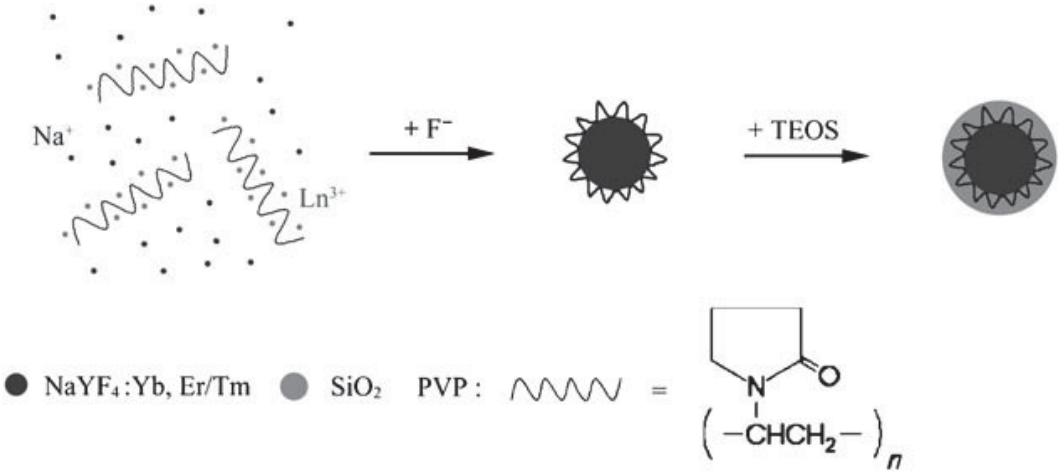

Figure 6.3. Synthesis of silica-coated PVP/$NaYF_4$ nanocrystals doped with lanthanide ions. TEOS=tetraethoxysilane [51].

An amine functionalised UCNP, UC-AOT, was synthesised using a modified hydrothermal microemulsion synthetic strategy assisted with bi-functional ligand 6-aminohexanoic acid [83]. Due to the presence of free amine moieties on their surfaces, the UC-AOT was well dispersed in water and can be covalently linked to other functional group as well (**Figure 6.4**).

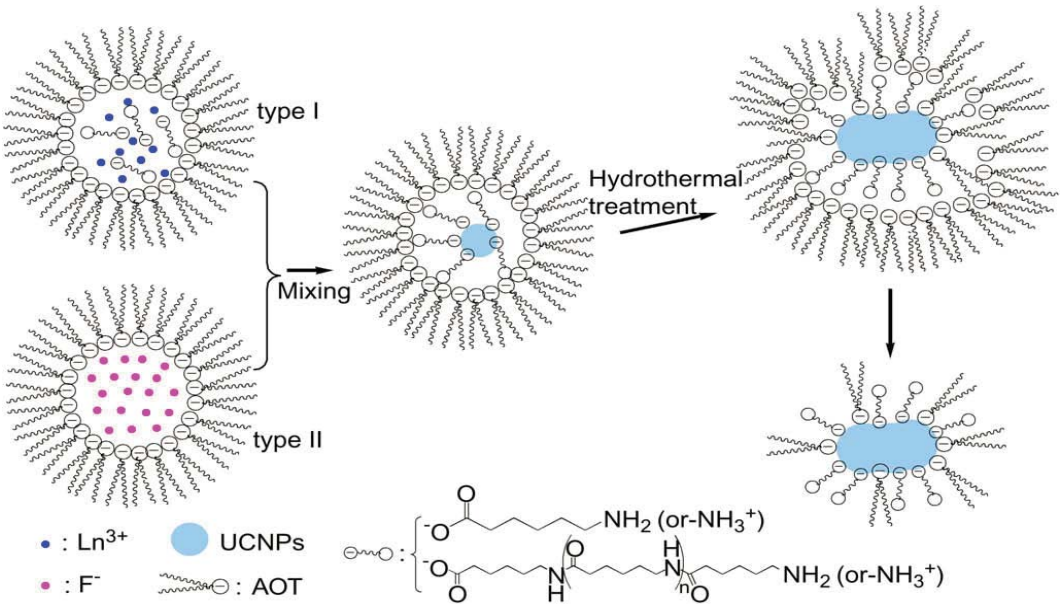

Figure 6.4. Synthesis mechanism for biocompatible UCNPs by a modified hydrothermal micro-emulsion route [83].

6.2. Materials and Methods

6.2.1. General

Two donors supplied latent fingermarks for this work. Non-CA-fumed fingermarks were deposited after the donors wiped their fingers over their forehead or facial area just prior to fingermark deposition. For comparison with rhodamine 6G, sets of three fingermarks (index, middle and ring fingers) were deposited on soft drink cans, plastic soft drink labels and Australian polymer banknotes, and then these samples were cut in halves (down the centre of the middle finger impression). The left side of each set was treated by CAF/rhodamine 6G staining, and the right side treated by CAF/UC-PEI or UC-AA staining. For CA-fumed fingermarks, the fingermarks were fumed immediately after deposition on the substrates; in this case, the fingers were not "charged" by wiping the fingers over the forehead or facial area prior to fingermark deposition.

Developed fingermarks were illuminated separately with white light (for conventional reflection mode imaging), with 530 nm green light from the Rofin Polilight (for conventional luminescence mode imaging), or by a laser pointer (Techlasers Enforcer) operating at a wavelength of 980 nm (for upconversion mode imaging). Images were recorded under the same conditions as in Chapter 4.

6.2.2. Synthesis and Characterization of Functionalised UCs

6.2.2.1. Synthesis and Characterization of UC-PEI Nanoparticles

Branched Polyethylenimine polymer ($(-NHCH_2CH_2-)_x(-N(CH_2CH_2NH_2)CH_2CH_2-)_y$), sodium chloride (≥99.0%), yttrium(III) chloride hexahydrate (99.99%), ytterbium(III) chloride (99.99%), erbium(III) chloride (99.99+%) and ammonium fluoride (98+%) were purchased from Sigma-Aldrich and were used as received. Milli-Q deionised water (DI water; 18.2Ω) was used to prepare stock solutions: polyethylenimine (5 wt%) and YCl_3, $YbCl_3$, $ErCl_3$, NaCl (all 0.2 M).

Synthesis

UC-PEI nanoparticles were synthesised using a modified literature procedure [41]. Aqueous solutions (0.2 M) of NaCl (2 ml), YCl_3 (1.6 ml), $YbCl_3$ (0.36 ml) and $ErCl_3$ (0.04 ml) were added to an ethanolic solution of PEI (prepared by dissolving 4 mL of stock PEI solution in 12 mL of ethanol). After thorough stirring, 0.0593 g of NH_4F was added. The mixture was transfered into a stainless autoclave with a Teflon tube as the liner. Then the autoclave was heated at 200 °C for 24 hours in an oil bath with continuous stirring. The resultant nanoparticles were collected by centrifugation, washed with ethanol and Milli-Q water three times, and dried using a vacuum freeze drier (John Morris Scientific, Alpha 2-4 LD Plus) for 24 hours.

Characterization

The synthesised UC-PEI particles were characterised by fluorescence spectrometry, scanning electron microscopy, and FTIR.

SEM images were obtained using a Phillips XL 30 series environmental scanning electron microscope with an accelerating voltage of 20 kV.

Fluorescence spectra for UC-PEI were measured by an Ocean Optics USB2000+ spectrometer, illuminated with a 1.5 watts laser diode (PSU-III LED/LD-WL206, from OEM Laser System, Inc) at 980 nm.

The FTIR spectra were measured using a Nicolet Magna-IR 760 Spectrometer with a DTGS KBr detector. The powder of sample UC-AA was dispersed in KBr discs and all spectra were obtained using 4 cm^{-1} resolution and 64 scans at room temperature.

6.2.2.2. Synthesis and Characterization of UC-AA

Synthesis of UC-AA nanoparticles

The UC-AA was prepared by modification of literature procedures [52, 84]. All the chemicals were of analytical grade and were used without further purification.

Oleic acid was obtained from Ajax Finechem Pty. Ltd (Sydney, Australia). All other chemicals were purchased from Sigma-Aldrich.

Synthesis of UC-Oleic Acid (UC-OA) nanoparticles

NaOH (1.2 g, 30 mmol), water (9 mL), ethanol (10 mL), and oleic acid (20 mL) were mixed under magnetic stirring to form a homogeneous solution. Then 0.5 mol/L rare-earth chloride (1.2 mL in total including 0.096 mL YCl_3, 0.240 mL $YbCl_3$ and 0.024 $ErCl_3$) was mixed together first and then added to the homogeneous solution under magnetic stirring. After that, 1.0 M aqueous NaF (4 mL) solution was added slowly. The mixture was stirred for 10 minutes and then transferred to a stainless autoclave with a Teflon tube inside as the liner. The autoclave was sealed, and heated at 160 °C for 8 hours. The system was naturally cooled to room-temperature, and all the products were poured into a beaker. Approximately 50 mL cyclohexane was used to dissolve and collect the *UC-OA*. The products were subsequently deposited by adding ethanol (about 80 mL) to the sample-containing cyclohexane solution. The resulting mixture was then centrifuged to obtain powder samples. Pure *UC-OA* powders can be acquired by washing the samples three times with ethanol to remove oleic acid and other remnants.

Converting Hydrophobic UC-OA nanoparticles into Hydrophilic UC-AA

0.1g UC-OA samples (synthesised from the last step), cyclohexane (100 mL), *tert*-butanol (70 mL), water (10 mL) and 5 wt % K_2CO_3 aqueous solution (5 mL) were mixed together and stirred at room temperature for 20 minutes. Then, 0.449 g $NaIO_4$ was added to 20 mL Milli-Q deionised water under stirring until it was completely dissolved. After that, 0.018 g $KMnO_4$ was added to the $NaIO_4$ solution to form the Lemieux-von Rudloff reagent. The Lemieux-von Rudloff reagent was added dropwise to the above solution and the mixture was stirred at about 40 °C for 2.5 hours. Subsequently, the product was isolated by centrifugation and washed with deionized water, acetone and ethanol. The product was then dispersed in 50 mL hydrochloric acid of pH 4-5, and the mixture was stirred for 30 minutes. Finally, the product was collected by centrifugation, washed twice with deionized water and

dried in a vacuum freezing drier (John Morris Scientific, Alpha 2-4 LD Plus) for 24 hours.

Besides UC-AA, a small quantity of UC(Ho)-AA ($NaYF_4$:Ho,Yb/azelaic acid) and UC(Tm)-AA ($NaYF_4$:Tm,Yb/azelaic acid) were also synthesised by using Holmium or Thulium chloride instead of Erbium chloride under the same conditions as described in the Section of *Synthesis of UC/Oleic Acid (UC/OA) nanoparticles*, but no characterization and fingermark detection were done for the UC(Ho)/AA and UC(Tm)/AA particles.

Characterization

The synthesised UC-AA particles were characterised by fluorescence spectrometry, Scanning Electron Microscopy, and FTIR.

SEM images were obtained using a Phillips XL 30 series environmental scanning electron microscope with an accelerating voltage of 20 kV.

Fluorescence spectra were measured by an Ocean Optics USB2000+ spectrometer, illuminated with a 1.5 watts laser diode at 980 nm in the Molecular and Health Technologies facility, Commonwealth Scientific and Industrial Research Organisation (CSIRO), Clayton, Australia.

The FTIR spectra were measured by a FTS7000 infrared spectrometer (Digilab, USA) with a DTGS KBr detector. The powder of sample UC-AA was dispersed in KBr discs and all spectra were obtained using 4 cm^{-1} resolution and 64 scans at room temperature.

6.2.2.3. Synthesis of UC-PVP

The UC-PVP was synthesised by modification of literature procedures [51]. All the chemicals were purchased from Sigma-Aldrich and used as received. The PVP/$NaYF_4$:Yb (20%), Er (2%) nanoparticles were synthesised according to the following procedure. $LnCl_3$ mixture was prepared as follows. $Y_2Cl_3 \cdot 6H_2O$ (237 mg, 0.78 mmol), $Yb_2Cl_3 \cdot 6H_2O$ (77.5 mg, 0.2mmol), and $Er_2Cl_3 \cdot 6H_2O$ (7.6 mg, 0.02mmol) were mixed together according to the ratio of Y 78%, Yb 20% and Er 2%.

This mixture was then heated to evaporate the water completely. Ethylene glycol (10 mL) was added to dissolve the $LnCl_3$ mixture. PVP (0.5560 g) and NaCl (0.0588 g, 1 mmol) were subsequently added to the $LnCl_3$ mixture and the solution was heated to 80 °C to form a homogeneous solution. Then NH_4F (0.1482g, 4 mmol) was dissolved in ethylene glycol (10 mL) at 80 °C and added dropwise to the $LnCl_3$ solution. The whole solution was stirred and kept at 80°C for 10 minutes. Afterwards the solution was heated to 160°C for 2 hours and then cooled to room temperature. The final product was collected by centrifugation, washed twice with absolute ethanol and dried in a vacuum freeze drier (John Morris Scientific, Alpha 2-4 LD Plus) for 24 hours. The luminescence of the synthesised product was checked using a 700 mW laser pointer (Techlasers Enforcer).

6.2.2.4. Synthesis of UC-AOT

All of the chemicals were of analytical grade and were used as received. NaF, ethanol, methanol, acetone, n-heptane, N,N-dimethylformamide (DMF), 6-aminohexanoic acid, sodium bis(2-ethylhexyl) sulfosuccinate (commonly known as AOT) and rare-earth chlorides ($LnCl_3$, Ln^{3+}: Y^{3+}, Yb^{3+}, Er^{3+}) were obtained from Sigma-Aldrich.

Synthesis of UC-AOT

The UC-AOT was prepared Based on a literature procedure[83]. In this synthesis, two types of micro-emulsions (types I and II) were respectively prepared by adding different aqueous phases to n-heptane solution. First 2.667 g AOT was dissolved in about 80 mL n-Heptane with stirring to form a clear solution (0.075 mol/L). In the type I micro-emulsion, 0.4 mL 6-aminohexanoic acid (0.375 mol/L) water solution and 0.2 mL rare-earth chloride (0.5 mol/L $LnCl_3$, Ln^{3+}: 78 mol% Y^{3+}+20 mol% Yb^{3+}+2 mol% Er^{3+}) water solution were added to 40 mL of the above n-heptane solution. In the type II micro-emulsion, 0.6 mL NaF (1 mol/L) was added into the rest 40 mL of n-heptane solution. The micro-emulsions were stirred for 1 hour repectively until the mixtures appeared clear which indicated the formation of the micro-emulsions. Then these two micro-emulsions were mixed and stirred for another 20 minutes. The resulting mixture was then transferred to a stainless

autoclave with a Teflon tube inside as the liner. The autoclave was sealed and heated at 180 °C for 6 hours before it was cooled to room temperature naturally. Then 8 mL acetone was added to the product and the mixture was centrifuged at 12,000 rpm for 20 minutes. Pure UCNP powders was obtained by washing the samples with the n-heptane and ethanol several times to eliminate excessive AOT and other remnants. The precipitates were then dried in a vacuum freezing drier (John Morris Scientific, Alpha 2-4 LD Plus) for 24 hours.

6.2.3. Fingermark Development

6.2.3.1. Fingermark Development using UC-PEI

UC-PEI as a dry powder

Although the original aim of the application of UC-PEI particles was for staining CA-fumed fingermarks, the possibility of using it as a powdering method was also explored. The UC-PEI particles were applied to non-CA-fumed fingermarks on the glass slides and polyethylene plastic bags using squirrel fingerprint brushes (Optimum Technology, Australia).

UC-PEI as a staining reagent after CAF

UC-PEI powder was dispersed in Milli-Q water at a concentration of 1% (w/v). The dispersion was sonicated for 10 minutes before application to fingermarks. The fingermark samples were placed on the table with the CA-fumed fingermarks facing upwards. A small amount (< 2mL) of UC-PEI solution was taken out using a pipette and then dropped to the CA-fumed fingermarks. The fingermarks were “soaked” in the suspension for 5 to 20 minutes and then rinsed in water and dried in air. The left side of each set of three fingermarks was treated by CAF/rhodamine 6G staining, and the right side treated by CAF/UC-PEI staining. CAF was performed in a CAF cabinet (FCC171; Carter-Scott Design, Melbourne) using the preset mode for fresh fingermarks (5 minutes initial fume time). After being fumed, the specimens were dipped into the rhodamine 6G working solution for about 10 seconds, rinsed with water, air dried and then visualised in luminescence mode at 530 nm with a 610 nm band pass barrier filter using the Rofin Poliview. The rhodamine 6G formulation was

that currently employed by the Australian Federal Police [48]. The right side of each set was treated by UC-PEI staining. Then, the UC-PEI stained fingermarks were illuminated and recorded in upconversion mode as described before. In other words, both sides were treated and visualized under optimal conditions for each half and then the recorded images compared.

6.2.3.2. Fingermark detection using UC-AA

UC-AA powder was dispersed in Milli-Q water at a concentration of 0.5% (w/v). The dispersion was sonicated for 10 minutes before application to fingermarks. The fingermark samples were placed on the table with the CA-fumed fingermarks facing upwards. A small amount (< 2mL) of UC-AA solution was taken out using a pipette and then dropped to the CA-fumed fingermarks. The fingermarks were "soaked" in the solution for 3 to 20 minutes and then rinsed in water and dried in air. For comparison with rhodamine 6G, the same procedures were conducted as those of UC-PEI. The left side of each set was treated by CAF/rhodamine 6G staining and illuminated and recorded in luminescence mode, and the right side treated by CAF/UC-AA staining and illuminated and recorded in upconversion mode. Both sides were treated and visualized under optimal conditions for each half and then the recorded images compared.

Fingermark detection using UC-PVP and UC-AOT were not considered since, as we shall see next, their luminescence is quite low. This is also mentioned at the end of this Chapter.

6.3. Results and Discussion

6.3.1. UC-PEI

6.3.1.1. Characterisation of the UC-PEI powder

The isolated UC-PEI was a white fine powder with about 0.12 g obtained from each batch.

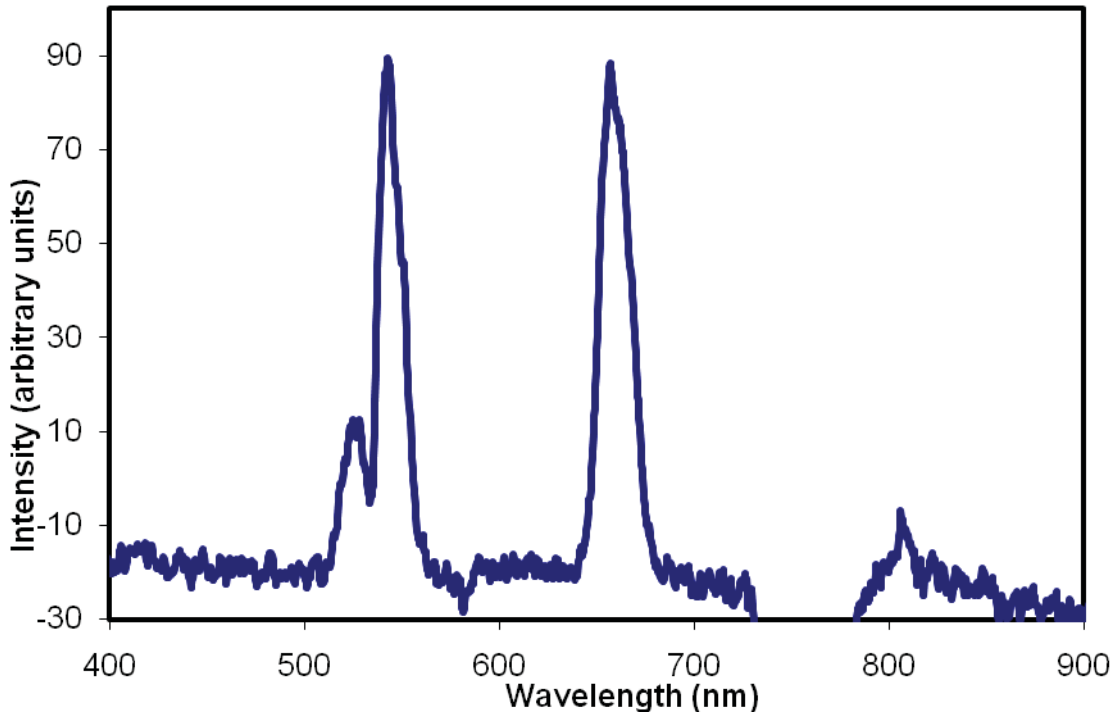

Figure 6.5. Luminescence emission spectrum for UC-PEI when illuminated by a 1.5 watt laser diode at 980 nm.

Figure 6.5 shows the luminescence emission spectrum of the UC-PEI particles in the solid state. Two emission peaks at 550 nm and 670 nm are observed, which are very similar in wavelength to those seen in the spectrum of unmodified $NaYF_4$:Er,Yb particles. However, the luminescence intensity was significantly weaker than that of the $NaYF_4$:Er,Yb nanoparticles. There may be several reasons for this. First, the existence of the α-cubic phase, which is unavoidable under the above synthetic conditions, makes the crystals less efficient in terms of luminescence emission intensity [41]. Two crystal phases for $NaYF_4$:Er,Yb have been reported, the α-cubic and β-hexagonal phases [37]. The luminescence intensity of the β-hexagonal phase is approximately ten times greater than that of the α-cubic phase [40]. Second, it is known that 100 nm is the threshold for high luminescence efficiency of certain UCs [85]. The average size of the UC-PEI particles was 50 nm (determined by analysis of SEM images) and they may more or less contain a significant number of crystal defects that will reduce the luminescence efficiency.

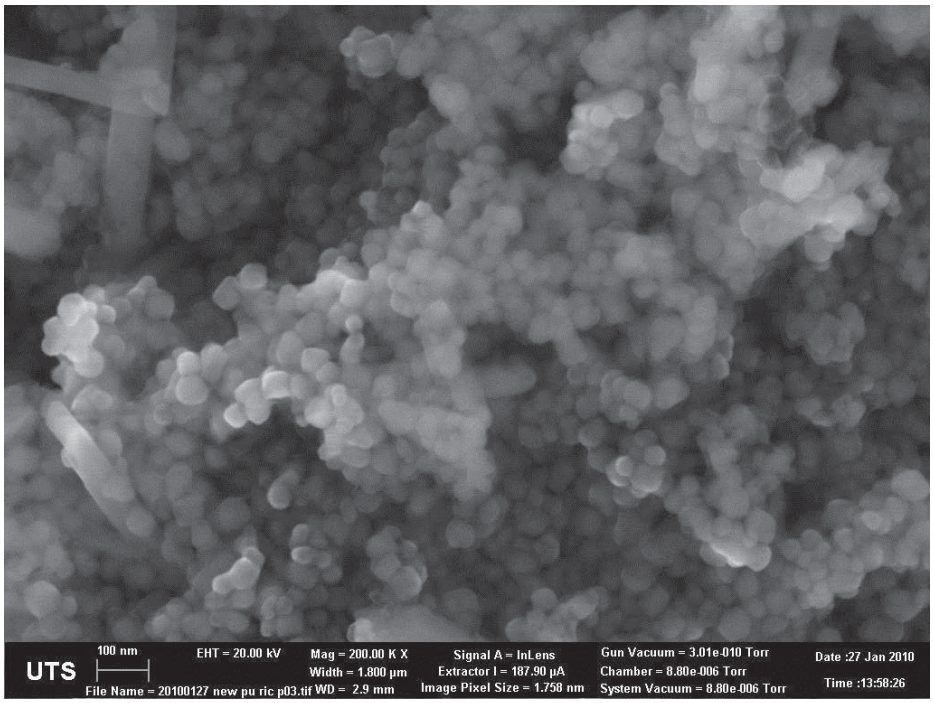

Figure 6.6. SEM image of the synthesised UC-PEI particles.

Figure 6.6 shows a representative SEM image and reveals that the majority of the synthesised nanoparticles appear spherical in shape. The average particle size is approximately 50 nm. There are also a small proportion of larger cubes with sides ~300 nm. Although PEI can stabilize the nanoparticles in the solution and hence control the growth of crystals, it was still difficult to get UC-PEI particles with ideal size (50 nm) [41]. It seemed that continuous stirring played an important role in reducing the quantity of large cubes and acquiring small globes with even size in the products.

The FTIR spectrum (**Figure 6.7**) shows bands that are assigned to PEI. These include bands arising from internal vibration of the amide bonds (1380–1630 cm^{-1}) and CH_2 stretching vibrations (2850–2960 cm^{-1}). These bands are absent in the spectra of the unmodified UC particles. The result showed that the PEI was attached to the UC particles.

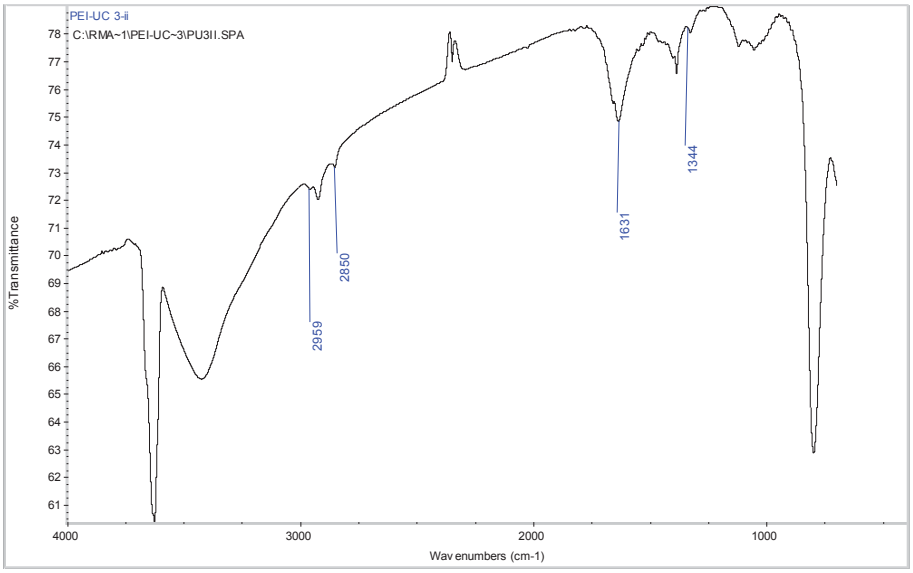

Figure 6.7. FTIR spectrum for the synthesised UC-PEI.

6.3.1.2. UC-PEI as a dry dowder for fingermark detection

Figure 6.8 shows fresh fingermarks developed on a glass slide using dry UC-PEI particles. The UC-PEI particles show a much poorer affinity for the fingermarks compared to other conventional fingermark powders such as aluminium powder. However, it is still able to develop reasonable images for fresh fingermarks on glass slides by repeating the powdering process several times. In summary, the UC-PEI was not an ideal fingermark detection powder.

Figure 6.8. Fresh fingermarks developed by UC-PEI particles on a glass slide (applied as a dry powder). Illuminated with a 980 nm laser light and imaged using a Rofin Poliview fitted with a 555nm band pass filter and using an exposure time of approximately 10 seconds.

6.3.1.3. UC-PEI for staining CA-fumed fingermarks

A UC-PEI dispersion in water (obtained by sonicating for 10 minutes) was found to be stable for at least 2 hours. When applied as a staining reagent, the UC-PEI was satisfactory on most of the surfaces treated. **Figure 6.9** shows fresh fingermarks on an aluminium soft drink can developed with CAF followed by UC-PEI staining. The fingermark images were with reasonably clear ridges and the background printing was effectively eliminated. In **Figure 6.10** the fingermark image is remarkably clear despite the highly luminescent background.

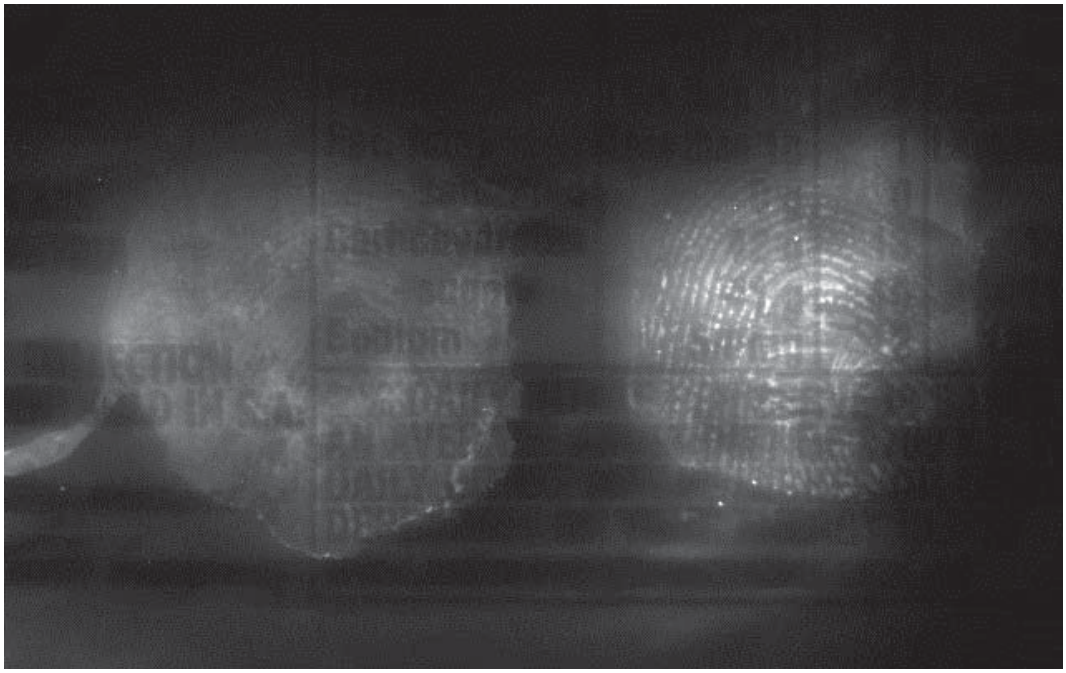

Figure 6.9. Fresh fingermarks on a soft drink can developed with CAF followed by UC-PEI staining. Illuminated using a 980 nm laser pointer with 20s exposure time and imaged using a Rofin Poliview system with a 555nm band pass filter.

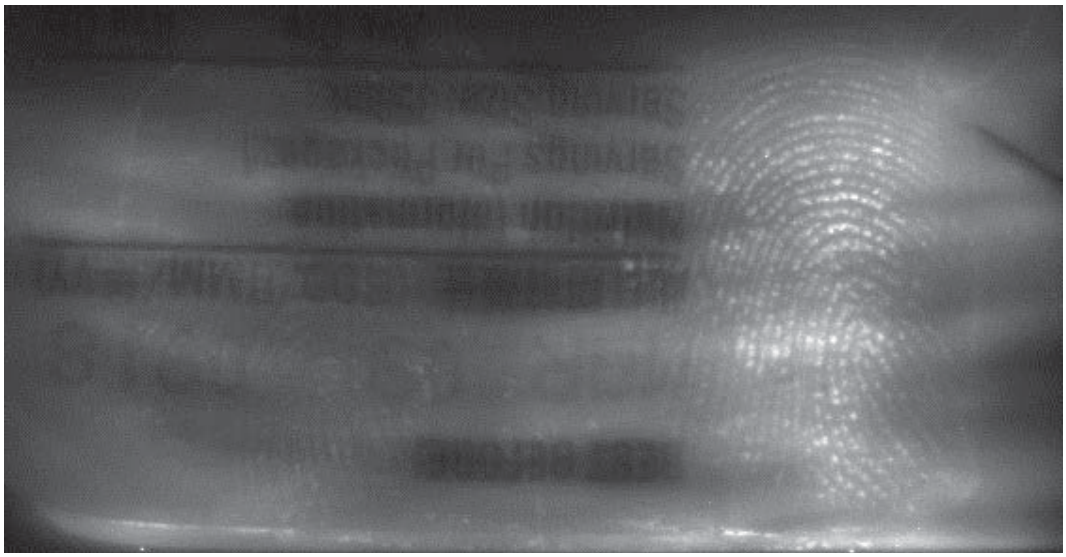

Figure 6.10. Fresh fingermarks on a plastic label developed with CAF followed by UC-PEI staining. Illuminated using a 980 nm laser pointer with 20s exposure time and imaged using a Rofin Poliview system with a 555nm band pass filter.

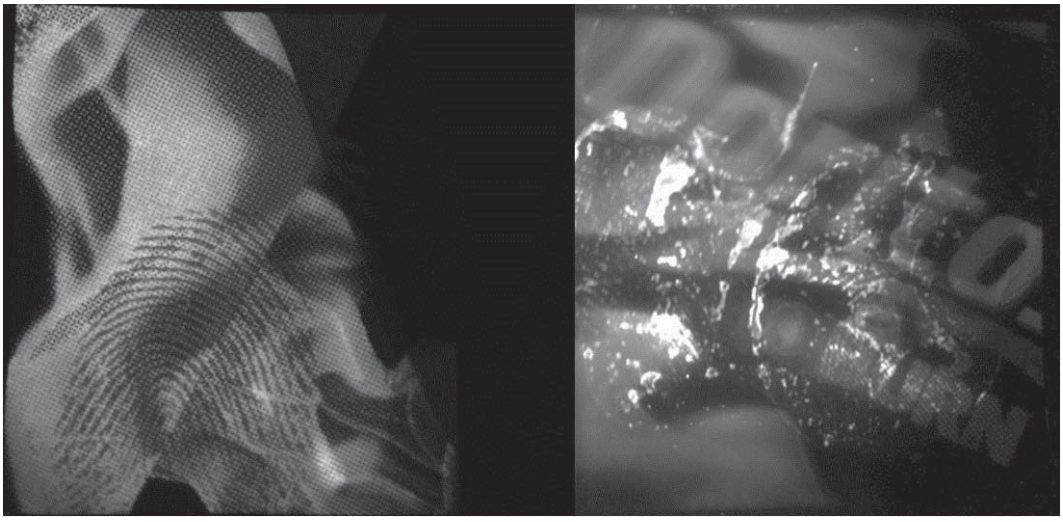

Figure 6.11. CAF fingermarks on a plastic soft drink label followed by different staining methods. (Left) rhodamine 6G staining, illumination at 530 nm with 610 nm band pass filter; (Right) UC-PEI staining, illumination at 980 nm and imaged using a Rofin Poliview with a 555nm band pass filter and an exposure time of approximately 10 seconds.

Figure 6.11 shows the effect of rhodamine 6G staining, in comparison with UC-PEI staining on CA-fumed fingermarks. Owning to the unevenness of background

luminescence, colour and pattern distribution, the effectiveness of CAF/rhodamine (or UC-PEI) staining also varies on different parts of the substrate. For example, by rhodamine 6G staining the left fingermark was visible, whereas the left half of the middle fingermark was completely invisible due to the background absorbance. However, the right half of the middle fingermarks was reasonably visible by UC-PEI staining which was under the same dark colour as the left half. Also the effectiveness of UC-PEI staining varies on different part of the surface, for example, the right fingermark was not much visible because the CA polymer was poorly stained at this part.

In **Figure 6.12**, on the left half of the soft drink label, the CAF/rhodamine 6G staining developed fingermarks were nearly invisible due to the background absorbance and printing luminescence interference, but on the right half, the CAF/UC-PEI staining developed fingermarks were much clearer and the background luminescence interference was relatively lighter. This shows the advantage of UC-PEI staining on the surfaces where conventional luminescence techniques are ineffective. However, in the CAF/UC-PEI staining developed fingermark, there were some letters with bright luminescence in the background that disturbed the upconversion luminescence. The reason for the bright letters in the background was not clear. A possible explanation is that upconversion luminescence has a wide range from 400 nm to 700 nm (see Figure 6.5) and the reflected light of the upconversion luminescence became excitation light itself. It can illuminate the luminescence (normal luminescence with stokes shift) of the letters in the background. Because the normal luminescence with stokes shift is much efficient than the upconversion luminescence, these letters in the background appeared very bright under long exposure time [54, 56].

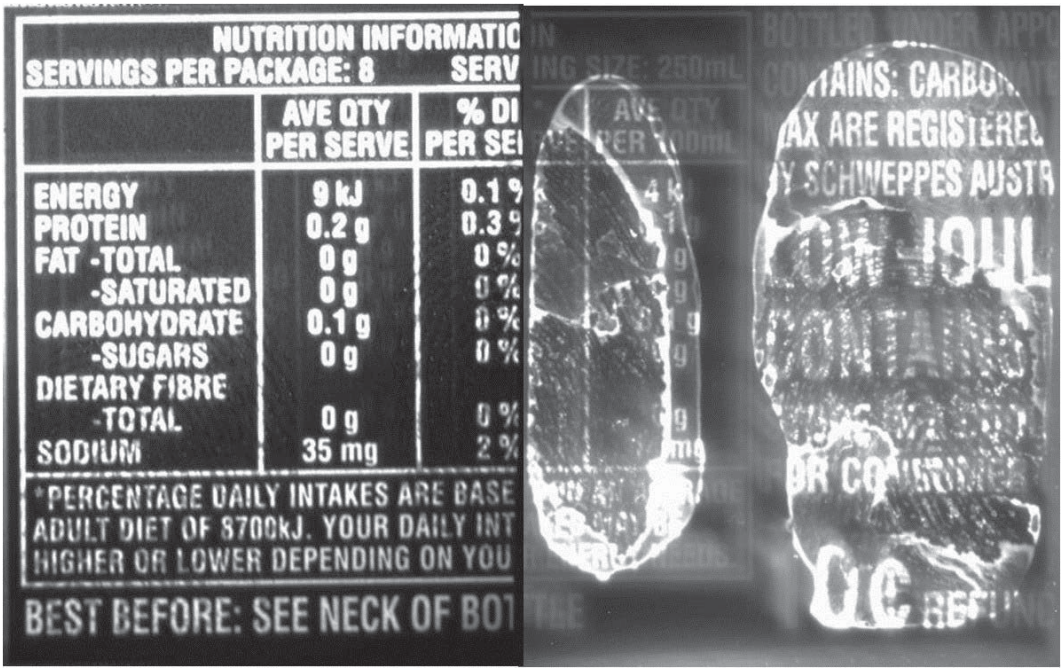

Figure 6.12. CAF fingermarks on a plastic label followed by different staining methods. (Left) rhodamine 6G staining, illumination at 530 nm with 610 nm band pass filter; (Right) UC-PEI staining, illumination at 980 nm and imaged using a Rofin Poliview with a 555nm band pass filter and an exposure time of approximately 33.7 seconds.

On the Australian polymer banknotes, another well-known "difficult" surface, the UC-PEI staining did not reveal any satisfactory images, not even any luminescence was seen either. Considering that clear fingermarks have been developed on the banknotes in the previous Chapters by $NaYF_4$:Er,Yb powder (**Figure 3.10**) and YVO_4:Er,Yb powder (**Figure 4.6**), this was owed more to CAF not being effective on the banknote, rather than the defect of UC-PEI [60]. CAF/staining solely is not able to develop fingermarks on the polymer banknotes and it has to be combined with vacuum metal deposition (VMD) or infrared chemical imaging [60, 65, 86, 87]. Further research may be conducted to explore the full possibility of UC-PEI for fingermark detection on polymer banknotes, together with the improvement of CAF.

6.3.1.4. The factors affecting imaging and fingermark detection using UC-PEI

Luminescence Intensity

The luminescence intensity of the functionalised UCs was closely related to the effectiveness of fingermark detection, i.e., the more luminescent the UCs, the better they were at fingermark detection. For example, the luminescence of UC-PEI fluctuated slightly from batch to batch due to the difficulty to control the quality of nanoparticles. The batches with stronger luminescence were better at fingermark detection than those with weaker luminescence. This observation was particular important in UC-AA which will be described in Section 6.3.2 since it was more difficult to control the quality of UC-AA in the synthesis reaction.

Detection method

Because the functionalised UC was difficult to be synthesised and purified under the conditions during this study, generally only a small amount of UC-PEI with ideal morphology and luminescence property can be obtained. As the result, the UC-PEI cannot be prepared in bulk solution and the whole fingermark samples (plastic, glass, soft drink cans and labels, etc) cannot be soaked in the solution. Instead, only the fingermarks on the samples can be "soaked" in the UC-PEI solution (<2 mL) which means only the UC-PEI particles in the small amount solution can possibly deposit on the fingermark ridges. That certainly reduced the chance of the CA-fumed fingermarks to be well stained and resulted that some fingermark details were invisible more or less under the illumination of laser, for example, the right fingermark in Figure 6.11.

Exposure Time

Another important factor in photographing upconversion luminescence is long exposure times owing to the weaker luminescence emission compared to conventional luminescence since upconversion is not an efficient optical process [54, 56]. Because of the long exposure times, the background was generally visible when illuminated by the luminescence emission from the (functionalised or not functionalised) UCs. Long exposure times also tended to result in a blurry

background. However, this background disturbance should still be much weaker than that encountered with traditional luminescence, although it can reduce the fingerprint contrast to some extent. To get better fingerprint images (better contrast and hence greater sensitivity), more concentrated UC suspensions or UC products with better luminescence are required to shorten exposure times.

6.3.2. UC-AA

6.3.2.1. Synthesis and characterization of UC-AA nanoparticles

The synthesised UC-AA was a white powder or a light pink powder owing to traces of $KMnO_4$. It could be well dispersed in water and was stable for over one year. The luminescence was visually much stronger than that of UC-PEI. However, the luminescence of UC(Ho)/AA and UC(Tm)/AA was much weaker than that of UC-AA. Only two batches of UC(Ho)/AA and UC(Tm)/AA were synthesised. Therefore, the weaker luminescence observed for UC(Ho)/AA and UC(Tm)/AA may not be representative due to the small quantity of synthesised product.

Since the luminescence emission of UC(Ho)/AA and UC(Tm)//AA was weak, they were not applied for fingermark detection in this project. Fingermark detection experiments were only conducted using UC-AA.

The luminescence emission spectrum (**Figure 6.13**) shows that the UC-AA had two peaks centred at 550 nm and 670 nm, which was the same as those observed for $NaYF_4$:Er,Yb and $NaYF_4$:Er,Yb/PEI. The luminescence of the UC-AA was very strong when illuminated by the 980 nm laser.

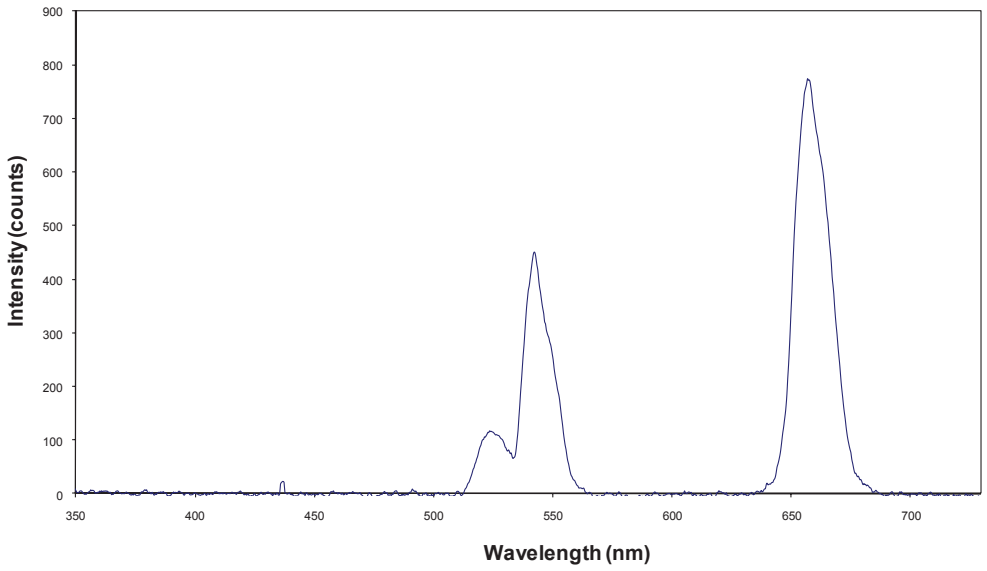

Figure 6.13. Luminescence emission spectrum for UC-AA, illuminated at 980 nm by a laser pointer.

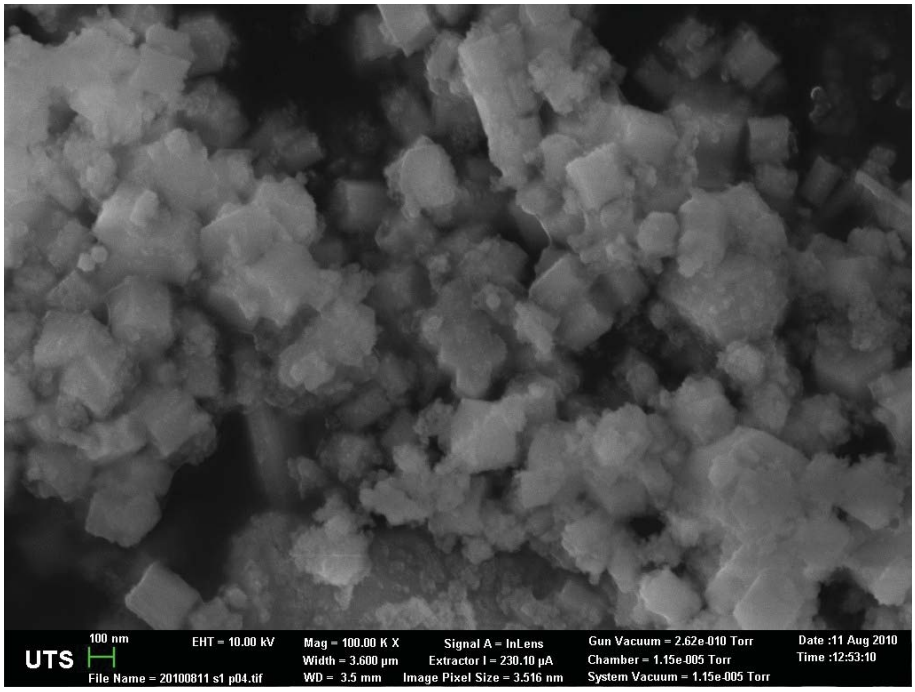

Figure 6.14. SEM image for UC-AA.

Figure 6.14 shows that the synthesised particles contained two different morphologies: one morphology was small spheres with diameters of 10–20 nm, which was similar to that in the published paper (10.8 ± 1.3 nm)[52]; another

morphology was cubes with sides measuring 100–150 nm. The two morphologies were equally represented in the reaction product. One observation was that the synthesised UC-AA should not be left in an ordinary vacuum drier as this lead to particle aggregation. It should be dried in a freezing vacuum drier for less than 24 hours. Longer drying time also resulted in aggregation.

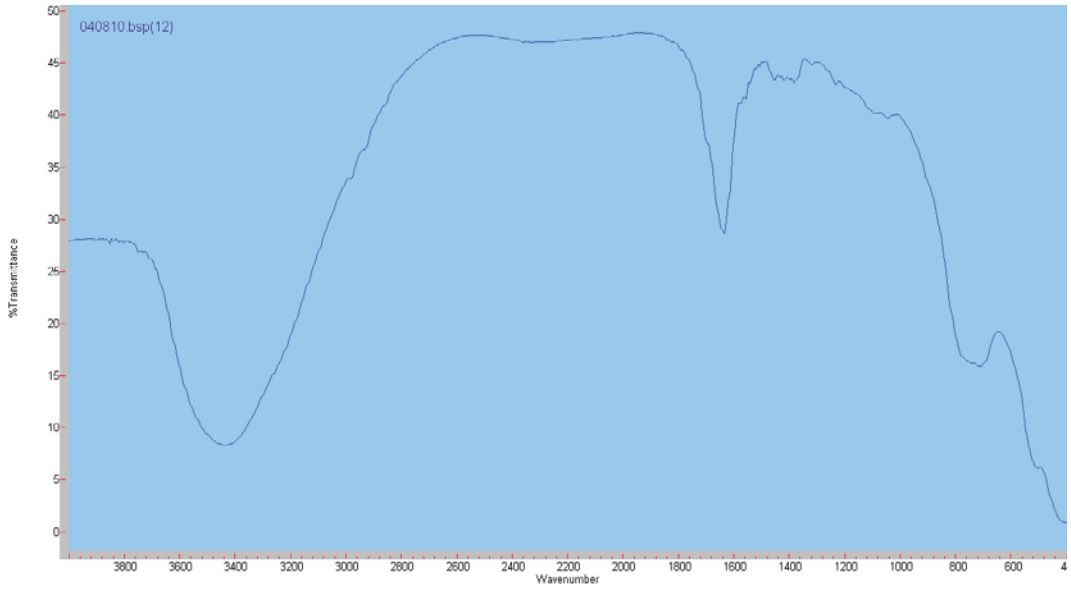

Figure 6.15. FTIR spectrum for $NaYF_4$: Er,Yb-Azelaic Acid.

The capping ligands on the surface of the UC-AA nanoparticles were identified by FTIR spectroscopy (**Figure 6.15**). The broad band at around 3450 cm^{-1} corresponded to the O-H stretching vibration. The transmission bands at around 3000 cm^{-1} were assigned to the stretching vibrations of methylene (CH_2) in the long alkyl chain. Bands corresponding to the carboxylic group were observed at around 1637 and 1550 cm^{-1}. The results confirmed that carboxylic groups were attached to the UC particles.

6.3.2.2. Fingermark detection

An UC-AA solution in water (obtained by sonicating for 10 minutes) can be stable for more than one year. When applied for staining CA-fumed fingermarks, the UC-AA showed affinity to fingermark ridges and was satisfactory on most of the surfaces treated. **Figure 6.16** shows fresh fingermarks on glass slides, plastic and aluminium foil developed with CAF followed by UC-AA staining. The arrow

showed the position of a CA-fumed only fingermark (on the left side of each sample) which was not stained by UC-AA. The CAF-only fingermark was invisible when imaged under the upconversion luminescence mode whereas the ridges of the CAF/UC-AA stained fingermark is very luminescent and clear except on the aluminium foil when imaged under the same time. This proved that the CA-fumed fingermarks were not visible under relatively short exposure time (in this case it was approximately 3 seconds) and the bright luminescence came from the UC-AA staining. It also proved that theoretically the functionalised UC staining can effectively eliminate the background disturbance.

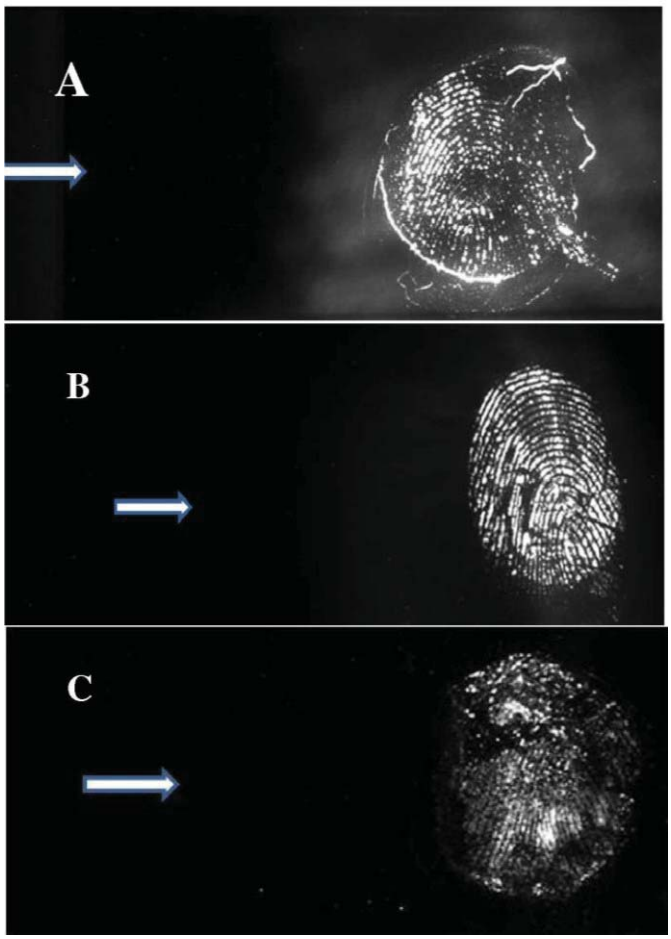

Figure 6.16. CA-fumed fingermark on glass (**A**), plastic (**B**) and aluminium (**C**) stained by UC-AA. Illumination at 980 nm and imaged using a Rofin Poliview with a 555nm band pass filter and an exposure time of approximately 3 seconds. The arrow shows the position of a CA-fumed only fingermark**.**

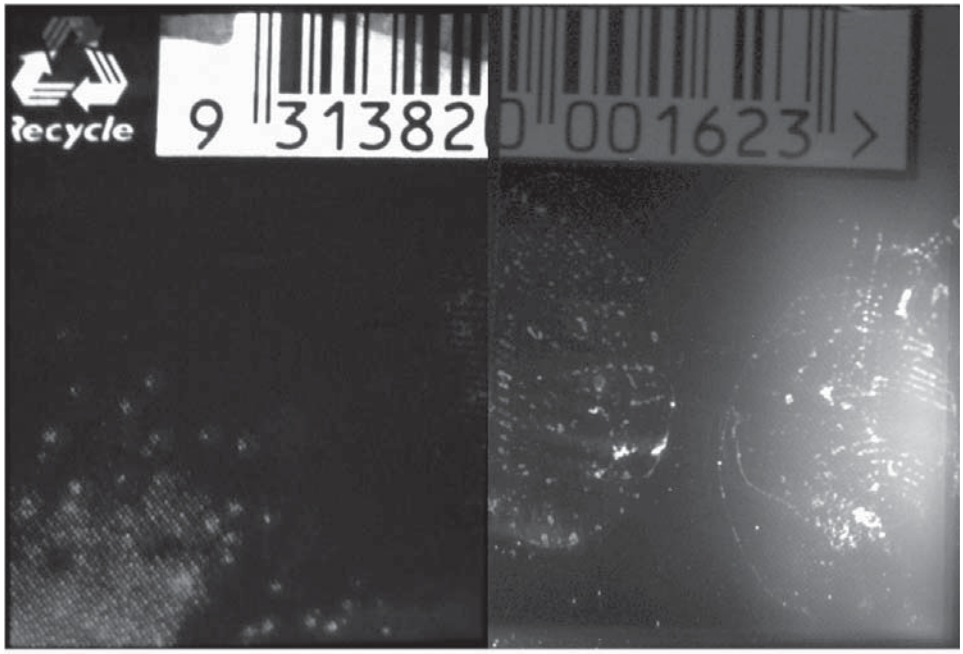

Figure 6.17. Fingermark developed on a soft drink plastic label: (left) rhodamine 6G staining, illumination at 530 nm with 610 nm band pass filter; (right) UC-AA staining, with illumination at 980 nm and imaged using a Rofin Poliview with a 555nm band pass filter and an exposure time of approximately 20 seconds.

Figure 6.17 shows fresh fingermarks on a plastic soft drink label developed with CAF followed by staining (rhodamine 6G on the left and UC-AA on the right). Because of background interference, the fingermarks on the left side are nearly invisible (only a few ridges were visible). On the contrary, the fingermarks on the right side are clearer despite some flaws. The right half of the middle fingermark seemed discontinuous and part of the right fingermark seemed invisible as well. Similarly, in **Figure 6.18** the fingermark images on the left side (stained by rhodamine 6G) are affected more seriously by the background printing than those on the right (stained by UC-AA). It also illustrates the advantage of UCs over traditional luminescent staining reagents under such conditions.

Figure 6.18. Fingermark developed on a soft drink can: (left) rhodamine 6G staining, illumination at 530 nm with 610 nm band pass filter; (right) UC-AA staining, illumination at 980 nm and imaged using a Rofin Poliview with a 555nm band pass filter and an exposure time of approximately 30 seconds.

Similar to UC-PEI, the UC-AA did not develop any satisfactory fingermark images on the Australian polymer banknotes. This may be primarily due to CAF not being effective on the banknote rather than a defect of UC-AA as discussed in Section 6.3.1.3. Further research is required to explore the full potential of UC-AA for fingermark detection on polymer banknotes, together with the improvement of CA fuming on this substrate.

6.3.2.3. The factors affecting imaging and fingermark detection using UC-AA

Luminescence Intensity

Generally the more luminescent the UCs, the better they were at fingermark detection. The luminescence intensity of UC-AA is high that theoretically made it an ideal fingermark reagent. However, during the synthesis process, the UC-AA always came out with MnO_2 impurities which was difficult to be got rid of. The luminescence of UC-AA was also quenched to some extent due to MnO_2 impurities.

The solubility of the UC-AA was affected by these MnO_2 impurities too. Overall it was more difficult to control the quality of UC-AA in the synthesis reaction than did for the UC-PEI.

Detection method

Pure UC-AA with ideal morphology and luminescence property is difficult to be synthesised under the conditions during this study. Generally only a very small amount of UC-AA can be obtained for fingermark detection. Similar to UC-PEI, the UC-AA cannot be prepared in bulk solution and only the fingermarks can be soaked in the solution instead of the whole samples where fingermarks were left on. It means that the CA-fumed fingermarks was far from being stained sufficiently and it resulted that some fingermark details were not fully revealed under the illumination of laser as shown in Figures 6.17 and 6.18.

Exposure Time

Long exposure times were generally employed for UC-AA-developed fingermarks. It also led that background was visible to some extent as in the imaging of UC-PEI-developed fingermarks. Long exposure times also tended to result in a blurry background which was very apparent in Figure 6.18. To get better fingerprint images with less background interference, more concentrated UC-AA solutions should be obtained and applied for fingermark detection with the advantage to shorten exposure times. And hence a better approach to synthesis and purify the UC-AA should be studied in the future.

6.3.3. UC-PVP

The synthesised product was not luminescent under the laser illumination; the synthetic process was repeated three times in total, but no luminescent materials were acquired. The reason was not clear because there are many factors that can affect the synthesis of nanoparticles. Owing to the limitation of time, no further experiments were conducted with this material.

6.3.4. UC-AOT

The synthesised product had very weak luminescence under the laser illumination and the syntheses were repeated three times in total, but only very weak luminescent materials were acquired. The reason was not clear because there are many factors that can affect the synthesis of nanoparticles. Owing to the limitation of time, no further experiments were conducted with this material. The luminescence of the UC/AOT was so weak that it was not a practical alternative for fingermark detection applications. Hence, no fingermark detection was conducted using the UC/AOT particles in this project.

Table 6.1. Summary for functionalised UCs

	UC-PEI	$NaYF_4$:Er (Ho,Tm),Yb-azelaic acid			UC-PVP	UC-AOT
		UC-AA	UC(Ho)-AA	UC(Tm)-AA		
Luminescence intensity	Strong	Very strong	Weak	Weak	Nil	Weak
Fingermark detection	Good	Fair to Good	--	--	--	--

6.4. Conclusions

This research explored the synthesis and use of several functionalised UCs including UC-PEI, UC-AA, UC-PVP and UC-AOT for staining CA-fumed fingermarks on various non-porous and semi-porous surfaces.

The overall results from the functionalised UCs for fingermark detection are summarised in **Table 6.1.** Both the UC-PEI and UC-AA showed strong luminescence under 980 nm laser illumination with the latter is more visually luminescent. The UC-PEI and UC-AA showed some advantage for fingermark detection on various difficult surfaces with high background luminescence and

printing, where conventional luminescence techniques such as rhodamine 6G staining are ineffective. However, they were not able to develop promising fingermarks on Australian polymer banknotes. Because upconversion luminescence is weaker than conventional luminescence, long exposure times under the Rofin Poliview system had to be employed for the imaging of fingermarks developed by functionalised UCs. This long exposure time resulted in a background that was generally visible to some extent, which was different from the theoretical scenario of bright fingermarks against a totally dark background. Due to the limit of timing and laboratory facilities in this study, only small amount of UC-PEI and UC-AA were synthesised and hence their potential for fingermark detection are not fully explored. However, functionalised UCs sometimes showed superior results to conventional luminescence techniques for fingermark detection on some difficult substrates and they can be improved significantly in further studies.

The synthesised UC-PVP showed no luminescence emission under the laser illumination and it was therefore not suitable as an UC for the detection of CA-fumed fingermarks. The synthesised UC-AOT showed very weak luminescence emission under the laser illumination and it was therefore not suitable as an UC for the detection of CA-fumed fingermarks. However, the potential of UC-PVP and UC-AOT as ordinary fingermark powders was not investigated since they were not as luminescent as the commercial UCs.

Chapter 7

General Conclusions

Chapter 7. General Conclusions

7.1. General Discussion and Conclusions

Fingermarks have been used for forensic identification since the late nineteenth century. It is one of the most valuable types of biometric evidence because the characteristic ridge patterns are considered, amongst other characteristics, as individual and immutable. Most fingermarks found at crime scenes are latent, so detection techniques have to be deployed to make them visible.

Recently, UCs have been largely studied in other areas of science for their unconventional anti-Stokes luminescence. Because of this property, UC nanoparticles have many advantages in biological applications, such as the non-invasive and deep penetration of NIR radiation. Upconversion is unusual when used on both natural surfaces and in consumer products. This means that fingermark detection techniques using UCs are, potentially, extremely sensitive and selective.

This project has investigated some fingermark detection techniques based on UCs and nanotechnology. The approaches included powdering, suspension and functionalised UC nanoparticles.

The $NaYF_4$:Er,Yb used in this study was a commercial UC powder and the YVO_4:Er,Yb powder was synthesised by the CSIRO laboratory in Melbourne. They were applied for fingermark detection as dry powdering and suspension methods. Both of them were excited by 980 nm lasers and emitted strong green visible luminescence. The $NaYF_4$:Er,Yb and the YVO_4:Er,Yb powders showed promising results for fingermark detection on a variety of luminescent and/or patterned backgrounds where traditional luminescence fingermark techniques gave poor results. The results illustrated the potential of UC (anti-Stokes) materials to develop fingermarks with high-contrast on substrates that would otherwise prove difficult.

However, the $NaYF_4$:Er,Yb and the YVO_4:Er,Yb powders are insoluble in water and other solvents, and this limits their application in the staining of CA-fumed fingermarks. Since CAF is probably the most common laboratory technique for fingermark detection on non-porous surfaces, it is worth investigating the possibility of making UCs soluble or dispersible in water by functionalising them with hydrophilic groups. Recently, these functionalised UCNPs have increasingly been used in medical imaging or as biological labels. In this project, we mainly illustrated the synthesis and assessment of a number of functionalised UCNPs, with UC-PEI and UC-AA being found suitable for fingermark detection on a range of non-porous and semi-porous surfaces.

The UC-PEI was synthesised by a one-pot heating method and the UC-AA was synthesised via a modified process of oxidizing oleic acid ligands to azelaic acid. The UC-PEI nanoparticles exhibited a spherical shape with an average size of about 50 nm, whereas the UC-AA showed two mixed morphologies: one was small spheres with diameters of 10–20 nm and another was big cubes with sides measuring 100–150 nm. The amino groups coming from the polyethylenimine made the UC-PEI nanoparticles disperse in water and the carboxylic group in the UC-AA made it soluble in water. Both the UC-PEI and the UC-AA emitted strong upconversion luminescence under the laser excitation at 980 nm. Fingermarks were deposited on various surfaces to compare CAF/UC-PEI and CAF/UC-AA with CAF/rhodamine 6G. The results showed that, on some surfaces where rhodamine 6G staining could not develop satisfactory fingermarks, UC-PEI or UC-AA staining could eliminate the background interference to some extent and achieve relatively good fingermarks. The result showed the potential of functionalised UC staining on surfaces where conventional luminescence techniques are ineffective. However, on the Australian polymer banknotes, neither of the UC-PEI or UC-AA staining revealed any satisfactory images, largely because CAF is not particularly effective on the banknotes due to the semi-porous nature of this substrate. Two other functionalised UCNPs, UC-PVP and UC-AOT, were synthesised but were not applied for fingermark detection owing to their low luminescence intensity.

The imaging of fingermarks developed by UCs was crucial in this study. A 980 nm laser pointer with 700 mW output proved to be the most suitable light source of those evaluated. Long exposure times were generally required for the recording of the upconversion luminescence, especially for the functionalised UCs, which exhibited much weaker luminescence than the commercial UC powders. A Rofin Poliview was found to be a suitable recording system when fitted with a 555 nm band-pass filter in front of the lens to block the reflected IR light from the laser (since the Poliview camera is sensitive to IR light). Safety measures had to be adopted all the times during the experiments to avoid potential eye damage.

In short, conventional luminescence techniques can develop satisfactory fingermarks in most cases. However, UCs and functionalised UCs show advantages on some difficult substrates and they are therefore an important supplementary method when conventional luminescence techniques are ineffective. The use of UCs and functionalised UCs has the potential to become a routine technique for fingermark detection when they are fully optimised through future research.

7.2. Future Directions

UCs have shown some advantage over traditional luminescence techniques on backgrounds with luminescence and/or pattern (printing) interference. Functionalised UCs are particularly interesting because of their application combined with CAF, which is generally regarded as being more sensitive than powdering methods. So far, only two functionalised UCs have been successfully applied to fingermark detection. However, dozens of functionalised UCs have recently been widely used in bio-imaging. These functionalised UCs either have hydrophilic groups or encapsulated hydrophobic nanocrystals with a SiO_2 or amphiphilic copolymer. These are soluble in water and have potential as a staining method for CA-fumed fingermarks. The critical part for the application of functionalised UCs for fingermark detection is the synthesis and purification of the nanoparticles. The quantum yield or luminescence efficiency for these functionalised UCs is another important factor. Certainly, the

formulation of functionalised UCs for fingermark detection needs to be optimized as well.

Another direction is to obtain smaller UC particles, with diameters less than 1 to 2 micrometres, since the diameter of the holes in the polycyanoacrylate layer that forms on the fingermark ridges is around 1 to 2 micrometres. These smaller particles are expected to be trapped inside the polycyanoacrylate layer and hence effectively stain the CA-fumed fingermarks. They could be used as a suspension or colloid, possibly with the help of a surfactant. These smaller particles could be acquired by controlled synthesis in different solvents, possibly with the help of certain surfactants. Alternatively, powerful, specially designed mills could be used to grind the commercial UC powders into smaller particles.

To improve the imaging, special-purpose NIR lasers could be manufactured. These lasers should have appropriate output which is powerful enough to excite the upconversion luminescence but not to ignite the exhibits. They should also have a large aperture to illuminate the whole fingermark area and avoid the manual scanning used in this study that may lead to blurry fingermark detail. A software, if possible, should be employed to control the swith-on and –off of the laser, the accurate exposure time of fingermark developed by UCs, and the real-time images should be displayed on computer screens.

In summary, UCs have demonstrated advantages over conventional luminescence techniques for fingermark detection on difficult backgrounds. They have the great potential to become an important routine technique for fingermark detection in the future provided that further research is undertaken to resolve some of the issues encountered.

References

1. C. Champod, C. Lennard, P. Margot, and M. Stoilovic, *fingerprints and other ridge skin impressions*. 2004, Boca Raton: CRC Press.
2. M.J. Choi, A.M. McDonagh, P. Maynard, and C. Roux, *Metal-containing nanoparticles and nano-structured particles in fingermark detection.* Forensic Science International, 2008. **179**(2-3): p. 87-97.
3. J.R. Lakowicz, *Principles of Fluorescence Spectroscopy,*. 1983, New York: Plenum Press.
4. *Schematic Representation of the Stokes Shift in a Luminescence Process*. 19/12/2011; Available from: http://upload.wikimedia.org/wikipedia/commons/a/af/Stokes_shift.png.
5. E.R. Menzel and J.A. Burt, *Laser detection of latent fingerprints: difficult surfaces.* Journal of Forensic Sciences, 1983. **30**(2): p. 364-370.
6. J. Almog, G. Levinton-Shamuilov, Y. Cohen, and M. Azoury, *Fingerprint Reagents with Dual Action: Color and Fluorescence.* J. Forensic Sciences, 2007. **52**(2): p. 330-334.
7. M. Stoilovic and C. Lennard, *Fingerprint Detection and Enhancement*. 3rd ed. 2010, Canberra: National Centre for Forensic Study.
8. E.R. Menzel, S.M. Savoy, S.J. Ulvick, K.H. Cheng, R.H. Murdock, and M.R. Sudduth, *photoluminescent semiconductor nanocrystals for fingerprint detection.* J. Forensic Sciences, 2000. **45**(3): p. 545-551.
9. E.R. Menzel, M. Takatsu, R.H. Murdock, K. Bouldin, and K.H. Cheng, *Photoluminescent CdS/Dendrimer nanocomposites for fingerprint detection.* J. Forensic Sciences, 2000. **45**(4): p. 770-773.
10. K.K. Bouldin, E.R. Menzel, M. Takatsu, and R.H. Murdock, *Diimide-enhanced fingerprint detection with photoluminescent CdS/Dendrimer nanocomposites.* J. Forensic Sciences, 2000. **45**(6): p. 1239-1242.
11. Y.-J. Jin, Y.-J. Luo, G.-P. Li, J. Li, Y.-F. Wang, R.-Q. Yang, and W.-T. Lu, *Application of photoluminescent CdS/PAMAM nanocomposites in fingerprint detection.* Forensic Science International, 2008. **179**(1): p. 34-38.
12. J. Dilag, H. Kobus, and A.V. Ellis, *Cadmium sulfide quantum dot/chitosan nanocomposites for latent fingermark detection.* Forensic Sci Int, 2009. **187**: p. 97-102.
13. M.Algarra, J.Jimenez-Jimenez, R. Moreno-Tost, B.B. Campos, and J.C.G.E.d. Silva, *CdS nanocomposites assembled in porous phosphate heterostructures for fingerprint detection.* Optical Materials, 2011. **33**: p. 893-898.
14. M. Sametband, I. Shweky, U. Banin, D. Mandler, and J. Almog, *Application of nanoparticles for the enhancement of latent fingerprints.* Chem. Commun., 2007: p. 1142-1144.
15. Y.F.Wang, R.Q.Yang, Y.J.Wang, Z.X.Shi, and J.J.Liu, *Application of CdSe nanoparticle suspension for developing latent fingermarks on the sticky side of adhesives.* Forensic Sci Int, 2009. **185**: p. 96-99.
16. A. Becue, S. Moret, C. Champod, and P. Margot, *Use of quantum dots in aqueous solution to detect blood fingermarks on non-porous surfaces.* Forensic Sci Int, 2009. **191**: p. 36-41.

17. F. Gao, J. Han, J. Zhang, Q. Li, X. Sun, J. Zheng, L. Bao, X. Li, and Z. Liu, *The synthesis of newly modified CdTe quantum dots and their application for improvement of latent fingerprint detection.* Nanotechnology, 2011. **22**(075705).
18. M.J. Choi, T. Smoother, A.A. Martin, A.M. McDonagh, P.J. Maynard, C. Lennard, and C. Roux, *Fluorescent TiO2 powders prepared using a new perylene diimide dye: Applications in latent fingermark detection* Forensic Science International, 2007. **173**(2-3): p. 154-160.
19. M.J. Choi, K.E. McBean, R.N.P. Hei, A.M. McDonagh, P.J. Maynard, C. Lennard, and C. Roux, *An evaluation of nanostructured zinc oxide as a fluorescent powder for fingerprint detection.* J. Mater. Sci., 2008. **43**: p. 732-737.
20. A. Becue, A.l. Scoundrianos, C. Champod, and P. Margot, *Fingermark detection based on the in situ growth of luminescent nanoparticles—Towards a new generation of multimetal deposition.* Forensic Science International, 2008. **179**(1): p. 39-43.
21. L. Liu, S.K. Gill, Y. Gao, L.J. Hope-Weeks, and K.H. Cheng, *Exploration of the use of novel SiO2 nanocomposites doped with fluorescent Eu3+/sensitizer complex for latent fingerprint detection.* Forensic Science International, 2008. **176**(2-3): p. 163-172.
22. B.J. Theaker, K.E. Hudson, and F.J. Rowell, *Doped hydrophobic silica nano- and micro-particles as novel agents for developing latent fingerprints.* Forensic Science International, 2008. **174**(1): p. 26-34.
23. U.S. Dinish, Z.X. Chao, L.K. Seah, and V.M. Murukeshan, *nanosecond resolution in fingerprint imaging using optical technique.* International Journal of Nanoscience, 2005. **4**(4): p. 695-700.
24. L. K. Seah, U.S. Dinish, W.F. Phang, Z.X. Chao, and V.M. Murukeshan, *Fluorescence optimisation and lifetime studies of fingerprints treated with magnetic powders* Forensic Science International, 2005. **152**(2-3): p. 249-257.
25. L.K. Seah, P. Wanga, V.M. Murukeshana, and Z.X. Chao, *Application of fluorescence lifetime imaging (FLIM) in latent finger mark detection.* Forensic Science International, 2006. **160**(2-3): p. 109-114.
26. R.H. Murdock and E.R. Menzel, *A computer interfaced time-resolved luminescence imaging system.* J. Forensic Sci., 1993. **38**: p. 521-529.
27. N. Akiba, N. Saitoh, and K. Kuroki, *Fluorescence Spectra and Images of Latent Fingerprints Excited with a Tunable Laser in the Ultraviolet Region.* J. Forensic Sciences, 2007. **52**(5): p. 1103-1106.
28. U.S. Dinish, Z.X. Chao, L.K. Seah, A. Singh, and V.M. Murukeshan, *Formulation and implementation of a phase-resolved fluorescence technique for latent-fingerprint imaging: theoretical and experimental analysis.* Applied Optics, 2005. **44**(3): p. 297-304.
29. U.S. Dinish, L.K. Seah, V.M. Murukeshan, and L.S. Ong, *Theoretical analysis of phase-resolved fluorescence emission from fingerprint samples.* Optics Communication, 2003. **223**: p. 55-60.
30. C.E. Allred and E.R. Menzel, *A novel europium-bioconjugate method for latent fingerprint detection* Forensic Science International, 1997. **85**: p. 83-94.
31. D. Wilkinson, *A one-step fluorescent detection method for lipid fingerprints; Eu(TTA)3·2TOPO.* Forensic Science International, 1999. **99**(1): p. 5-23.

32. D.A. Wilkinson and J.E. Watkin, *Europium aryl-β-diketone complexes as fluorescent dyes for the detection of cyanoacrylate developed fingerprints on human skin* Forensic Science International, 1993. **60**(1-2): p. 67-79.
33. E.R.A. Lock, W.D. Mazzella, and P. Margot, *A New Europium Chelate As a Fluorescent Dye for Cyanoacrylate Pretreated Fingerprints-EuTTAPhen: Europium ThenoylTrifluoroAcetone Ortho-Phenanthroline.* Journal of Forensic Sciences, 1995. **40**(4): p. 654-658.
34. N. Meylan, C.J. Lennard, and P.A. Margot, *Use of A Gaseous Electrical Discharge to Induce Luminescence in Latent Fingerprints.* Forensic Science International, 1990. **45**: p. 73-83.
35. L.M. Davies, N.E. Jones, J.S. Brennan, and S.K. Bramble, *A New Visibly-Excited Fluorescenct Component in Latent Fingerprint Residue Induced by Gaseous Electrical Discharge.* Journal of Forensic Sciences, 2000. **45**(6): p. 1294-1298.
36. C.G. Worley, S.S. Wiltshire, T.C. Miller, G.J. Havrilla, and V. Majidi, *Detection of Visible and Latent Fingerprints Using Micro-X-ray Fluorescence Elemental Imaging.* Powder Diffraction, 2006. **21**(2): p. 136-139.
37. J.F. Suyver, A. Aebischer, D. Biner, P. Gerner, J. Grimm, S. Heer, K.W. Kra¨mer, C. Reinhard, and H.U. Gu¨del, *Novel materials doped with trivalent lanthanides and transition metal ions showing near-infrared to visible photon upconversion.* Optical Materials, 2005. **27**: p. 1111-1130.
38. E. Bullock, *Up-conversion phosphors for use in latent fingermark detection*, in *Faculty of science*. 2006, University of Technology, Sydney: Sydney. p. 98.
39. C. Artemis, *Luminescent Colours*. 2006, Artemis Chemicals: Essex, England.
40. S. Heer, K. Kompe, H. Gudel, and M. Haase, *Highly efficient multicolor upconversion emission in transparent colloids of lanthanide-doped NaYF4 nanocrystals.* Advanced Materials, 2004. **16**(23-24): p. 2102-2105.
41. F. Wang, D.K. Chatterjee, Z. Li, Y. Zhang, X. Fan, and C. Wang, *Synthesis of polyethylenimine/NaYF4 nanoparticles with upconversion fluorescence.* Nanotechnology, 2006. **17**: p. 5786-5791.
42. A.M. Pires, S. Heer, H.U. G¨udel, and O.A. Serra, *Er, Yb Doped Yttrium Based Nanosized Phosphors: Particle Size,"Host Lattice" and Doping Ion Concentration Effects on Upconversion Efficiency.* J Fluoresc, 2006. **16**: p. 461-468.
43. Y. Bai, K. Yang, Y. Wang, X. Zhang, and Y. Song, *Enhancement of the upconversion photoluminescence intensity in Li+ and Er3+ codoped Y2O3 nanocrystals.* Optics Communications, 2008. **281**: p. 2930-2932.
44. G. Zhuo, X. Wang, D. Wang, C. Wang, X. Zhao, Z. Shao, and M. Jiang, *Two-photon induced optical-power limiting and upconverted superradiance properties of a new organic dye HEASPI.* Optics & Laser Technology, 2001. **33**: p. 209-212.
45. W. Koechner, *Solid-State Laser Engineering*, W.T.Rhodes, Editor. 2006, Springer: Atlanta.
46. W. Zhao and F.N. Castellano, *Upconverted emission from Pyrene and Di-terr-butylpyrene using Ir(ppy)3 as triplet sensitizer.* J. Phys. Chem. A, 2006. **110**: p. 11440-11445.

47. J.-M. Cosquer, *Security ink for high-valued security document - anti-Stokes inks.* Newsletter of International Government Printing and Publishing Association, January 2003: p. 8-9.
48. M. Stoilovic and C. Lennard, *Fingermark Detection & Enhancement*. 4th ed. 2010, Canberra: National Centre for Forensic Studies.
49. C. Lennard, *Personal Communication.* 2010.
50. Z. Li and Y. Zhang, *An efficient and user-friendly method for the synthesis of hexagonal-phase NaYF4:Yb,Er/Tm nanocrystals with controllable shape and upconversion fluorescence.* Nanotechnology, 2008. **19**: p. 345606.
51. Z. Li and Y. Zhang, *Monodisperse silica-coated polyvinylpyrrolidone/NaYF4 nanocrystals with multicolor upconversion flurescence emission.* Angew. Chem. Int. Ed., 2006. **45**: p. 7732-7735.
52. Z. Chen, H. Chen, H. Hu, M. Yu, F. Li, Q. Zhang, Z. Zhou, T. Yi, and C. Huang, *Versatile synthesis strategy for carboxylic acid-functionalized upconverting nanophosphors as biological lables.* J. AM. CHEM. SOC., 2008. **130**: p. 3023-3029.
53. H. Hu, M. Yu, F. Li, Z. Chen, X. Gao, L. Xiong, and C. Huang, *Facile epoxidation strategy for producing amphiphilic up-converting rare-earth nanophosphors as biological lables.* Chem. Mater., 2008. **20**: p. 7003-7009.
54. F. Auzel, *Upconversion and Anti-Stokes Processes with f and d Ions in Solids.* Chem. Rev., 2004. **104**: p. 139-173.
55. R. Ma, E. Bullock, P. Maynard, B. Reedy, R. Shimmon, C. Lennard, C. Roux, and A. McDonagh, *Fingermark Detection on Non-Porous and Semi-Porous Surfaces Using NaYF4:Er,Yb Up-converter Particles.* Forensic Science International, 2011. **207**(1-3): p. 145-149.
56. A. Dowd, *Personal Communication.* 2011.
57. J.H. Zeng, J. Su, Z.H. Li, R.X. Yan, and Y.D. Li, *Synthesis and upconversion luminescence of Hexagonal-phase NaYF4:Yb,Er^{3+} phosphors of controlled size and morphology.* Advanced Materials, 2005. **17**(2119-2123).
58. R. Henderson and K. Schulmeister, *Laser Safety*, ed. J. Navas. 2004, Bristol and Philadelphia: Institute of Physics Publishing.
59. R.E. Gaensslen and H.C. Lee, *Advances in fingerprint technology*. 2001, Boca Raton: CRC Press.
60. N. Jones, M. Kelly, M. Stoilovic, C. Lennard, and C. Roux, *The development of latent fingerprints on polymer banknotes.* J. Forensic Identification, 2003. **53**(1): p. 50-77.
61. H. Bandey and T. Kent, *Superglue Treatment of Crime Scenes, A Trial of the Effectiveness of the Mason Vactron SUPERfume Process*. 2003, Home Office, Police Scientific Development Branch: Sandridge, St Albans, Hertfordshire.
62. A. Becue, S. Moret, C. Champod, and P. Margot, *Use of quantum dots in aqueous solution to detect blood fingermarks on non-porous surfaces.* Forensic Sci. Int., 2009. **191**: p. 36-41.
63. C. McLaren, C. Lennard, and M. Stoilovic, *Methylamine Pretreatment of Dry Latent Fingermarks on Polyethylene for Enhanced Detection by Cyanoacrylate Fuming.* Journal of Forensic Identification, 2010. **60**(2): p. 199-222.
64. G.S. Sodhi and J. Kaur, *Powder methods for detecting latent fingerprints: a review.* Forensic Science International, 2001. **120**: p. 172-176.

65. M. Tahtouh, J. Kalman, C. Roux, C. Lennard, and B. Reedy, *The detection and enhancement of latent fingermarks using infrared chemical imaging.* Journal of Forensic Sciences, 2005. **50**(1): p. 64-72.
66. V. Drapel, A. Becue, C. Champod, and P. Margot, *Identification of promising antigenic components in latent fingermark residues.* Forensic Science International, 2009. **184**: p. 47-53.
67. J.H. Olenik, *Super glue - a modified technique for the development of latent fingerprints.* Journal of Forensic Sciences, 1984. **29**(3): p. 881-884.
68. L.A. Lewis, R.W. Smithwick, G.L. Deavult, B. Bollinger, and S.A. Lewis, *Processes Involved in the development of latent fingerprints using the cyanoacrylate Fuming method.* Journal of Forensic Sciences, 2001. **46**(2): p. 241-246.
69. C. Lennard, *Personal Communication*. 2010.
70. D.J. Shaw, *Introduction to Colloid and Surface Chemistry*. 4th ed. 1991, Oxford: Butterworth-Heinemann Ltd.
71. A. Lynch and C. Rowland, *Fine-grinding mills*, in *The history of grinding*. 2005, Society for Mining, Metallurgy, and Exploration, Inc. (SME) littleton, Colorado. p. 133-147.
72. R. Ma, R. Shimmon, A. McDonagh, P. Maynard, C. Lennard, and C. Roux, *Fingermark detection on non-porous and semi-porous surfaces using YVO4:Er,Yb luminescent upconverting particles.* Forensic Science International, accepted, 2011.
73. L. Xiong, Z. Chen, Q. Tian, T. Cao, C. Xu, and F. Li, *High Contrast Upconversion Luminescence Targeted Imaging in Vivo Using Peptide-Labeled Nanophosphors.* Anal. Chem., 2009. **81**: p. 8687-8694.
74. L. Xiong, T. Yang, Y. Yang, C. Xu, and F. Li, *Long-term in vivo biodistribution imaging and toxicity of polyacrylic acid-coated upconversion nanophosphors.* Biomaterials, 2010. **31**: p. 7078-7085.
75. H. Hu, L. Xiong, J. Zhou, F. Li, T. Cao, and C. Huang, *Multimodal-Luminescence Core–Shell Nanocomposites for Targeted Imaging of Tumor Cells.* Chem. Eur. J., 2009. **15**: p. 3577-3584.
76. M. Yu, F. Li, Z. Chen, H. Hu, C. Zhan, H. Yang, and C. Huang, *Laser Scanning Up-Conversion Luminescence Microscopy for Imaging Cells Labeled with Rare-Earth Nanophosphors.* Analytical Chemistry, 2009. **81**(3): p. 930-935.
77. H. Hu, M. Yu, F. Li, Z. Chen, X. Gao, L. Xiong, and C. Huang, *Facile Epoxidation Strategy for Producing Amphiphilic Up-Converting Rare-Earth Nanophosphors as Biological Labels.* Chem. Mater., 2008. **20**: p. 7003-7009.
78. J. Wu, Q. Tian, H. Hu, Q. Xia, Y. Zou, F. Li, T. Yi, and C. Huang, *Self-assembly of peptide-based multi-colour gels triggered by up-conversion rare earth nanoparticles.* Chem. Commun., 2009: p. 4100-4102.
79. T. Cao, T. Yang, Y. Gao, Y. Yang, H. Hu, and F. Li, *Water-soluble NaYF4:Yb/Erupconversion nanophosphors: Synthesis, characteristics and application in bioimaging.* Inorganic Chemistry Communications, 2010. **13**: p. 392-394.
80. W.T. Godbey , K.K. Wu , and A.G. Mikos, *Poly(ethylenimine) and its role in gene delivery.* Journal of Controlled Release, 1999. **60**(2-3): p. 149–160.

81. J.N. Cha, Y. Zhang, S.P. Wong, S. Raoux, C. Rettner, L. Krupp, and V. Deline, *Biomimetic Approaches for Fabricating High-Density Nanopatterned Arrays.* Chem. Mater., 2007. **19**: p. 839-843.
82. R.U. Lemieux and E. Von Rudloff, *Periodate-Permanganate Oxidations: I.Oxidation of Olefins.* Canadian Journal of Chemistry, 1955. **33**: p. 1701-1709.
83. L.-Q. Xiong, Z.-G. Chen, M.-X. Yu, F.-Y. Li, C. Liu, and C.-H. Huang, *Synthesis, characterization, and in vivo targeted imaging of amine-functionalized rare-earth up-converting nanophosphors.* Biomaterials, 2009. **30**: p. 5592-5600.
84. R. Naccache, F. Vetrone, V. Mahalingam, L.A. Cuccia, and J.A. Capobianco, *Controlled Synthesis and Water Dispersibility of Hexagonal Phase NaGdF4:Ho3+/Yb3+ Nanoparticles.* Chem. Mater., 2009. **21**(4): p. 717-723.
85. C. Zha, *Personal communication.* 2008: Melbourne.
86. M. Tahtouh, S.A. Scott, J.R. Kalman, and B.J. Reedy, *Four novel alkyl 2-cyanoacylate monomers and their use in latent fingermark detection by mid-infrared spectral imaging.* Forensic Sci Int, 2011. **207**: p. 223-238.
87. M. Tahtouh, J.R. Kalman, and B.J. Reedy, *Synthesis and characterization of four alkyl 2-cyanoacrylate monomers and their precursors for use in latent fingerprint detection.* Journal of Polymer Science, Part A: Polymer Chemistry, 2011. **49**: p. 257-277.